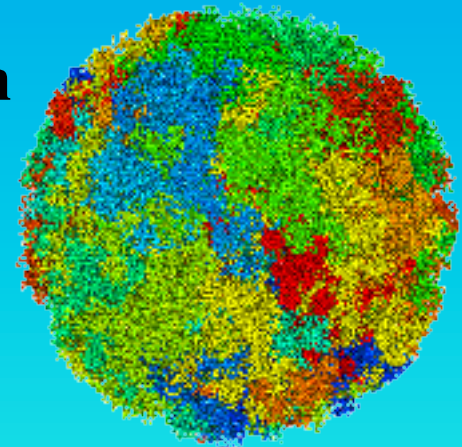
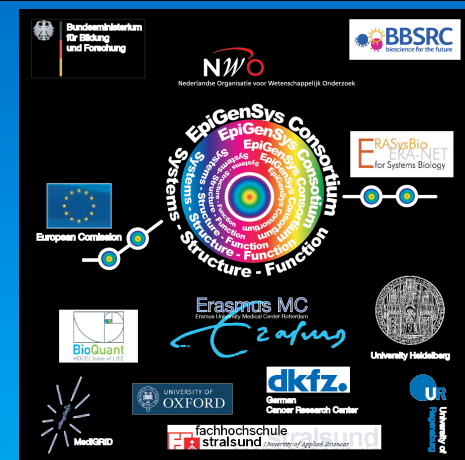
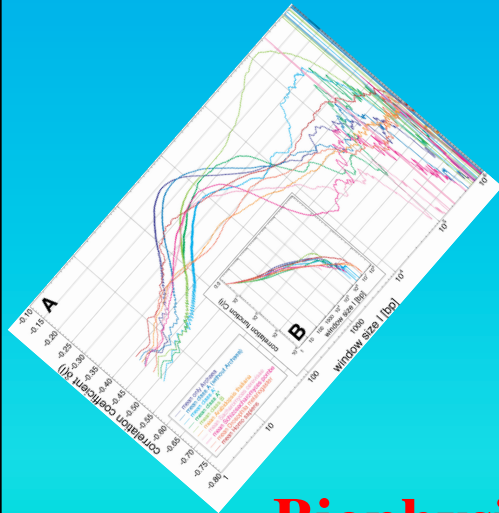


**A Systems Genomic Approach
combining
Simulations and Experiments
reveals the detailed
3D Multi-Loop Aggregate/Rosette
Chromatin Architecture
and
Functional Dynamic Organization
of
Genomes**

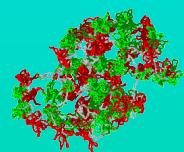
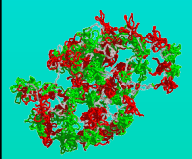


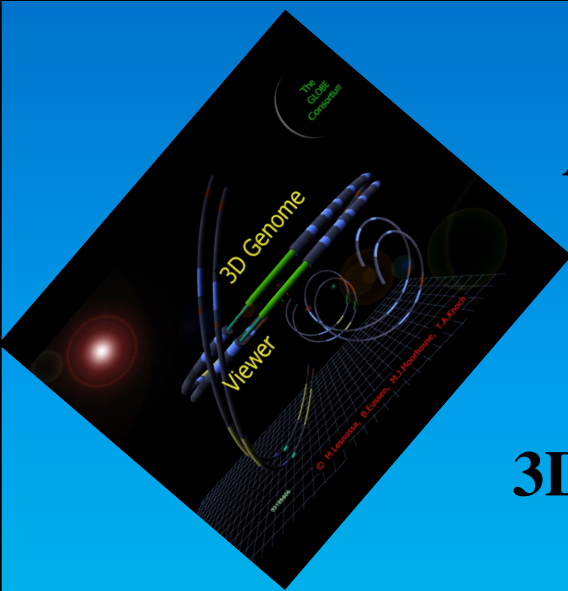
Tobias A. Knoch

Biophysical Genomics & Erasmus Computing Grid

Erasmus Medical Center

TA.Knoch@taknoch.org





A Systems Genomic Approach combining Simulations and Experiments reveals the details of 3D Multi-Loop Architecture Chromatin

Functional Organization of a Genome

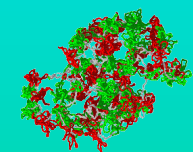
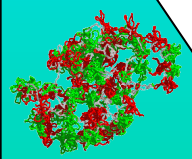
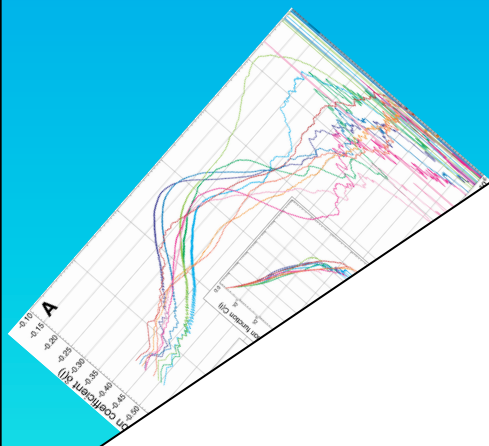
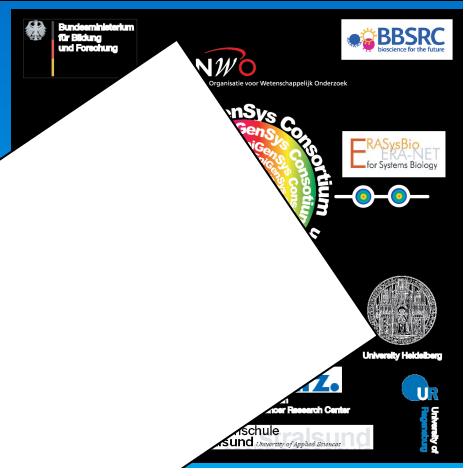
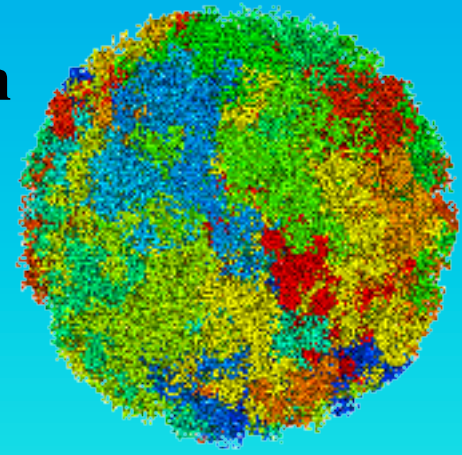
**Results and Perspectives
Finally Solved Challenge!**

Nobias A. Knoch

Genomics & Erasmus Computing Grid

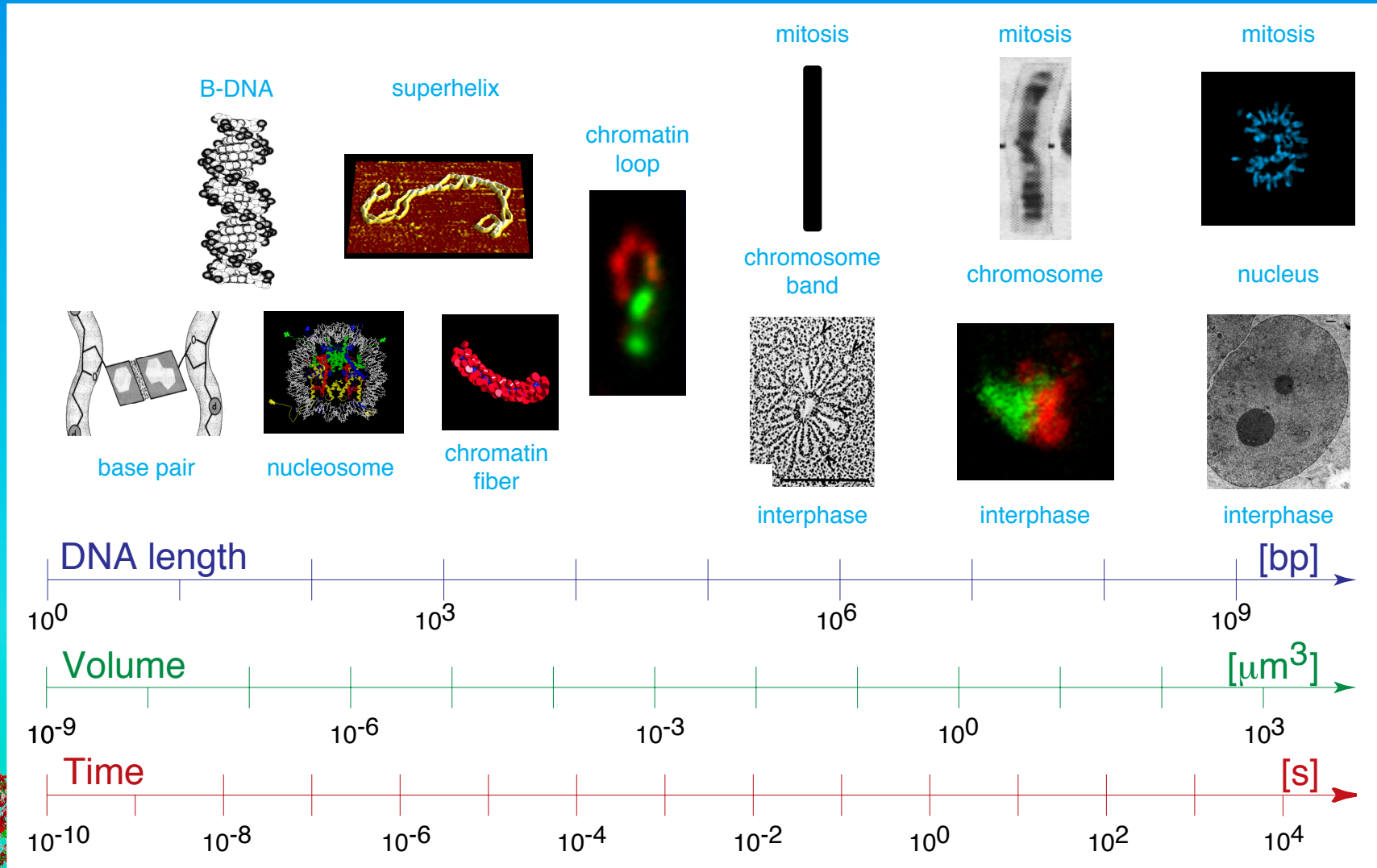
Erasmus Medical Center

TA.Knoch@taknoch.org



Dynamic and Hierarchical Genome Organization

The different organization levels of genomes bridge several orders of magnitude concerning space and time. How all of these organization levels connect to processes like gene regulation, replication, embryogeneses, or cancer development is still unclear?

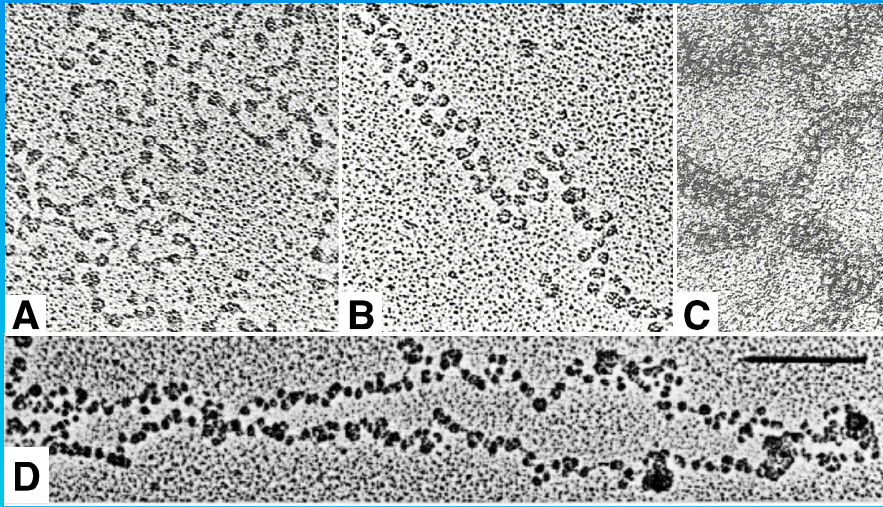


Chromatin Conformation and Higher-Order Topologies

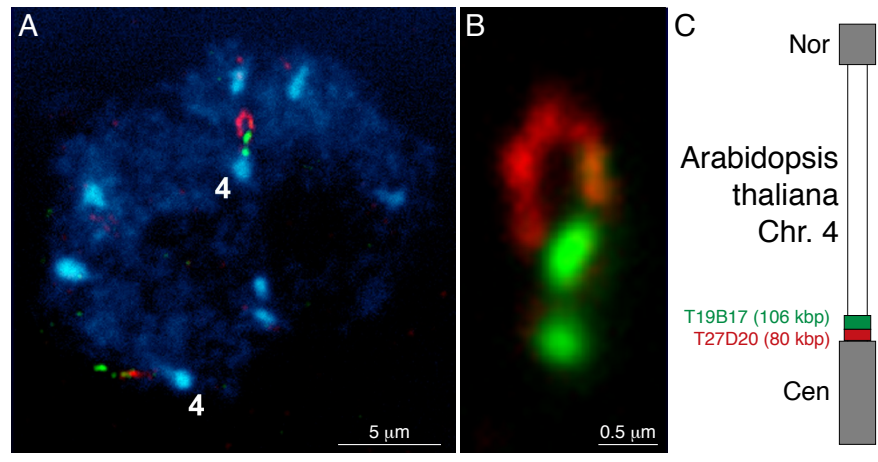
It becomes increasingly clearer, that the chromatin conformation is a random organization of nucleosomes, which depending on external or modification conditions has different condensation degrees, with a prevalence for the 30nm fiber with ~6nucleosomes per 11nm. This seems to make loops which further cluster to form aggregates more or less rosette-like which then constitute the chromosome.



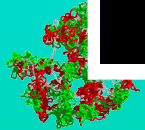
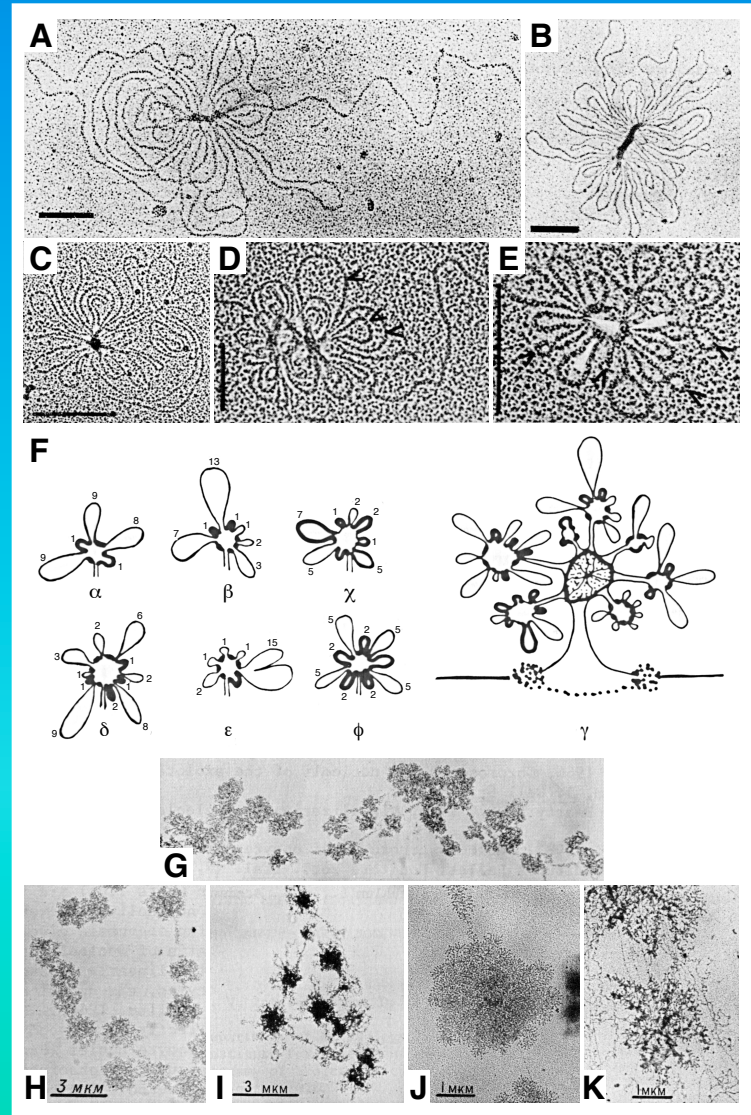
A-C: Voet & Voigt; D: Reznik *et al.*



Courtesy P. Fransz, Amsterdam



A: B. Aramova *et al.*; C: Salganik *et al.*; D-G: Frznik *et al.*; G-K: Tsvetkov & Pavlov

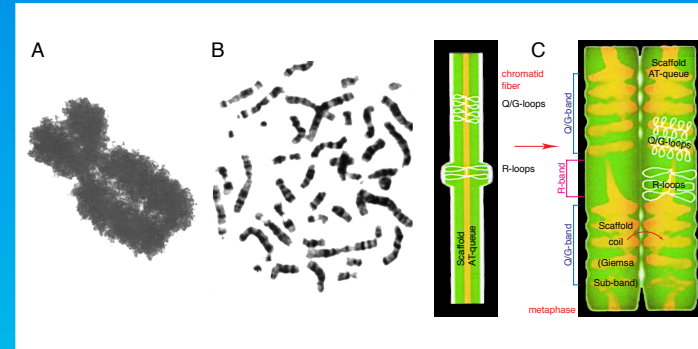
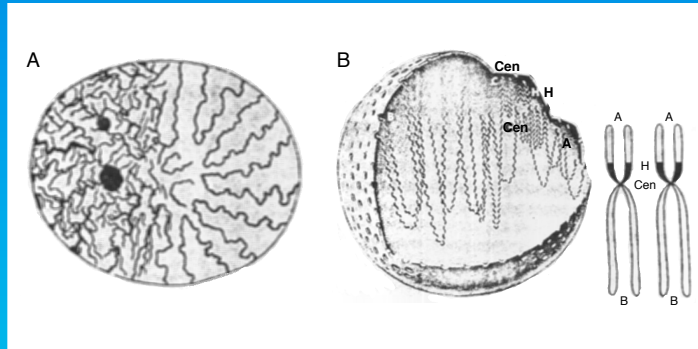


Integral Models of Cell Nuclear Organization I

Already Rabl and Boveri were aware of the obvious fact that the organization of genomes has to be consistent from the sequence level to the morphology of the whole cell nucleus. Although they might be different in detail their common seem is recursive folding and clustering thereof with variation/ modification and dynamics accounting for different nuclear states and function.

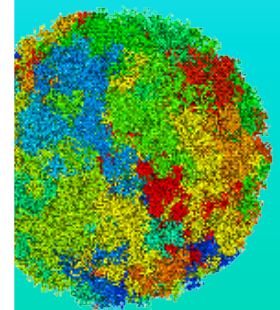
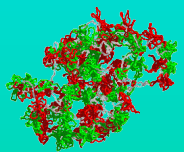
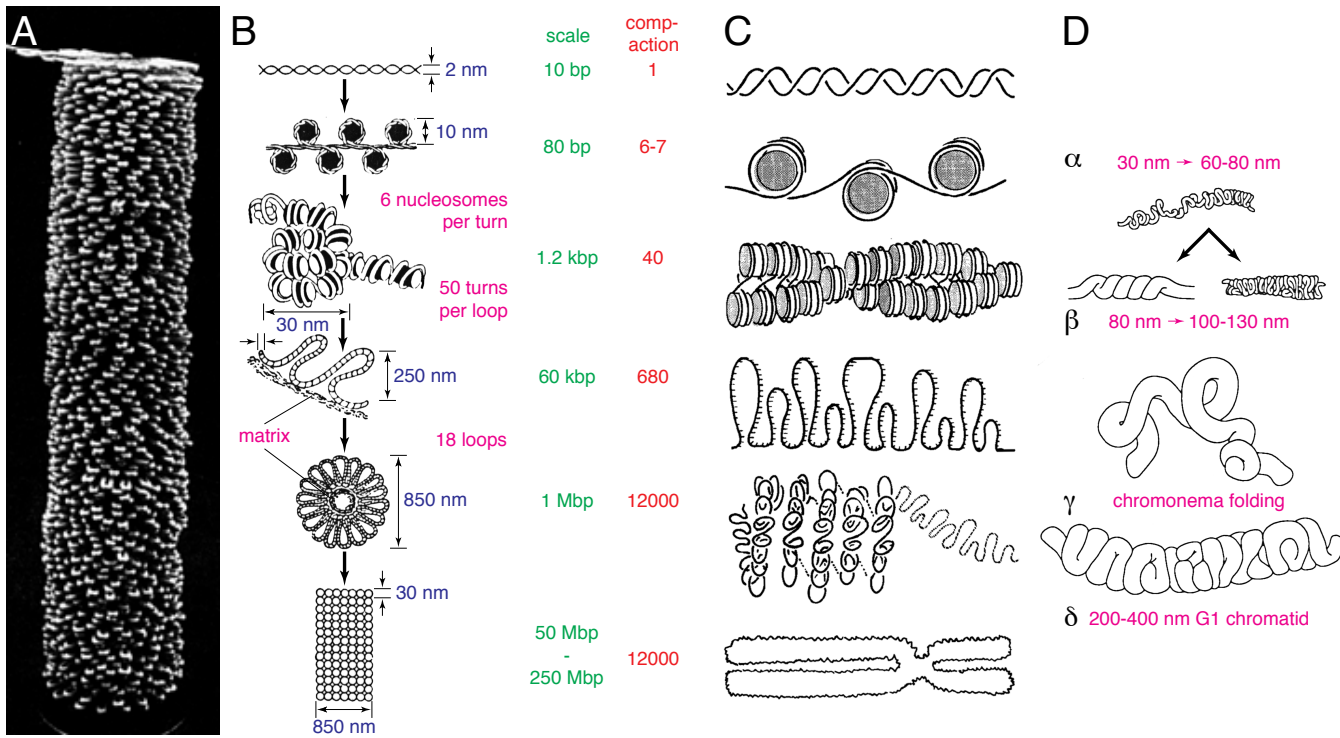


Rabl & Boveri



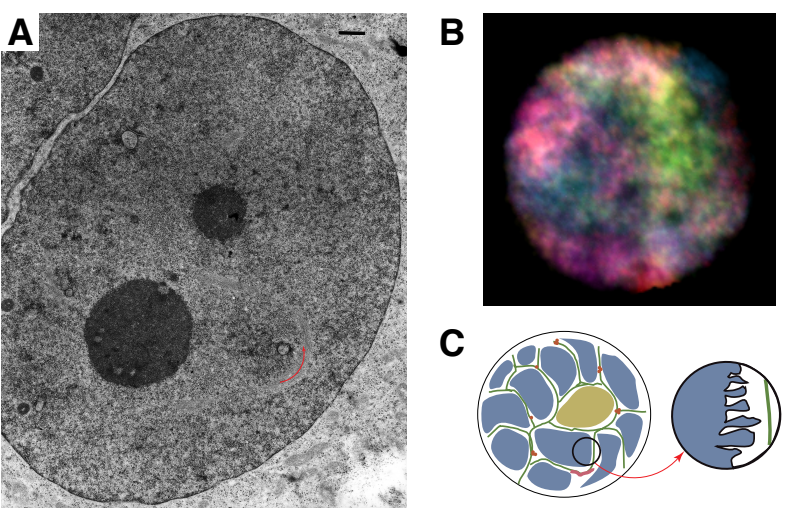
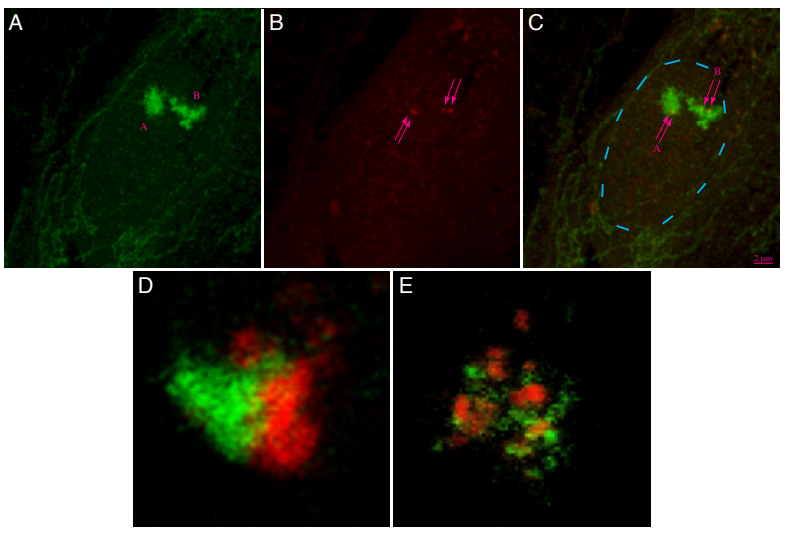
A: Bloom & Fawcett
B: Alberts *et al.*
C: Paulson & Laemmli

A, B: Pienta & Coffey; C: Alberts *et al.*; D: Belmont & Bruce

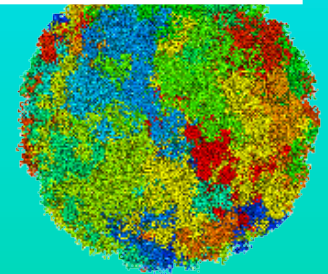
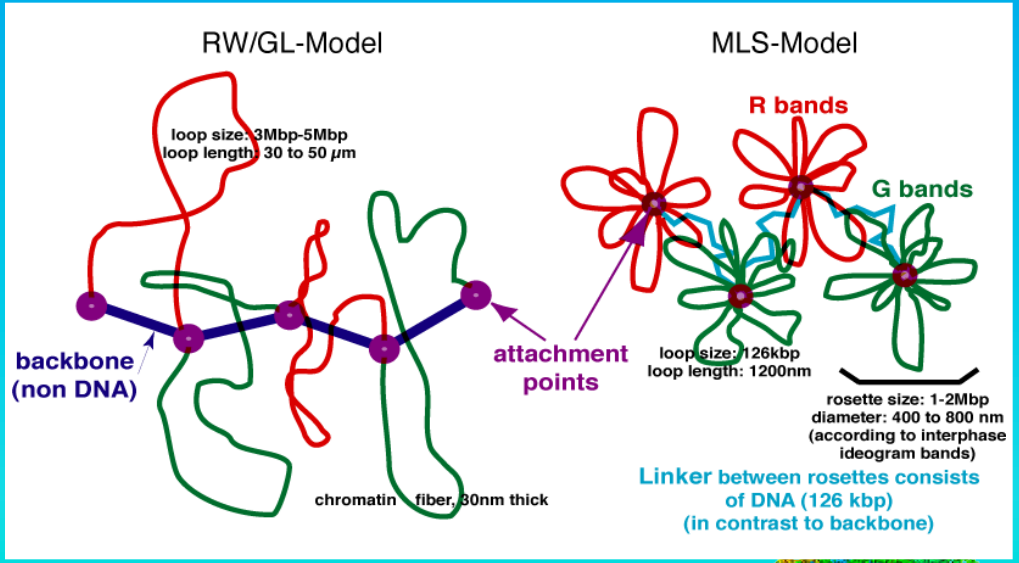


Integral Models of Cell Nuclear Organization

The biggest advantage of integral models is the again obvious and simple fact, that they allow the validation from the consistency of different levels of organization from the other levels. Thus, e.g. the so called Interchromosomal Domain Model can be ruled out by simple voluminous thought...



Random-Walk/Giant-Loop Multi-Loop-Subcompartment Model



A: courtesy K. Richter; B: courtesy K. Greulich-Bode

D: courtesy S. Dietzel; E: courtesy D. Zink

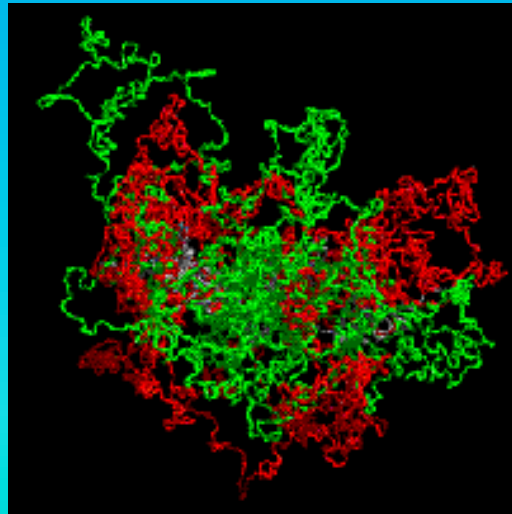
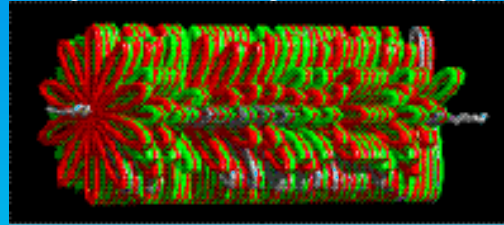
Simulation of Single Chromosomes

The 30 nm chromatin fiber is modeled as a polymer chain with stretching, bending, and excluded volume interactions. Monte Carlo and Brownian Dynamic methods lead to thermodynamical equilibrium configurations.

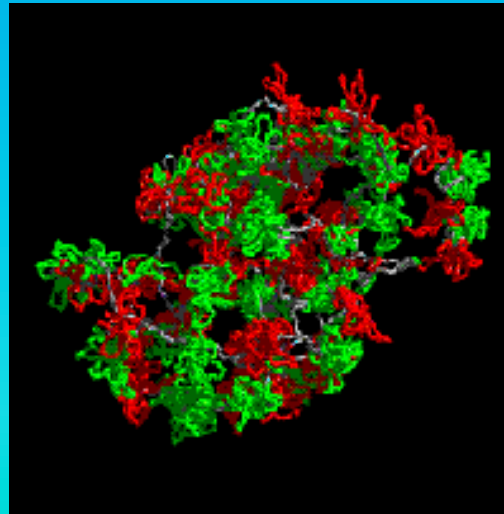
All models form chromosome territories with big voids and different chromatin morphologies. Experimental territory and subcompartment diameters agree best with an MLS model with 80 to 120 kbp loops and linkers.



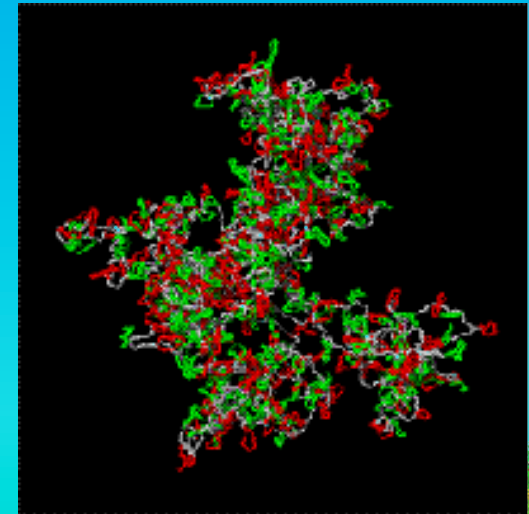
Metaphase starting configuration with ideogram bands in red/green, linker in grey.



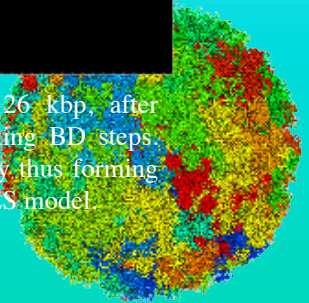
RW/GL model, loop size 5 Mbp, after ~80.000 MC and 1000 relaxing BD steps. Large loops intermingle freely and reach out of the chromosome territory, thus forming no distinct features like in MLS model.



MLS model, loop size 126kbp, linker size 126 kbp, after ~50.000 MC and 1000 relaxing BD steps. Here rosettes form subcompartments as separated organizational and dynamic entities.



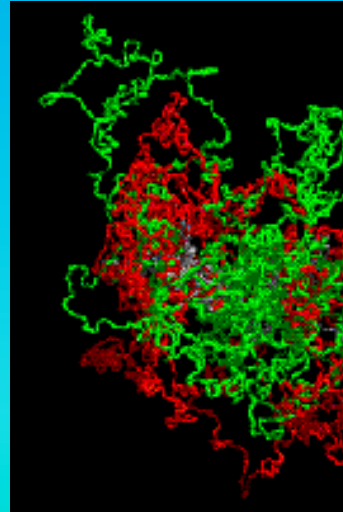
RW/GL model, loop size 126 kbp, after ~80.000 MC and 1000 relaxing BD steps. Large loops intermingle freely thus forming no distinct features like in MLS model.



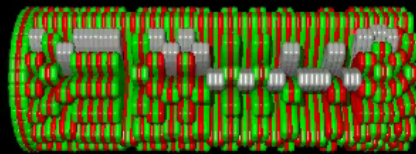
Simulation of Single Chromosomes

The 30 nm chromatin fiber is modeled as a polymer chain with stretching, bending, and excluded volume interactions. Monte Carlo and Brownian Dynamic methods lead to thermodynamical equilibrium configurations.

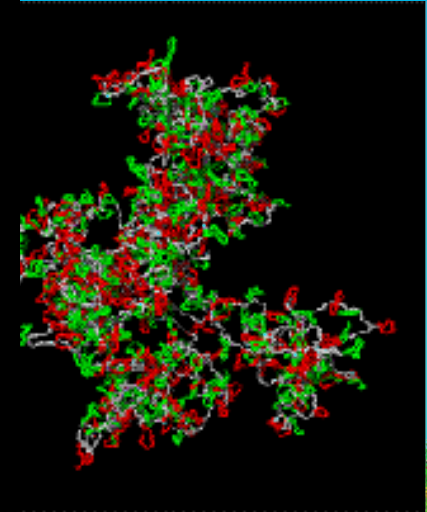
All models form chromosome territories with big voids and different chromatin morphologies. Experimental territory and subcompartment diameters agree best with an MLS model with 80 to 120 kbp loops and linkers.



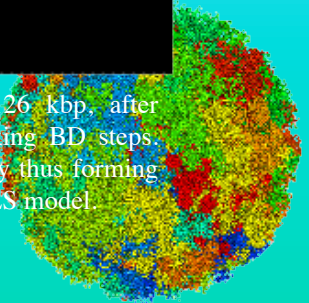
RW/GL model, loop size ~80.000 MC and 1000 relaxing BD steps. Large loops intermingle freely and reach out of the chromosome territory, thus forming no distinct features like in MLS model.



120 kbp, after ~30.000 MC and 1000 relaxing BD steps. Here rosettes form subcompartments as separated organizational and dynamic entities.



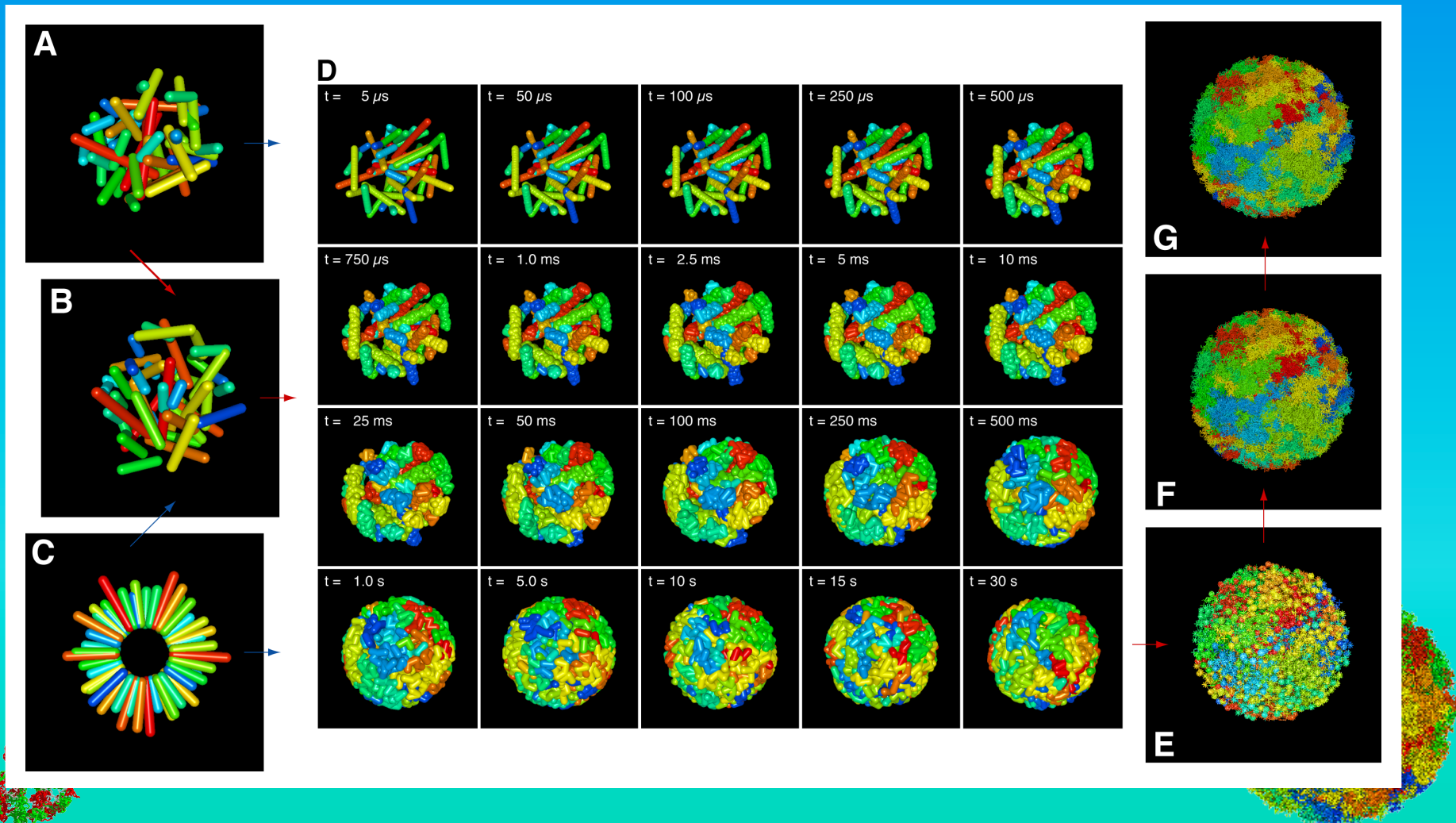
model, loop size 126 kbp, after ~80.000 MC and 1000 relaxing BD steps. Large loops intermingle freely thus forming no distinct features like in MLS model.



Simulation of Whole Nuclei with all 46 Chromosomes

Starting with some metaphase arrangement of cylindrical chromosomes, interphase nuclei with a 30 nm fiber resolution and at thermodynamical equilibrium are created in 4 steps using simulated annealing and Brownian Dynamics methods with stretching, bending, excluded volume and a spherical boundary interactions.

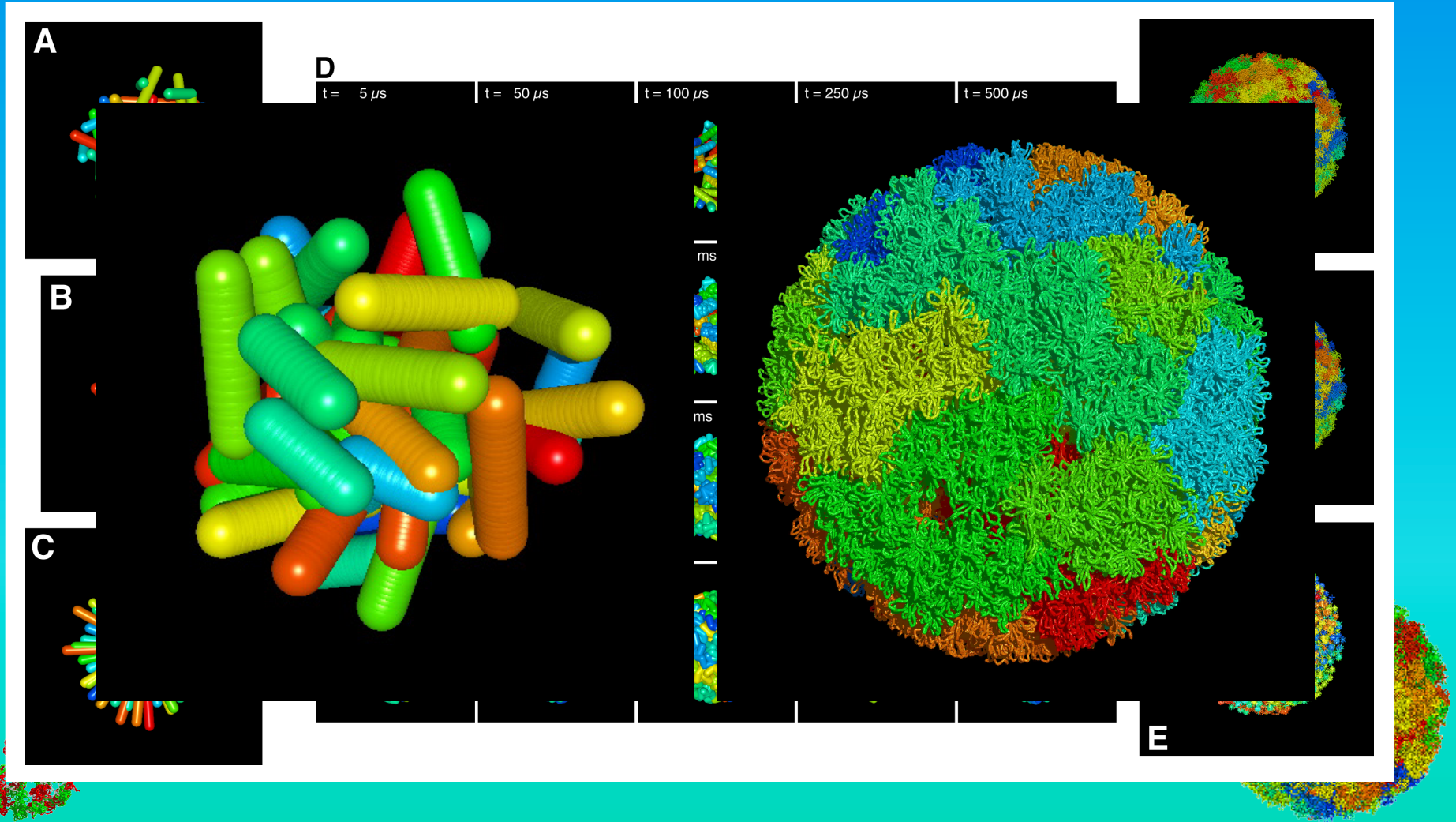
The chromosome territory position depends on their metaphase position and is reasonably stable.



Simulation of Whole Nuclei with all 46 Chromosomes

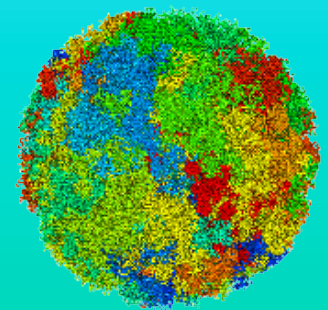
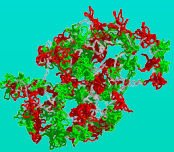
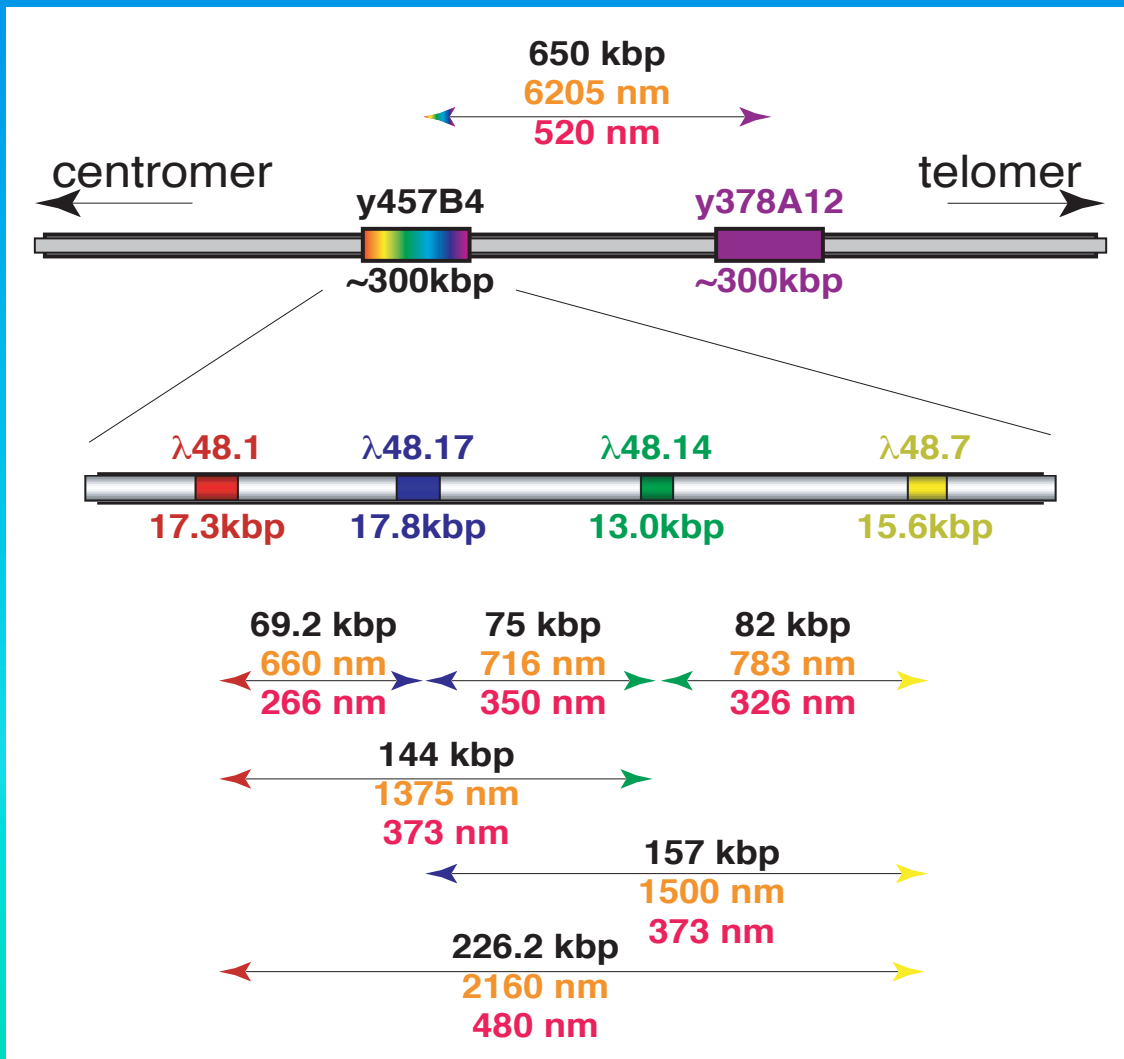
Starting with some metaphase arrangement of cylindrical chromosomes, interphase nuclei with a 30 nm fiber resolution and at thermodynamical equilibrium are created in 4 steps using simulated annealing and Brownian Dynamics methods with stretching, bending, excluded volume and a spherical boundary interactions.

The chromosome territory position depends on their metaphase position and is reasonably stable.



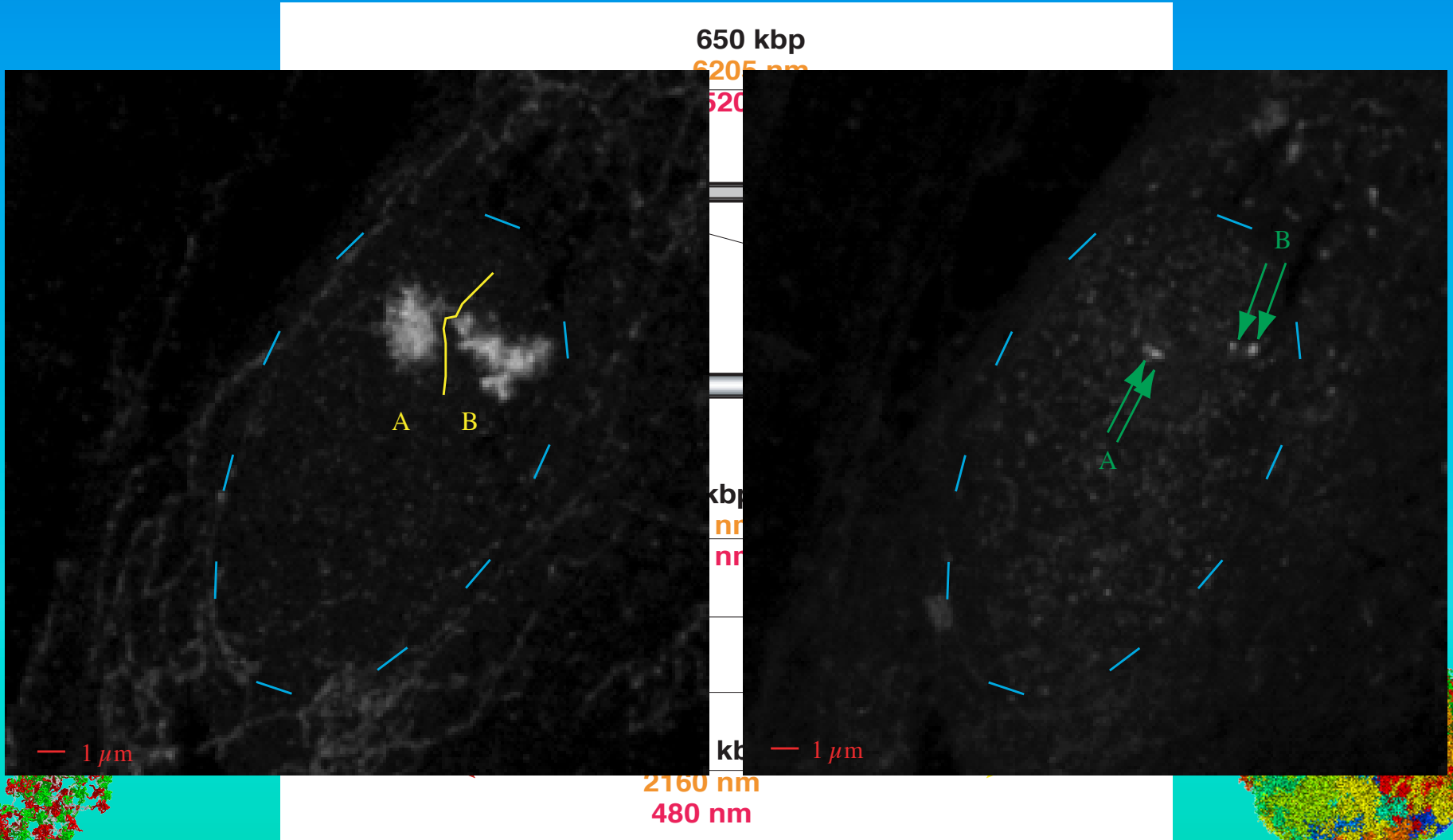
3D Architecture of the Prader-Willi Region

Fluorescence *in situ* hybridization with various protocols of small probes within the Prader-Willi region combined with spectral precision distance confocal laser scanning microscopy and comparison with large-scale computer simulations shows a Multi-Loop Subcompartment organization of the Prader-Willi region.



3D Architecture of the Prader-Willi Region

Fluorescence *in situ* hybridization with various protocols of small probes within the Prader-Willi region combined with spectral precision distance confocal laser scanning microscopy and comparison with large-scale computer simulations shows a Multi-Loop Subcompartment organization of the Prader-Willi region.



3D Architecture of the Prader-Willi Region

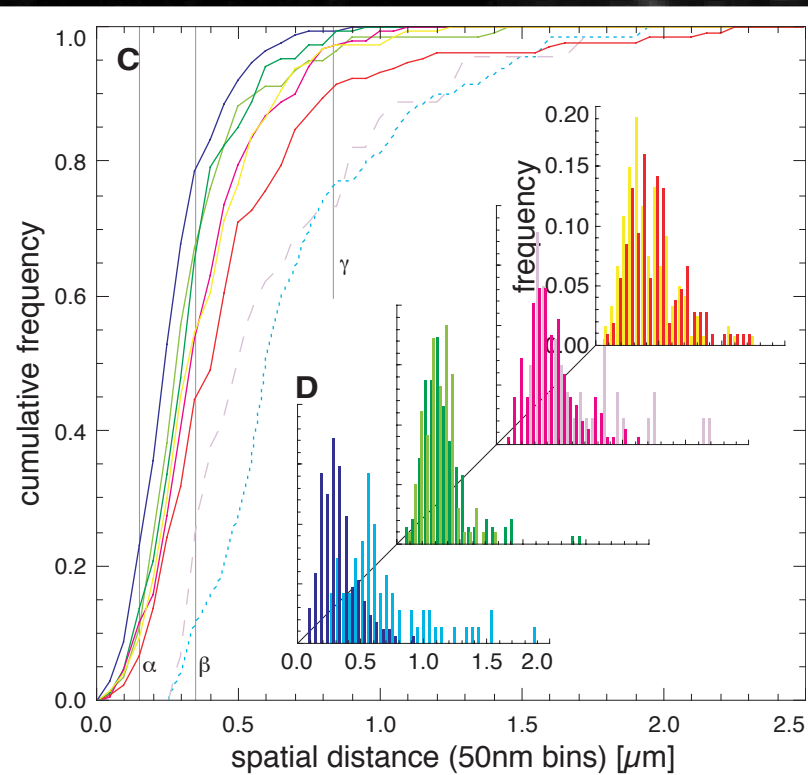
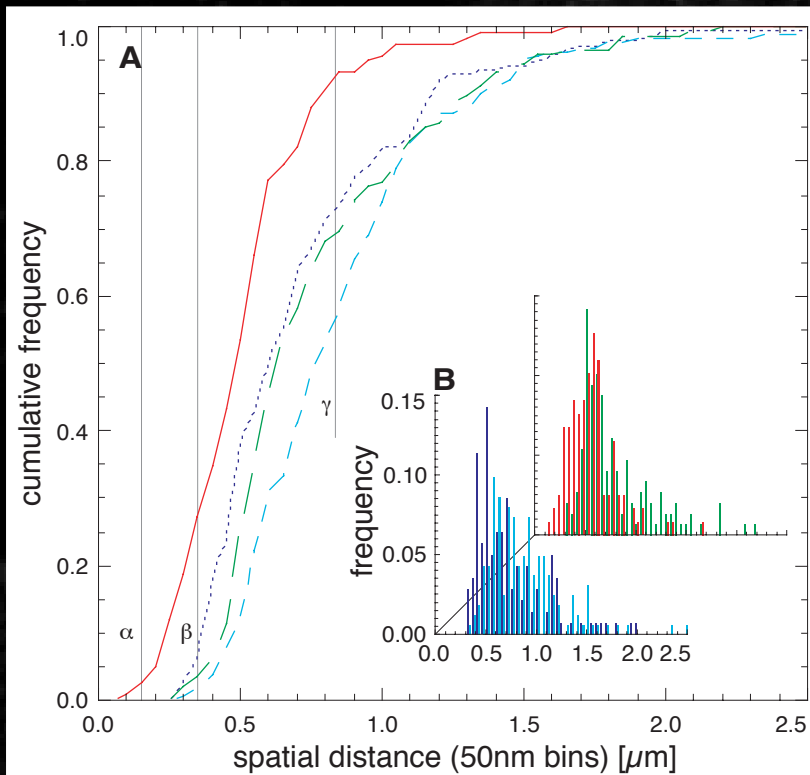
Fluorescence *in situ* hybridization with various protocols of small probes within the Prader-Willi region combined with spectral precision distance confocal laser scanning microscopy and comparison with large-scale computer simulations shows a Multi-Loop Subcompartment organization of the Prader-Willi region.



650 kbp

6205 nm

520



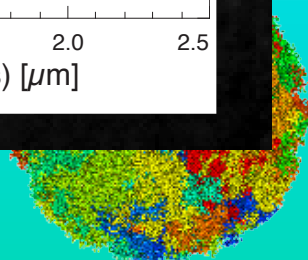
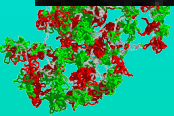
1 μm

KU

1 μm

2160 nm

480 nm



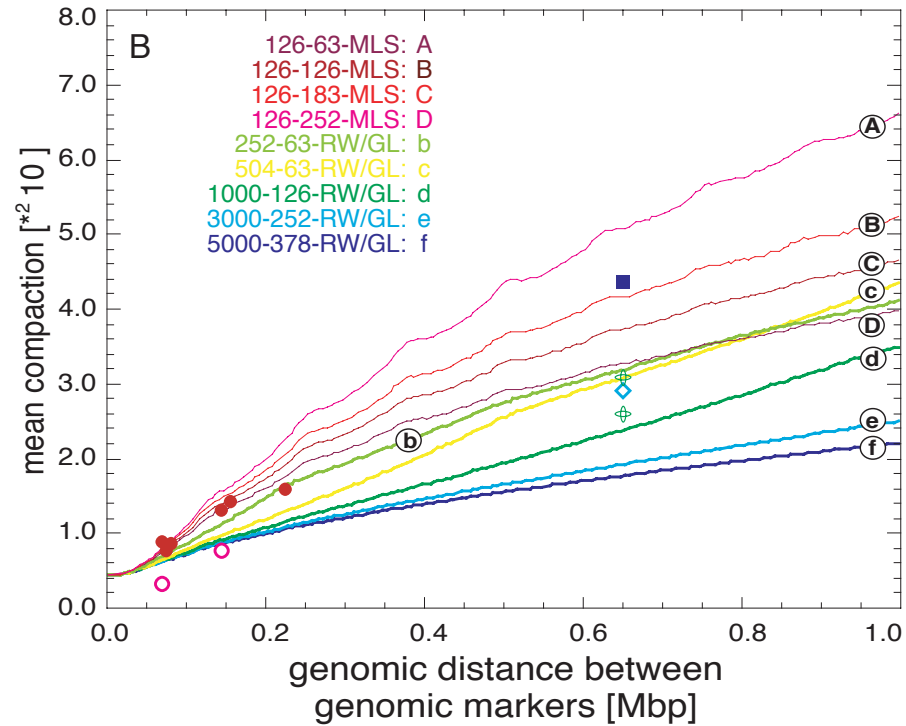
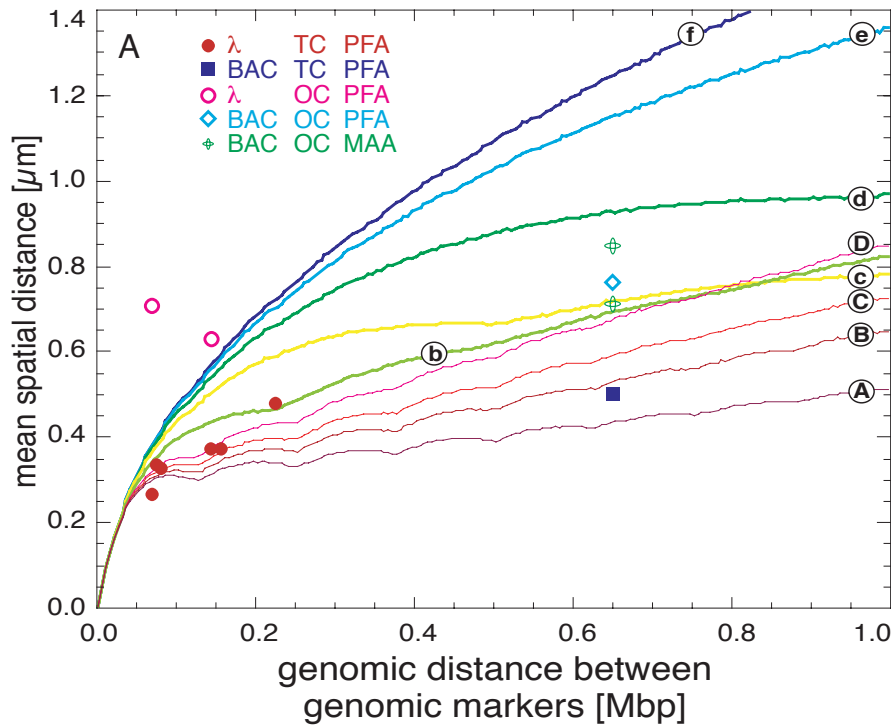
3D Architecture of the Prader-Willi Region

Fluorescence *in situ* hybridization with various protocols of small probes within the Prader-Willi region combined with spectral precision distance confocal laser scanning microscopy and comparison with large-scale computer simulations shows a Multi-Loop Subcompartment organization of the Prader-Willi region.



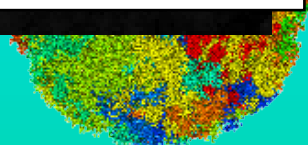
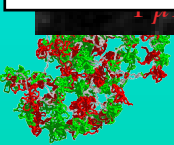
650 kbp

6205 nm



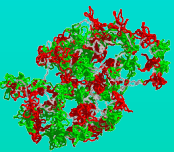
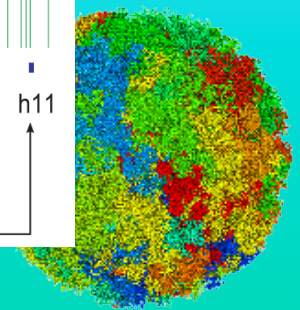
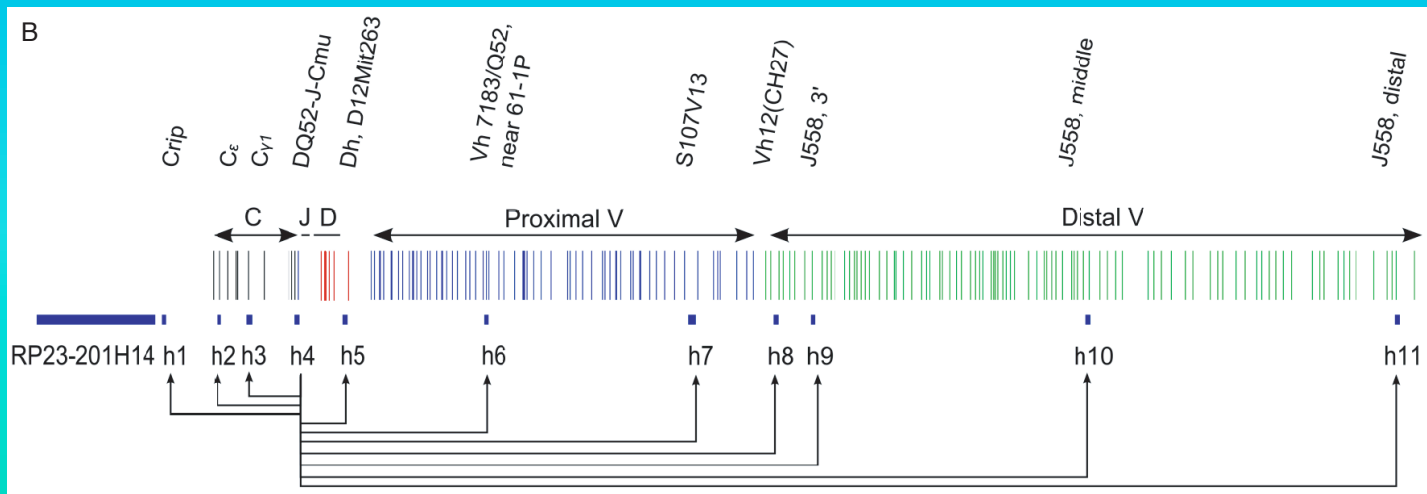
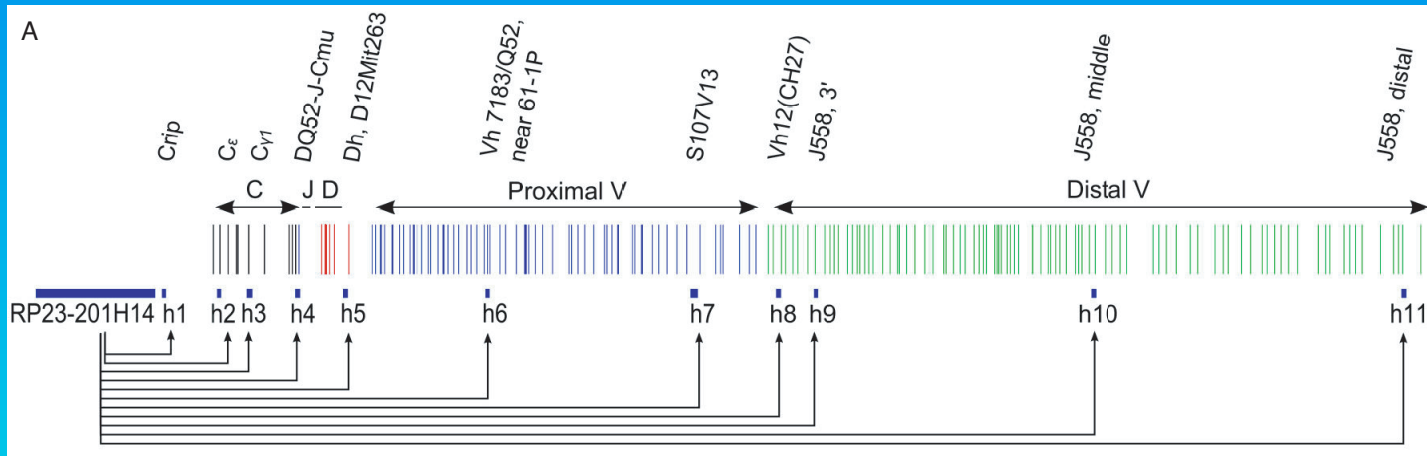
2160 nm

480 nm



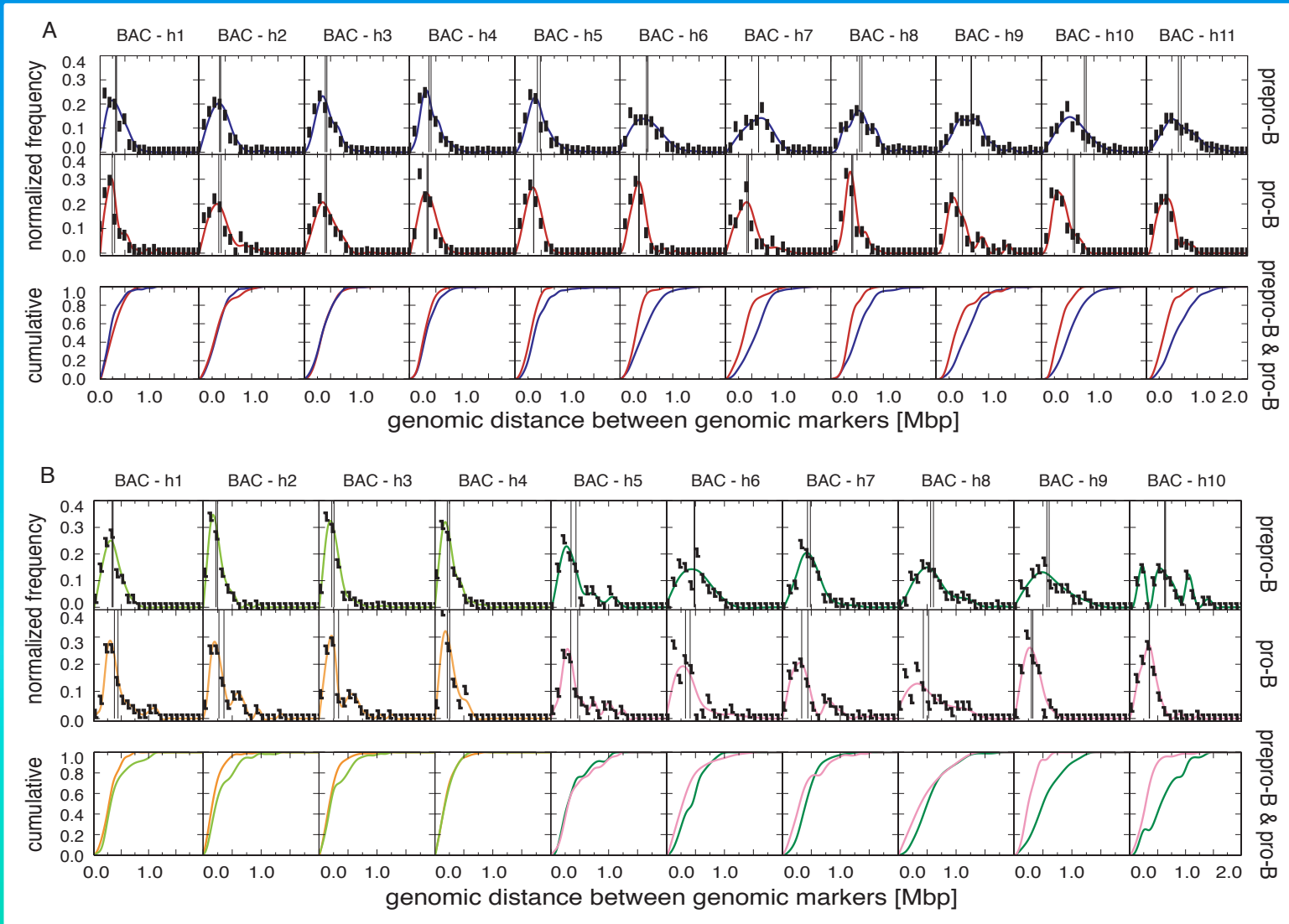
3D Architecture & Function of the IgH Locus

Fluorescence *in situ* hybridization of the IgH locus combined with spectral precision distance epifluorescence microscopy, analytical trilateration and comparison with computer simulations shows again a Multi-Loop Subcompartment organization of the IgH locus with functional relevant distances.



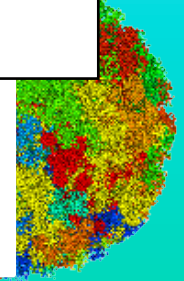
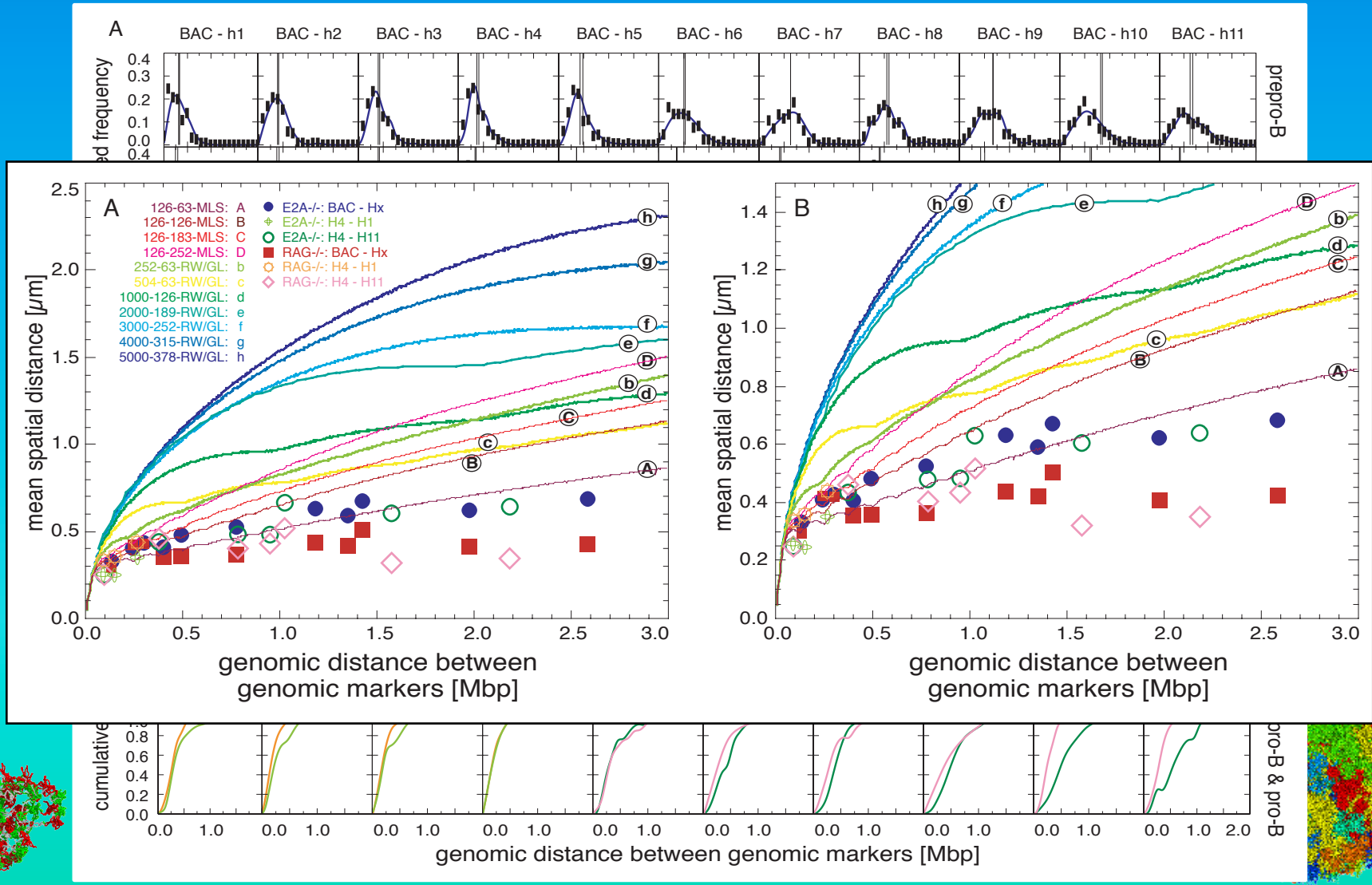
3D Architecture & Function of the IgH Locus

Fluorescence *in situ* hybridization of the IgH locus combined with spectral precision distance epifluorescence microscopy, analytical trilateration and comparison with computer simulations shows again a Multi-Loop Subcompartment organization of the IgH locus with functional relevant distances.



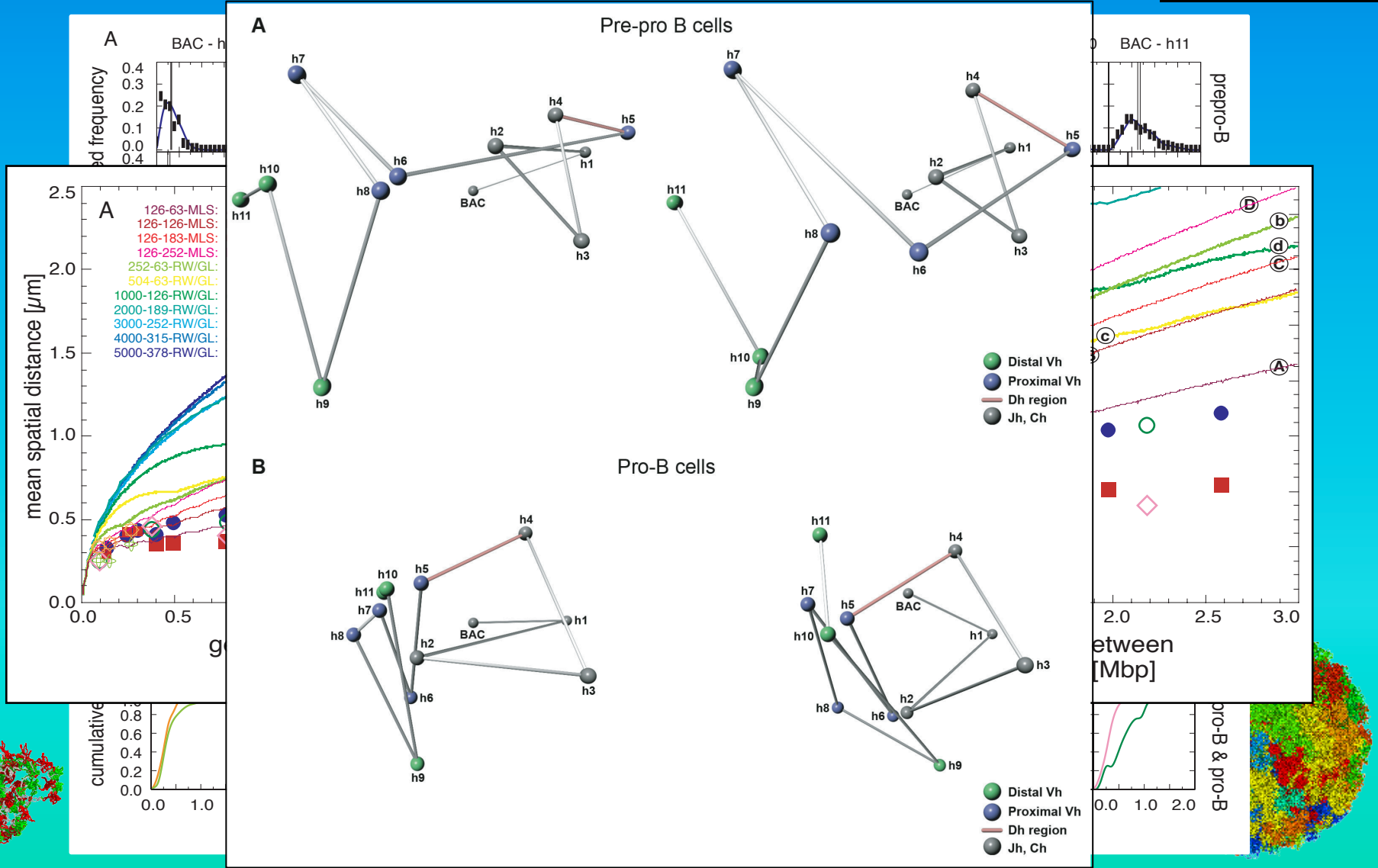
3D Architecture & Function of the IgH Locus

Fluorescence *in situ* hybridization of the IgH locus combined with spectral precision distance epifluorescence microscopy, analytical trilateration and comparison with computer simulations shows again a Multi-Loop Subcompartment organization of the IgH locus with functional relevant distances.



3D Architecture & Function of the IgH Locus

Fluorescence *in situ* hybridization of the IgH locus combined with spectral precision distance epifluorescence microscopy, analytical trilateration and comparison with computer simulations shows again a Multi-Loop Subcompartment organization of the IgH locus with functional relevant distances.



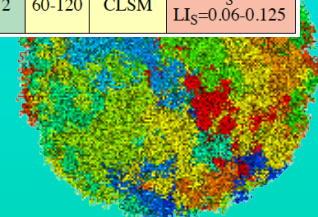
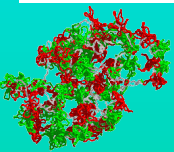
“Synoptic” 3D Architecture of Various Loci

A history “synoptic” comparison of the spatial distance mapping from their original background and aim, FISH methodological protocols, via microscopic imaging and restoration analysis procedures, to their interpretation, reveals that with time Multi-Loop Subcompartment models are favoured.



Study	Location	Preparation of Cells			FISH			Microscopy		Fit to model
		Cell cycle	KCl [nM]	Fixative	Melting	Label	Colours	# of nuclei	Image acquisition	
Fig. 3B, Trask '89	DHFR	UA41 G1-cf	75 dropped	MAA 3:1	FM 50 %	Biotin	1	20-37	photo, wall	RWGL 0.08-J RWGL 1.0
Fig. 3B, Lawrence '90	Dystrophin	WI38F G1	75 dropped	MAA 3:1	FM 50 %	Biotin	1	20-60	photo, wall	RWGL 0.5-1
Fig. 3A, Trask '91	Xq28	F G1-cf	75 dropped	MAA 3:1	FM 50 %	Biotin	1	30-60	photo, wall	RWGL 0.7 J RWGL 2.0- >5.0
Fig. 3B, Trask '91	Xq28	F G1-cf	75 dropped	MAA 3:1	FM 50 %	Biotin Dig	2	30-60	photo, wall	RWGL 1.0-3.0
Fig. 3, v.d. Engh '92 or Fig. 5A, Trask '93	4p16.3	F G1-cf	75 dropped	MAA 3:1	FM 50 %	Biotin Dig	2	?	photo, d-board	$L_S \leq 0.1$ for $GS < 0.5 <$ $RWGL > 5.0$
Fig. 5B, Trask '93	6p21	F G1-cf	75	MAA 3:1	FM 50-70 %	Biotin Dig	2	?	photo, d-board	$L_S \leq 0.1$ for $GS < 1.0 <$ $RWGL 1.0-5.0$
Fig. 5, Senger '93	MHC 6p21.31	HFF G1-cf	?	?	FM 50 %	Biotin	1	> 30	photo, wall	$MLS L_S \& LI_S =$ $0.12-0.25$ $RWGL 0.1-0.5$
Fig. 5, Senger '93	MHC 6p21.31	HFF G1-cf	?	?	FM 50 %	Biotin Dig	2	> 30	photo, wall	$MLS L_S = 0.1$ $LI_S = 0.18$ $RWGL 0.1-0.5$
Fig. 1, Warrington '94	4p16.3	F G1-cf	75	MAA 3:1	FM 50 %	Biotin Dig	2	?	?	$RWGL > 5.0$
Tab. 1, Warrington '94	5q31-33	L	?	?	?	?	?	?	CLSM BioRad	$RWGL > 5.0$
Fig. 2B, Yokota '95	4p16.3	F G1-cf	40 dropped	MAA 3:1	FM 70 %	Biotin Dig	2	40-360	photo, d-board	$RWGL 2.0-4.0$
Fig. 3B, Yokota '95	4p16.3	F G1-cf	-	PFA 4 %	FM 70 %	Biotin Dig	2	40-350	photo, d-board	$MLS L_S \& LI_S =$ $0.1-0.125$

Study	Location	Preparation of Cells			FISH			Microscopy		Fit to model
		Cell cycle	KCl [nM]	Fixative	Melting	Label	Colours	# of nuclei	Image acquisition	
Fig. 2A, Yokota '97	4p16.3 R-band	F G1-cf	40 dropped	MAA 3:1	FM 70 %	Biotin Dig	2	37-178	photo, d-board	$RWGL 2.0-3.0$
Fig. 2B, Yokota '97	6p21.3 R-band	F G1-o	40 dropped	MAA 3:1	FM 70 %	Biotin Dig	2	37-178	photo, d-board	$RWGL 4.0-5.0$
Fig. 2C, Yokota '97	21q22.2 G-band	F G1-o	40 dropped	MAA 3:1	FM 70 %	Biotin Dig	2	37-178	photo, d-board	$RWGL 1.0-2.0$
Fig. 2D, Yokota '97	Xp21.3 G-band	F G1-o	40 dropped	MAA 3:1	FM 70 %	Biotin Dig	2	37-178	photo, d-board	$RWGL 0.5-0.9$
Fig. 2D, Yokota '97	Xq28 R-band	F G1-of	40 dropped	MAA 3:1	FM 70 %	Biotin Dig	2	37-178	photo, d-board	$RWGL 1.0-5.0j$
Fig. 2A, Yokota '97	Xp21.3 G-band	F	-	PFA 4 %	FM 70 %	Biotin Dig	2	37-178	photo, d-board	$RWGL 0.25$ $MLS L_S = 0.126$ $LI_S = 0.200$
Fig. 2A, Yokota '97	Xq28 R-band	F	-	PFA 4 %	FM 70 %	Biotin Dig	2	37-178	photo, d-board	$RWGL 1.0$
Fig. 4B, Yokota '97	Xp21.3 G-band	HeLa	40 dropped	MAA 3:1	FM 70 %	Biotin Dig	2	37-178	photo, d-board	$RWGL 0.25$ $MLS L_S = 0.126$ $LI_S = 0.200$
Fig. 4B, Yokota '97	Xq28 R-band	HeLa	40 dropped	MAA 3:1	FM 70 %	Biotin Dig	2	37-178	photo, d-board	$RWGL 1.0$
Monier '97	11q13	F	-	PFA 4 %	FM 70 %	Biotin Dig	1	22-69	CLSM	$MLS L_S = 0.126$ $LI_S = 180$
Monier '97	11q13	L	-	PFA 4 %	FM 70 %	Biotin Dig	1	22-69	CLSM	$MLS L_S = 0.1$ $LI_S = 0.18-0.24$
Knoch '98/ Rauch '99	15q11-21	F	-	PFA 4 %	FM 70 %	Biotin Dig	1 & 2	60-120	CLSM	$MLS L_S = 0.1$ $LI_S = 0.06-0.125$

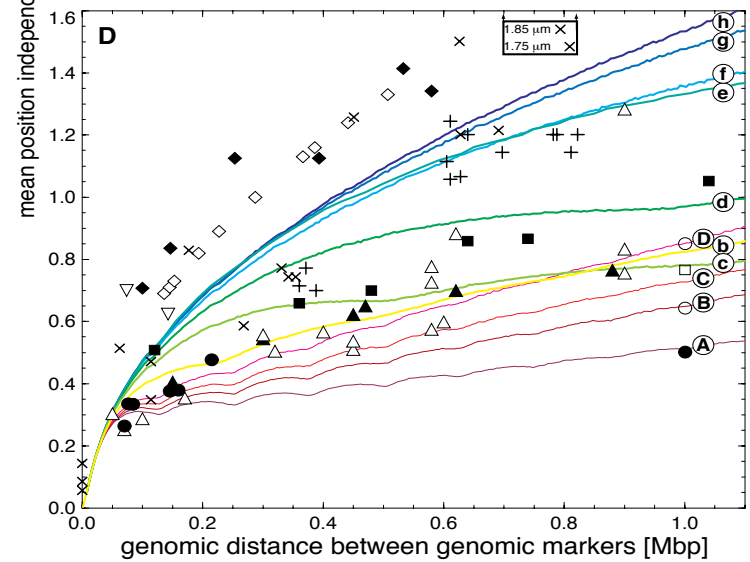
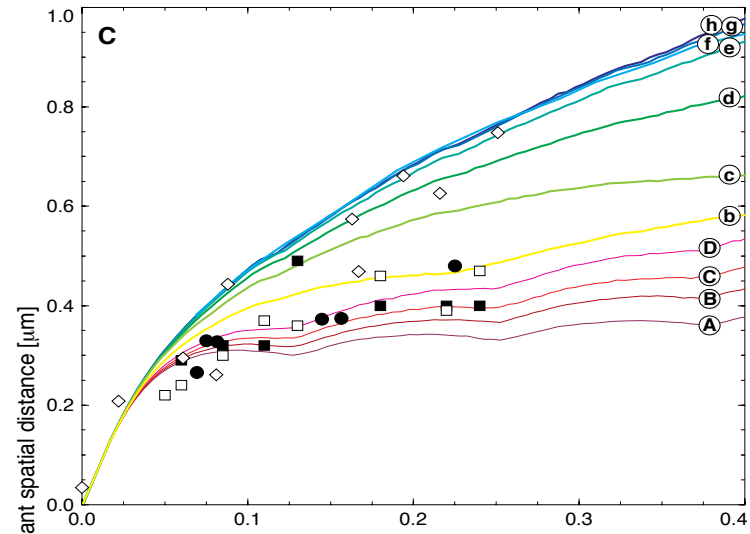
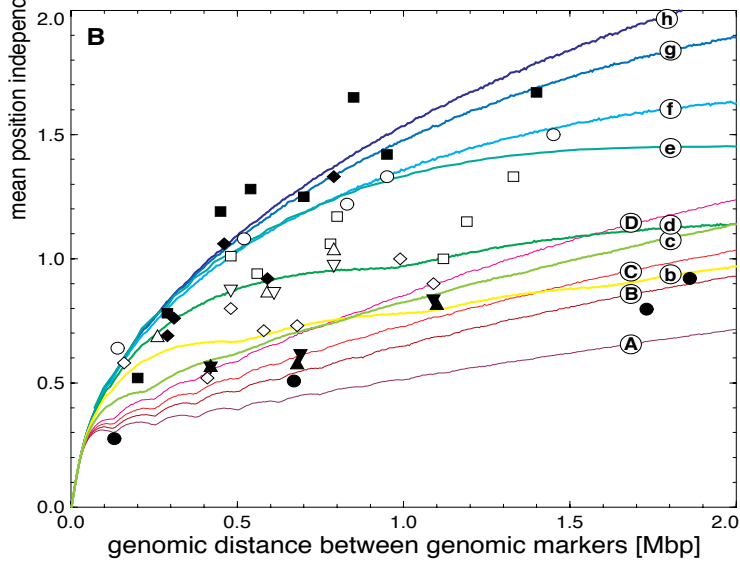
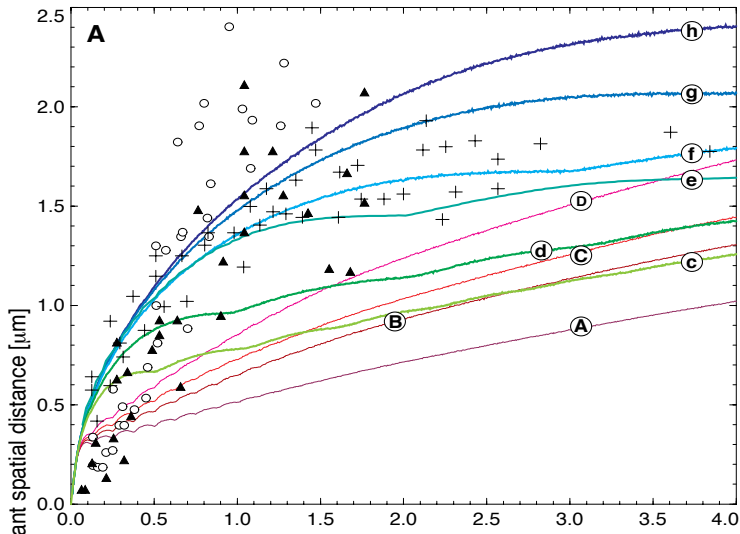


“Synoptic” 3D Architecture of Various Loci

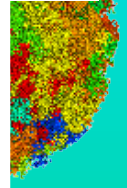
A history “synoptic” comparison of the spatial distance mapping from their original background and aim, FISH methodological protocols, via microscopic imaging and restoration analysis procedures, to their interpretation, reveals that with time Multi-Loop Subcompartment models are favoured.



Study
Fig. 3B, Trask '89
Fig. 3B, Lawrence '91
Fig. 3A, Trask '91
Fig. 3B, Trask '91
Fig. 3, v.d. Trask '93
Fig. 5B, Trask '93
Fig. 5, Senger '93
Fig. 5, Senger '93
Fig. 1, Warrington
Tab. 1, Warrington
Fig. 2B, Ye '95
Fig. 3B, Ye '95

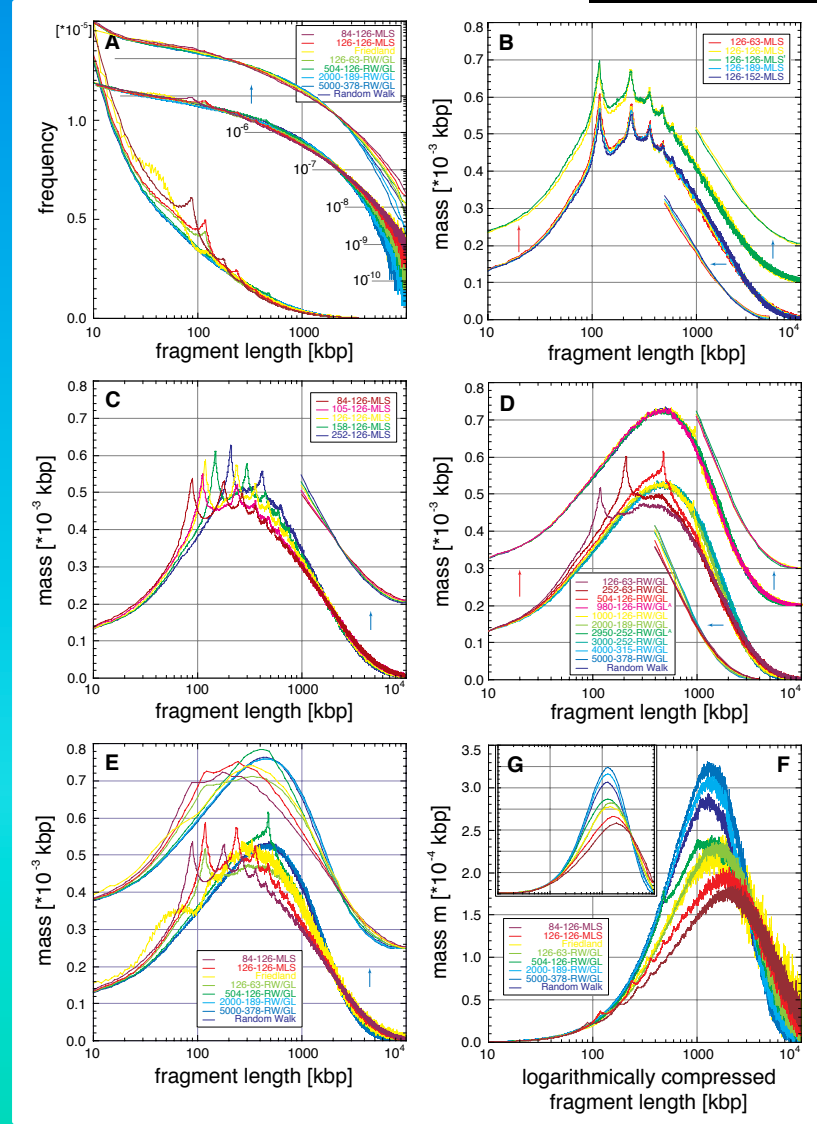
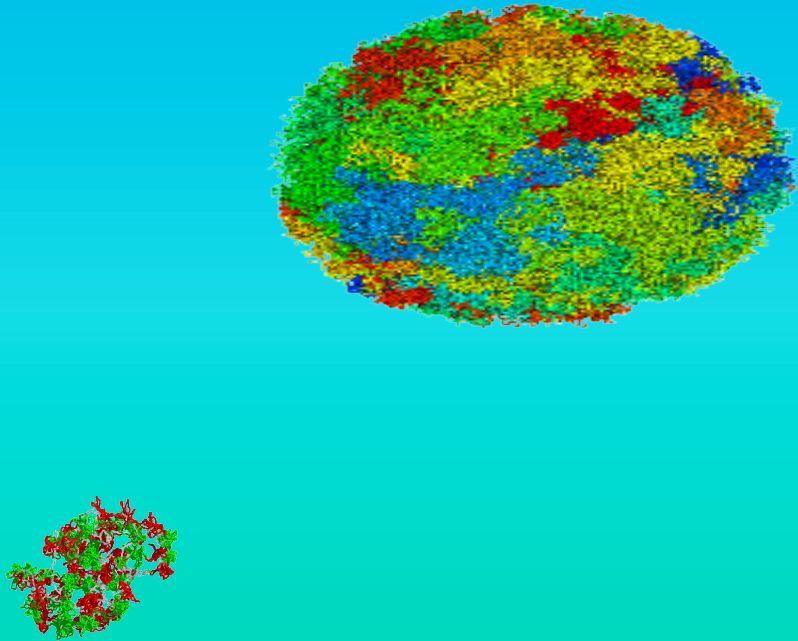


to model
L 2.0-3.0
L 4.0-5.0
L 1.0-2.0
L 0.5-0.9
L 1.0-5.0j
L 0.25 L _S =-0.126 0.200
L 1.0
L 0.25 L _S =-0.126 0.200
L 1.0
L _S =-0.126 180
L _S =-0.1 0.18-0.24
L _S =-0.1 0.06-0.125



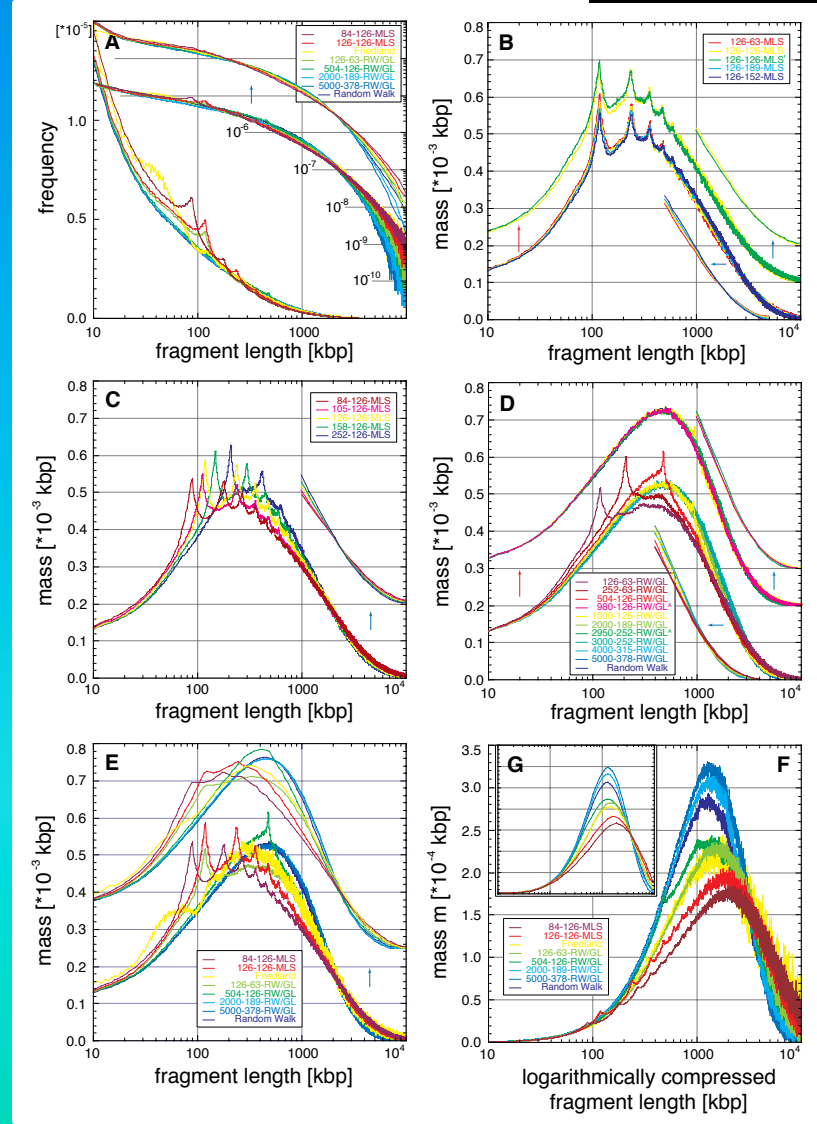
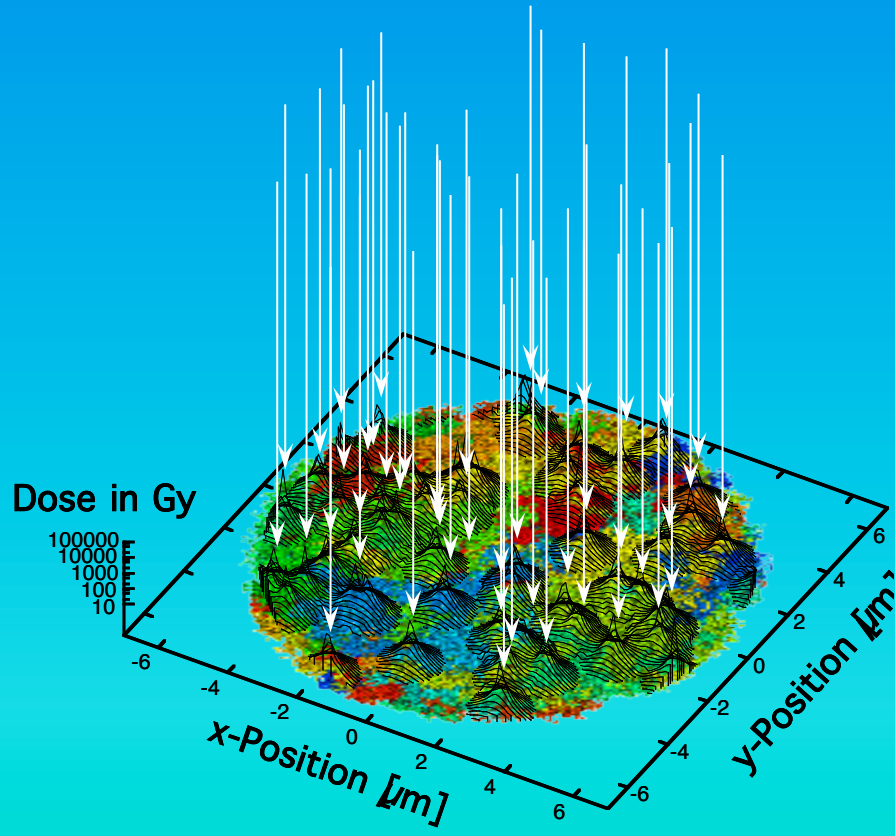
DNA Fragment Distribution after Ione-Irradiation

The length distribution of DNA fragments after irradiation with e. g. C or Ca with an inhomogeneous spatial double strand breakage probability depends on the detailed folding topology of the chromatin fiber and the RW/GL and MLS models differ largely.



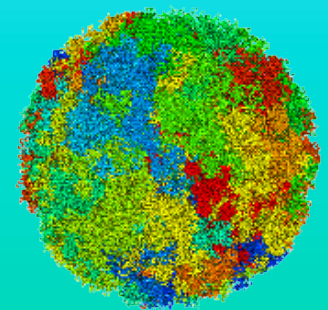
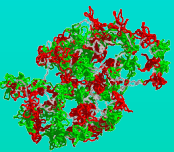
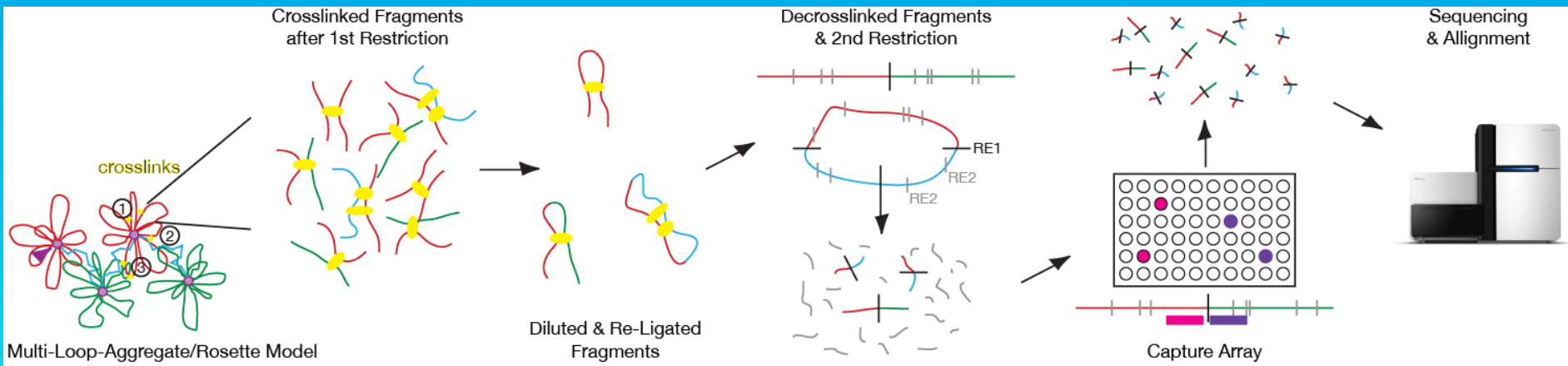
DNA Fragment Distribution after Ione-Irradiation

The length distribution of DNA fragments after irradiation with e. g. C or Ca with an inhomogeneous spatial double strand breakage probability depends on the detailed folding topology of the chromatin fiber and the RW/GL and MLS models differ largely.



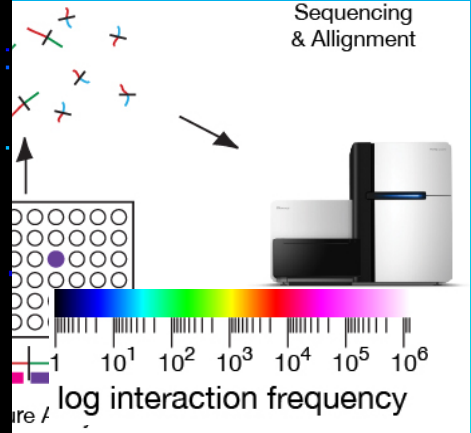
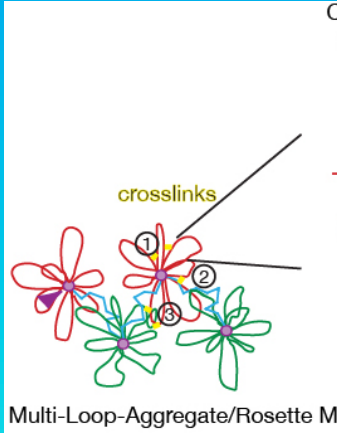
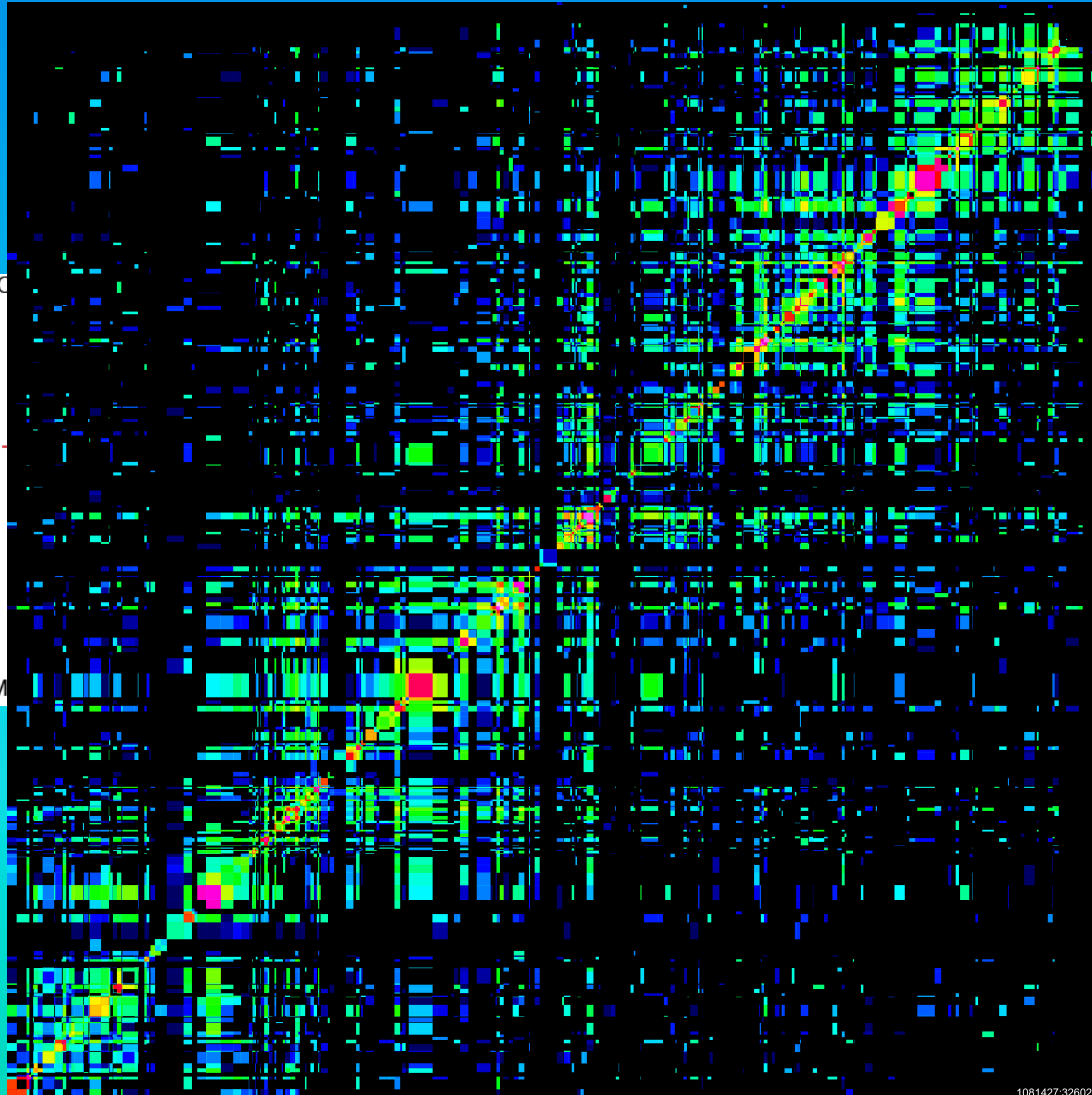
Selective Chromosome Interaction Capture (T2C)

T2C is a novel selective high-resolution high-throughput chromosome interaction capture, in which the relation between, region size, resolution, interaction frequency range, and sequencing depth can be designed towards the goal of the experiment. T2C reaches the limit of the “genomic” uncertainty principle and statistical mechanics.

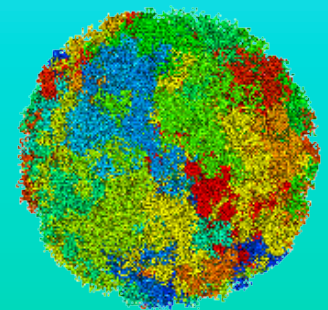


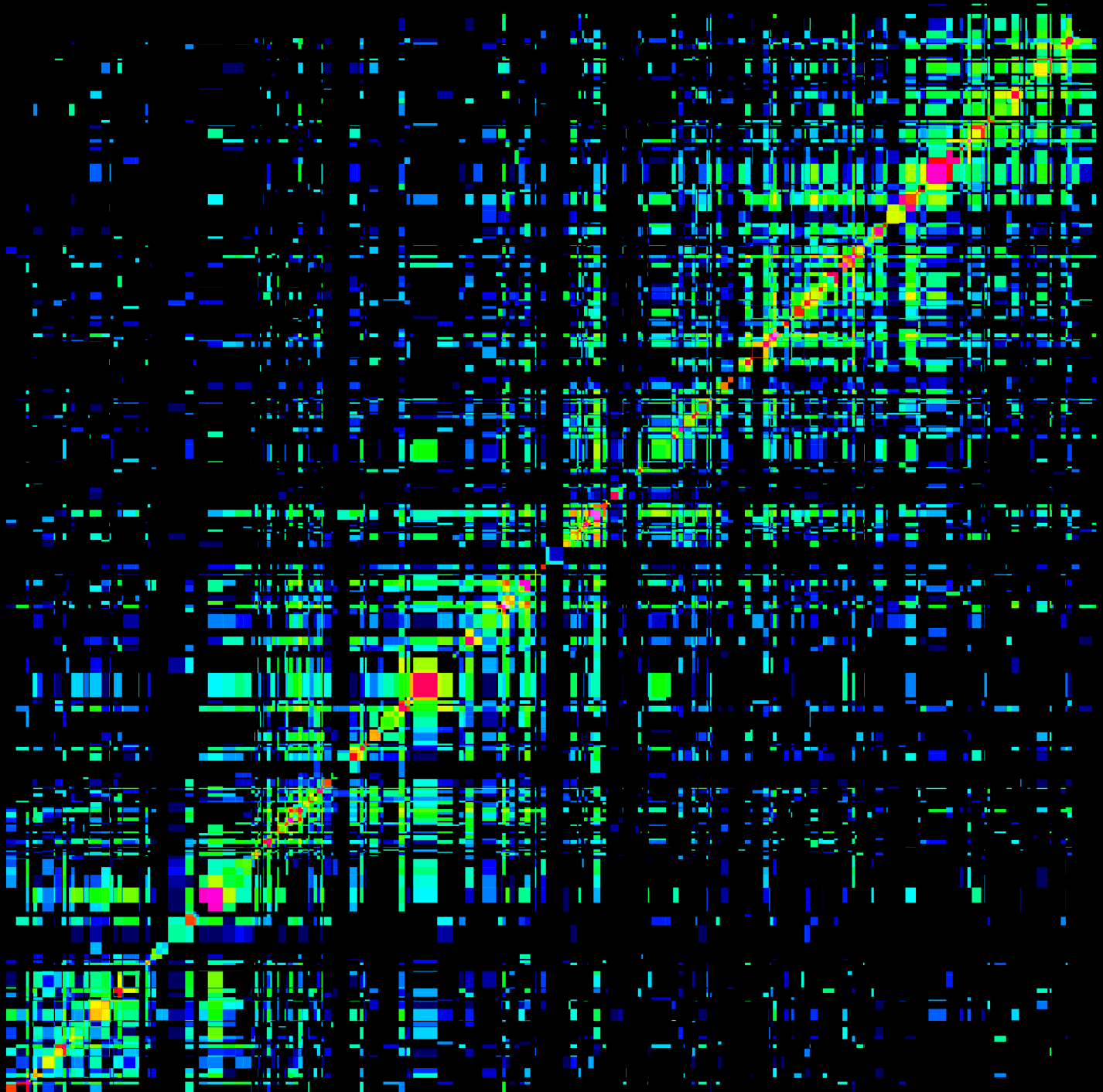
Selective Chromosome Interaction Capture (T2C)

T2C is a novel selective high-resolution high-throughput chromosome interaction capture, in which the relation between, region size, resolution, interaction frequency range, and sequencing depth can be designed towards the goal of the experiment. T2C reaches the limit of the “genomic” uncertainty principle and statistical mechanics.



HS IGF locus
~2.1 Mbp



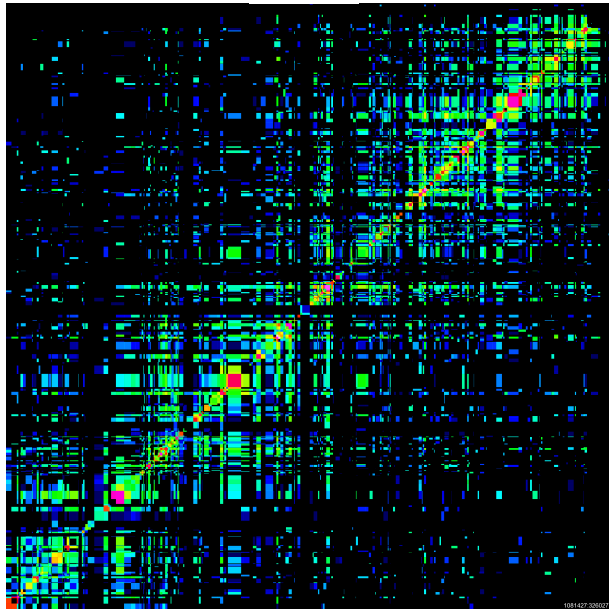


Stable Consensus Architecture of Genomes

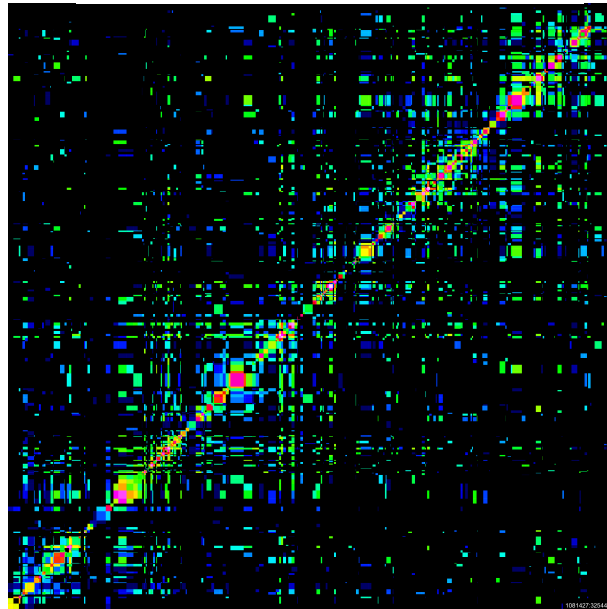
Due to the high signal-to-noise ratio of T2C reaching 5-6 orders of magnitude interaction maps reveal definitely an extremely high degree of similarity between different species, cell types, or functional states, thus functional differences are variation of a stable theme persisting through the cell cycle



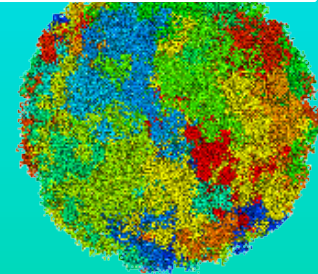
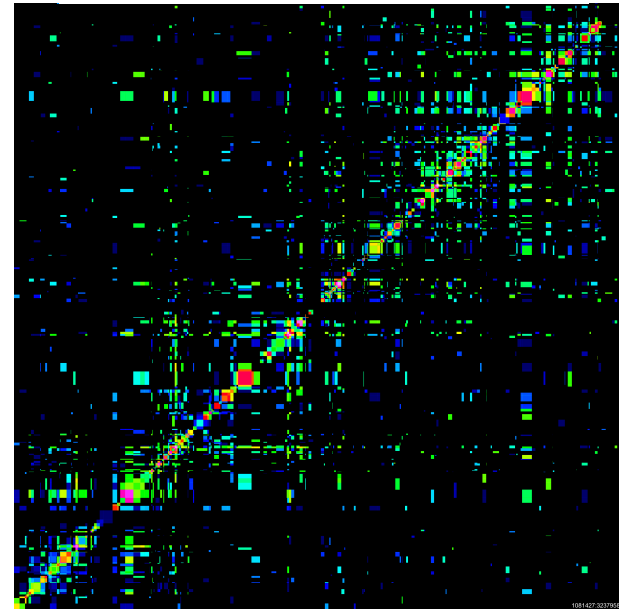
HB2



TEV-HEK293T cohesin intact



HRV-HEK293T cohesin cleaved

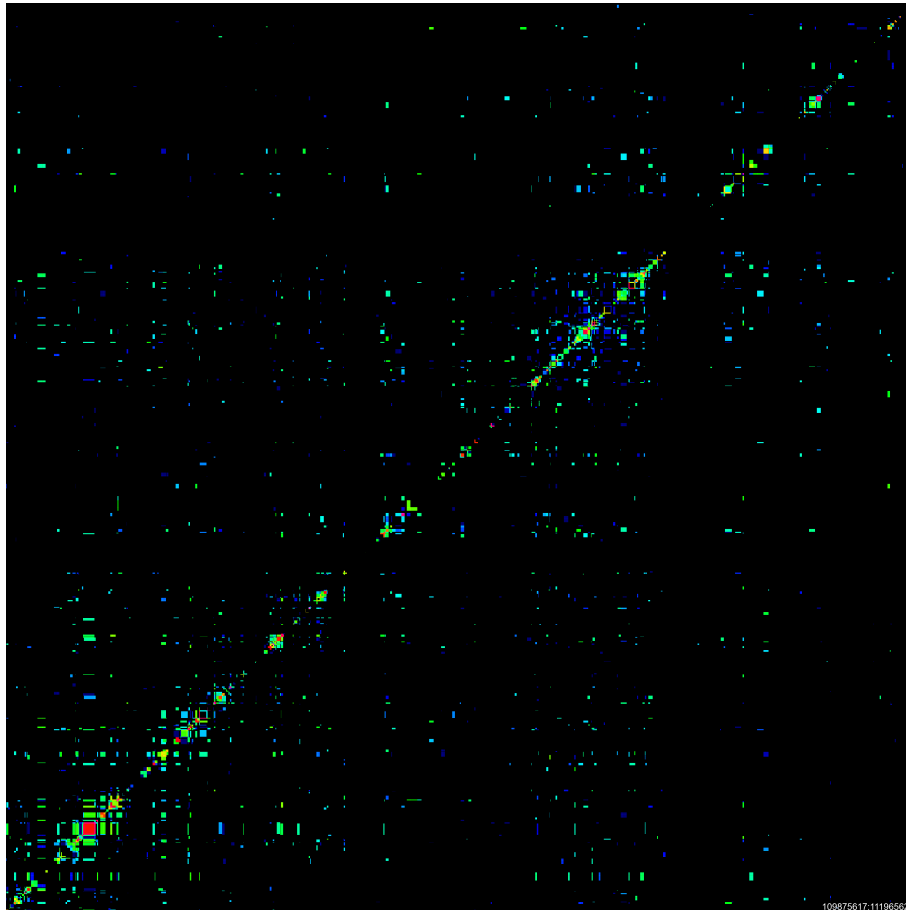


Stable Consensus Architecture of Genomes

Due to the high signal-to-noise ratio of T2C reaching 5-6 orders of magnitude interaction maps reveal definitely an extremely high degree of similarity between different species, cell types, or functional states, thus functional differences are variation of a stable theme persisting through the cell cycle

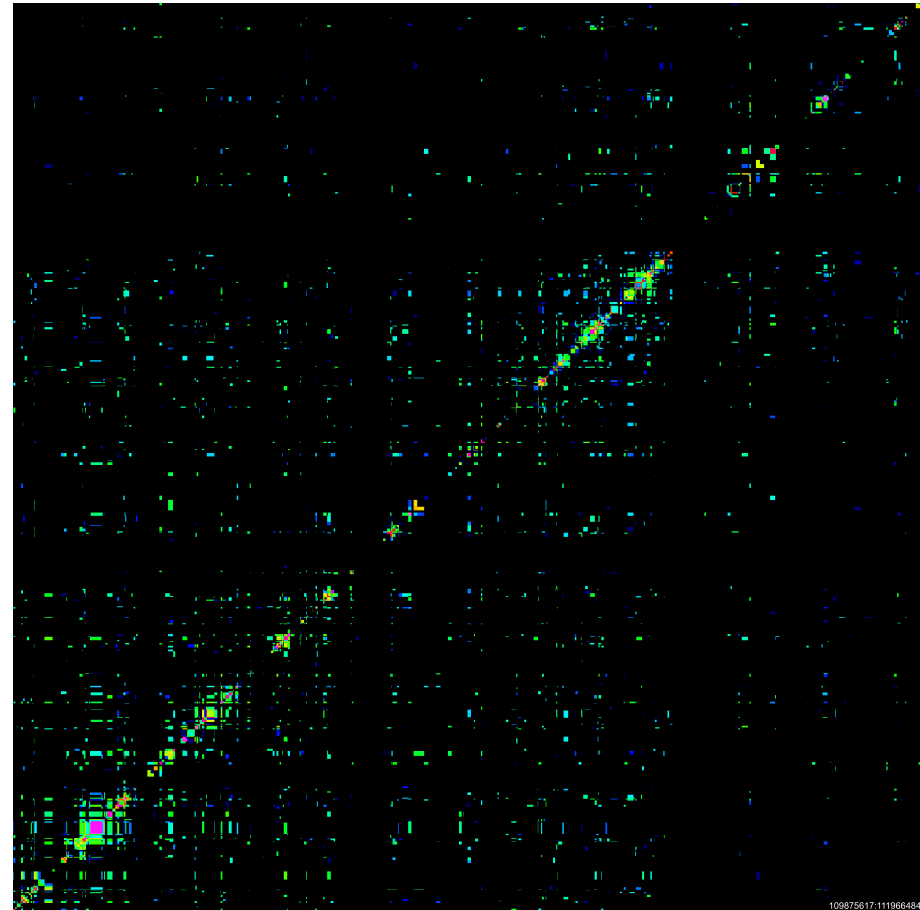


Fetal Brain (inactive β -Globin)



109875617:111965624

Fetal Liver (active β -Globin)



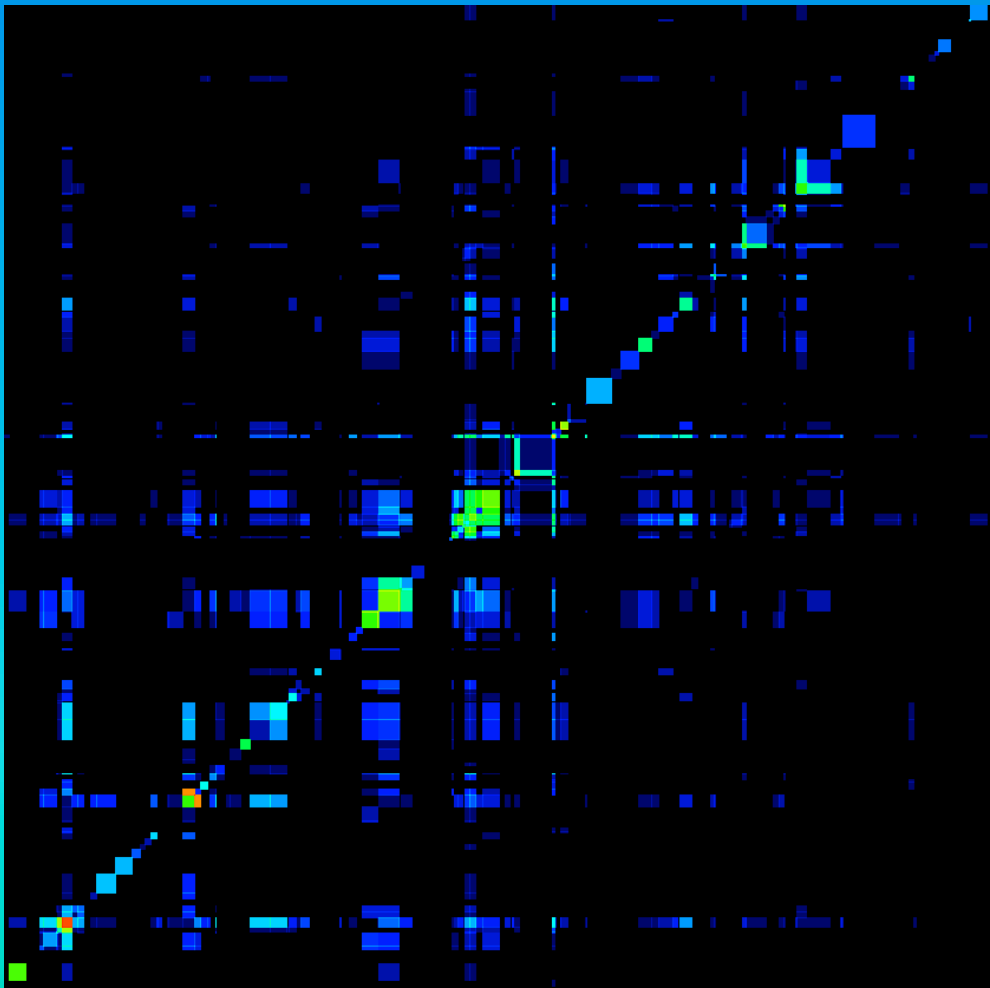
109875617:111966484

MM β -Globin 2.1 Mbp

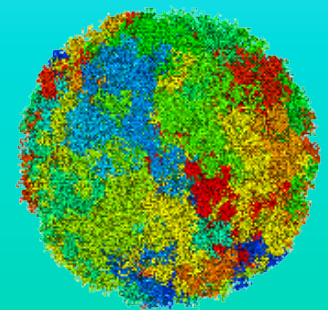
Fine Structure of Loop Aggregates/Rosettes

Depending on the resolution, the loops within a domain and their arrangement in loop aggregates/rosettes can be shown as well as the details of how the loops are organized at their base as well as their aggregated rosette core: parallel loop fibres exist at the loop base with ~6kbp and these form the core.

A collage of logos and diagrams. At the top left is the logo for 'Bundesministerium für Bildung und Forschung'. To its right is 'N7/O' with the text 'Nucleosome Organization and Chromatin Dynamics'. Further right is 'BBRC'. Below these are the 'European Commission' logo and 'Erasmus MC' logo. In the center is a circular diagram with 'ExGenSys' and 'Chromatin' text, and 'Structure - Function' at the bottom. To the right of this is 'Erasmus MC' and 'University of Hamburg'. At the bottom are logos for 'UNIVERSITY OF OXFORD', 'dkfz', 'Fachhochschule', and 'U'. There is also a small diagram of a loop structure.

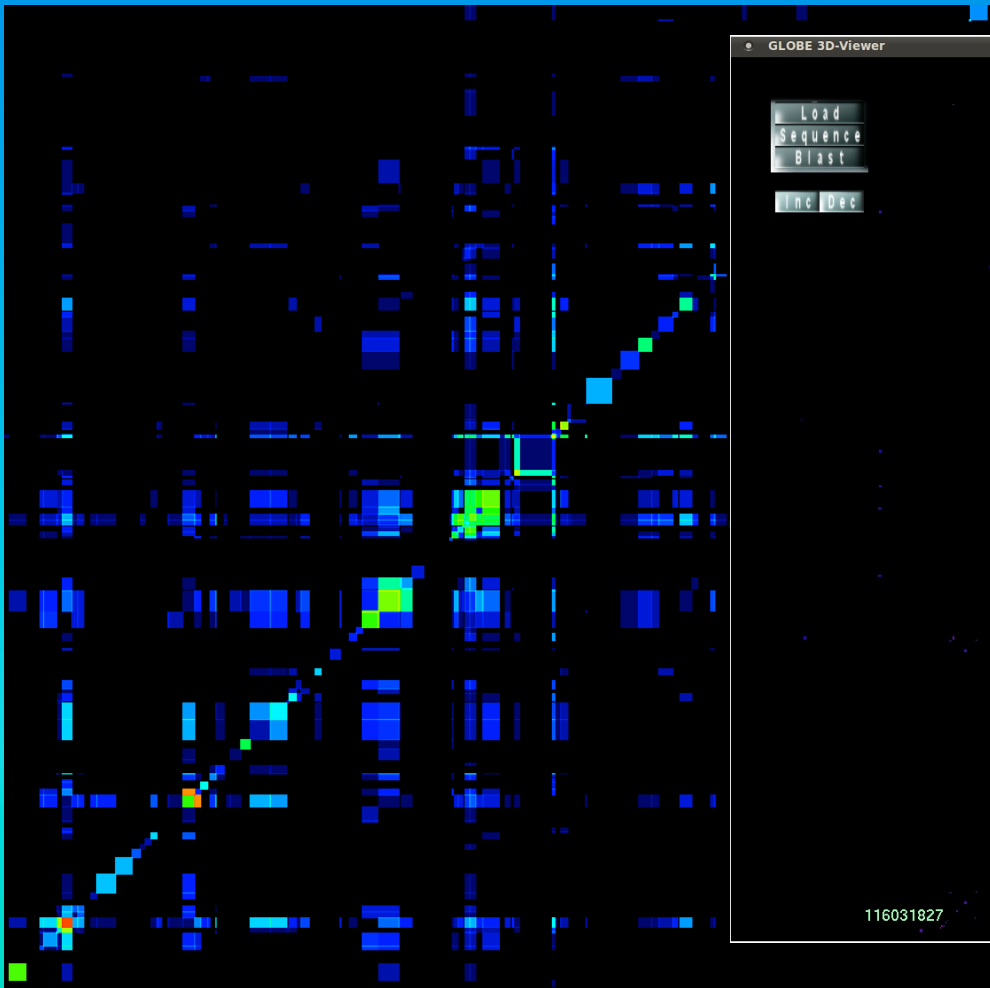


~ 400 kbp

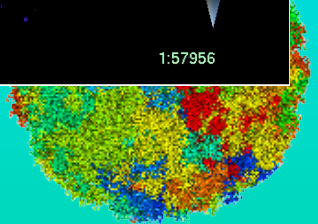
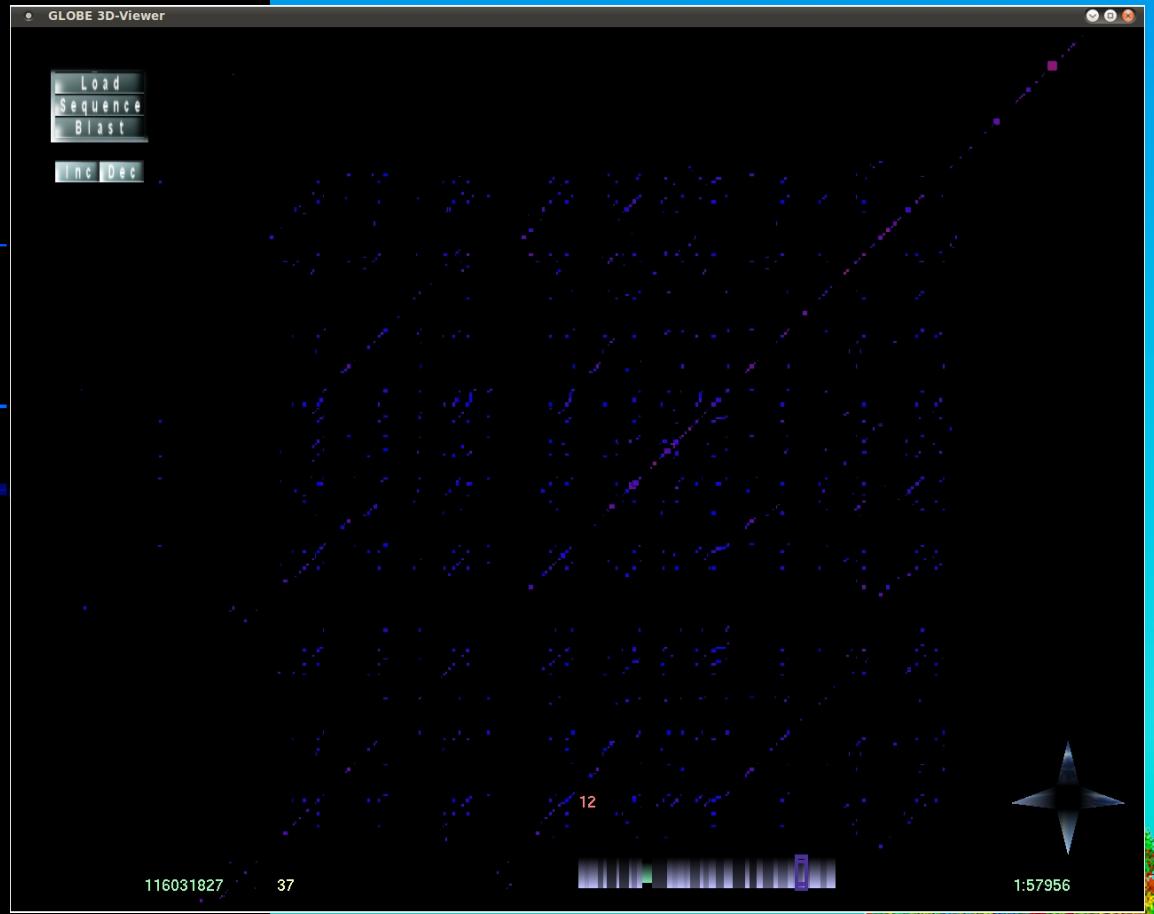


Fine Structure of Loop Aggregates/Rosettes

Depending on the resolution, the loops within a domain and their arrangement in loop aggregates/rosettes can be shown as well as the details of how the loops are organized at their base as well as their aggregated rosette core: parallel loop fibres exist at the loop base with ~6kbp and these form the core.



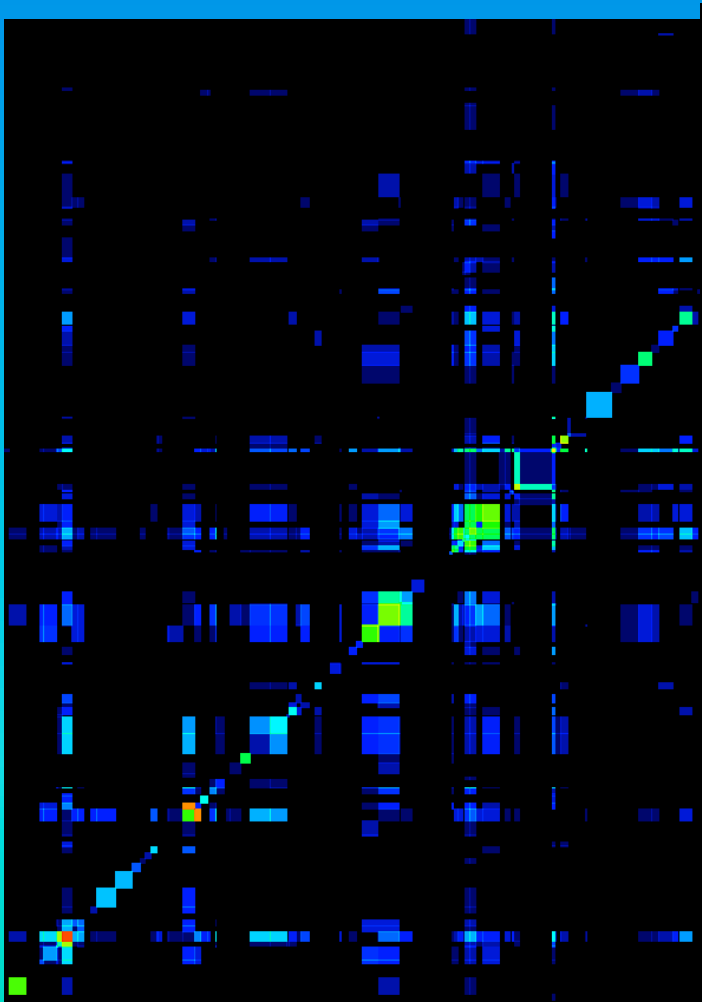
~ 400 kbp



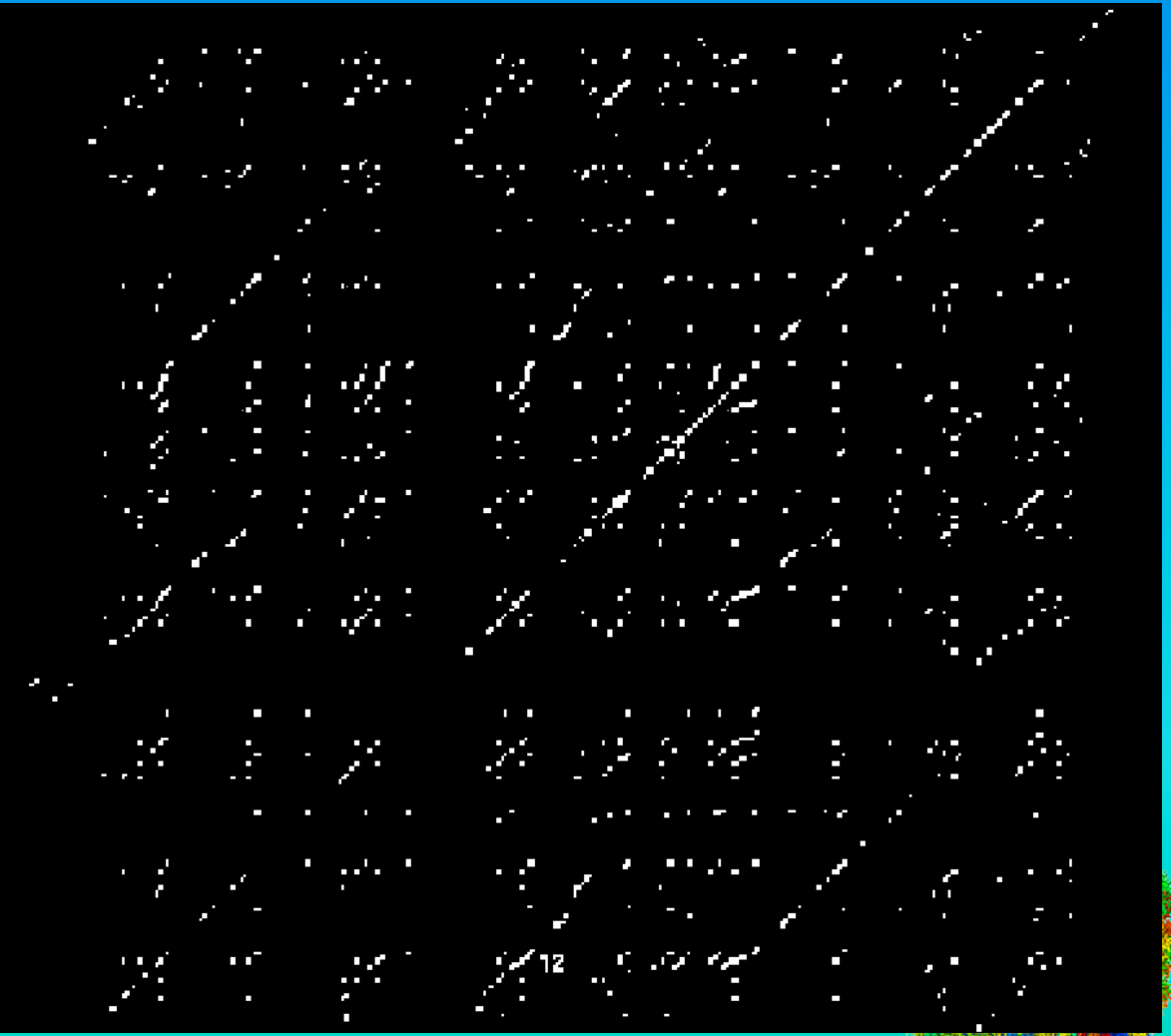
Fine Structure of Loop Aggregates/Rosettes

Depending on the resolution, the loops within a domain and their arrangement in loop aggregates/rosettes can be shown as well as the details of how the loops are organized at their base as well as their aggregated rosette core: parallel loop fibres exist at the loop base with ~6kbp and these form the core.

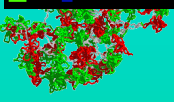
A collage of logos from various funding agencies and research institutions, including BBSRC, NWO, European Commission, EpiGenSys, Erasmus MC, and others.



~ 400 kbp



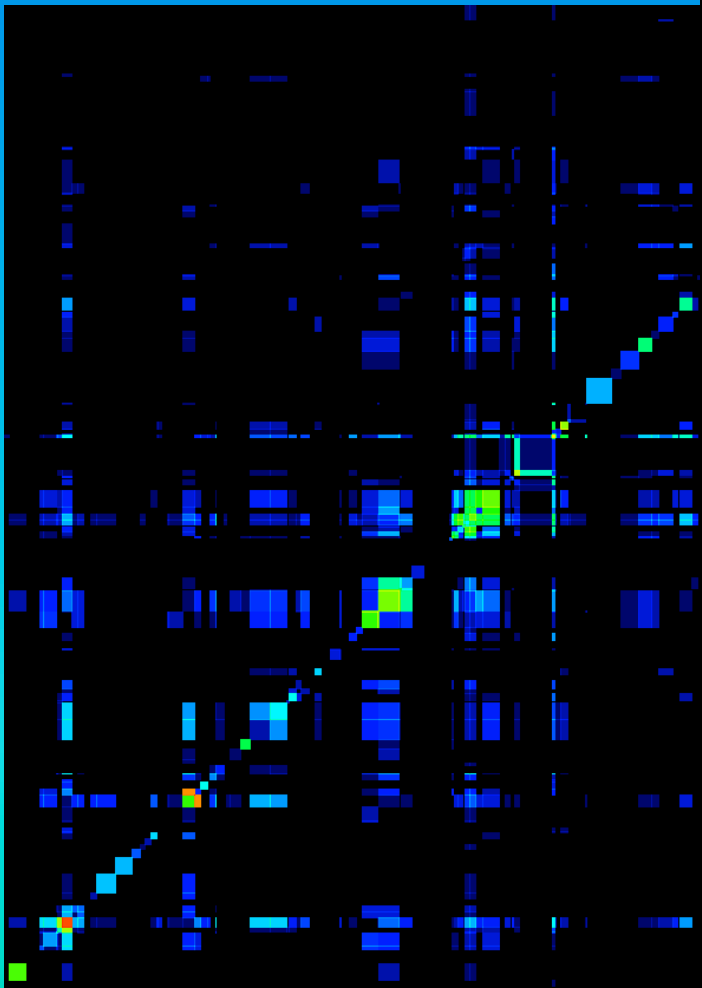
~ 380 kbp



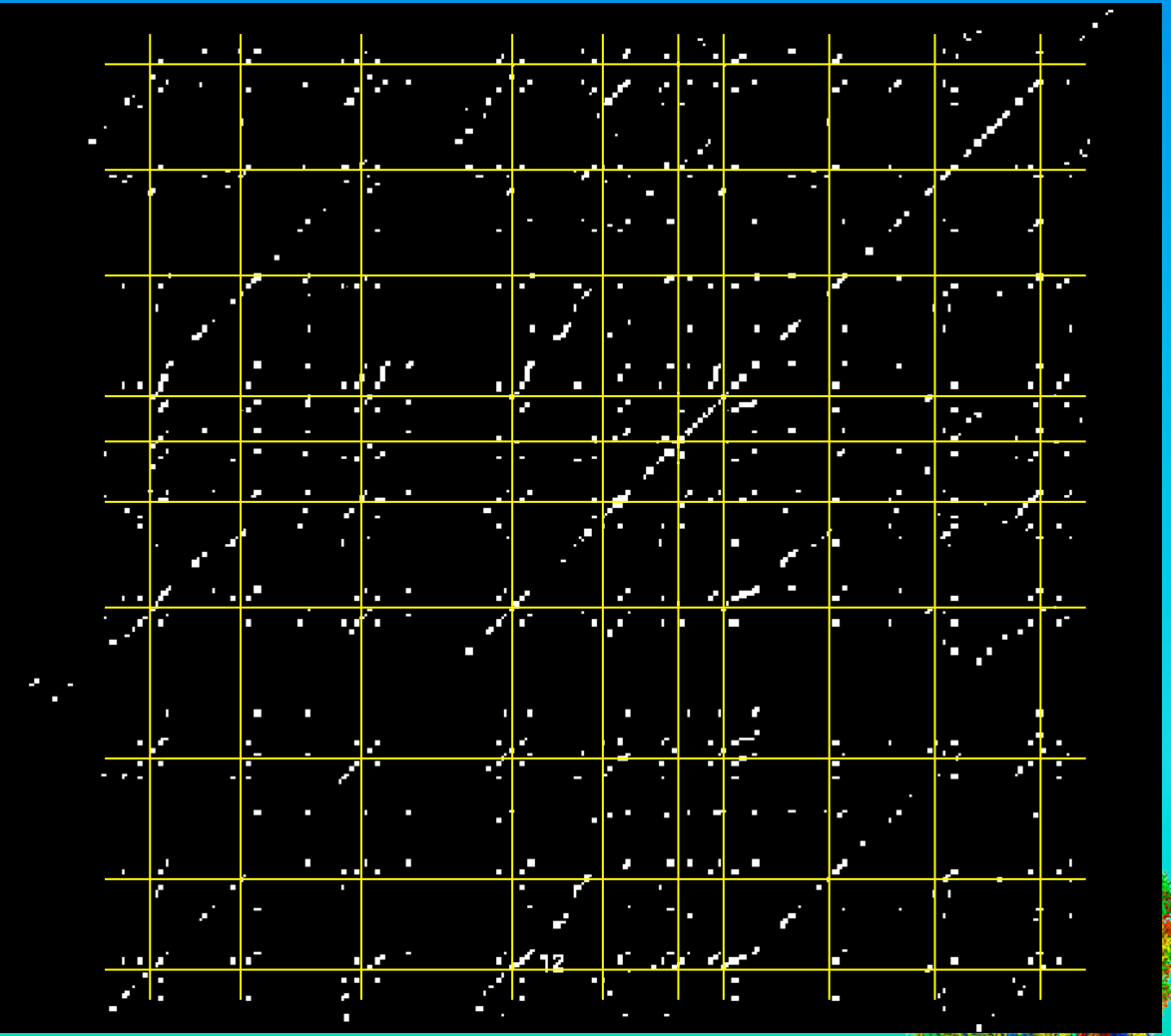
Fine Structure of Loop Aggregates/Rosettes

Depending on the resolution, the loops within a domain and their arrangement in loop aggregates/rosettes can be shown as well as the details of how the loops are organized at their base as well as their aggregated rosette core: parallel loop fibres exist at the loop base with ~6kbp and these form the core.

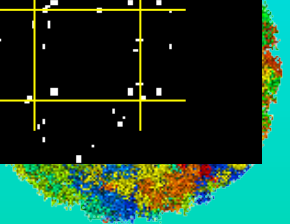
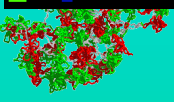
A collage of logos from various research institutions and funding bodies, including BBSRC, NWO, European Commission, Erasmus MC, University of Oxford, and others.



~ 400 kbp

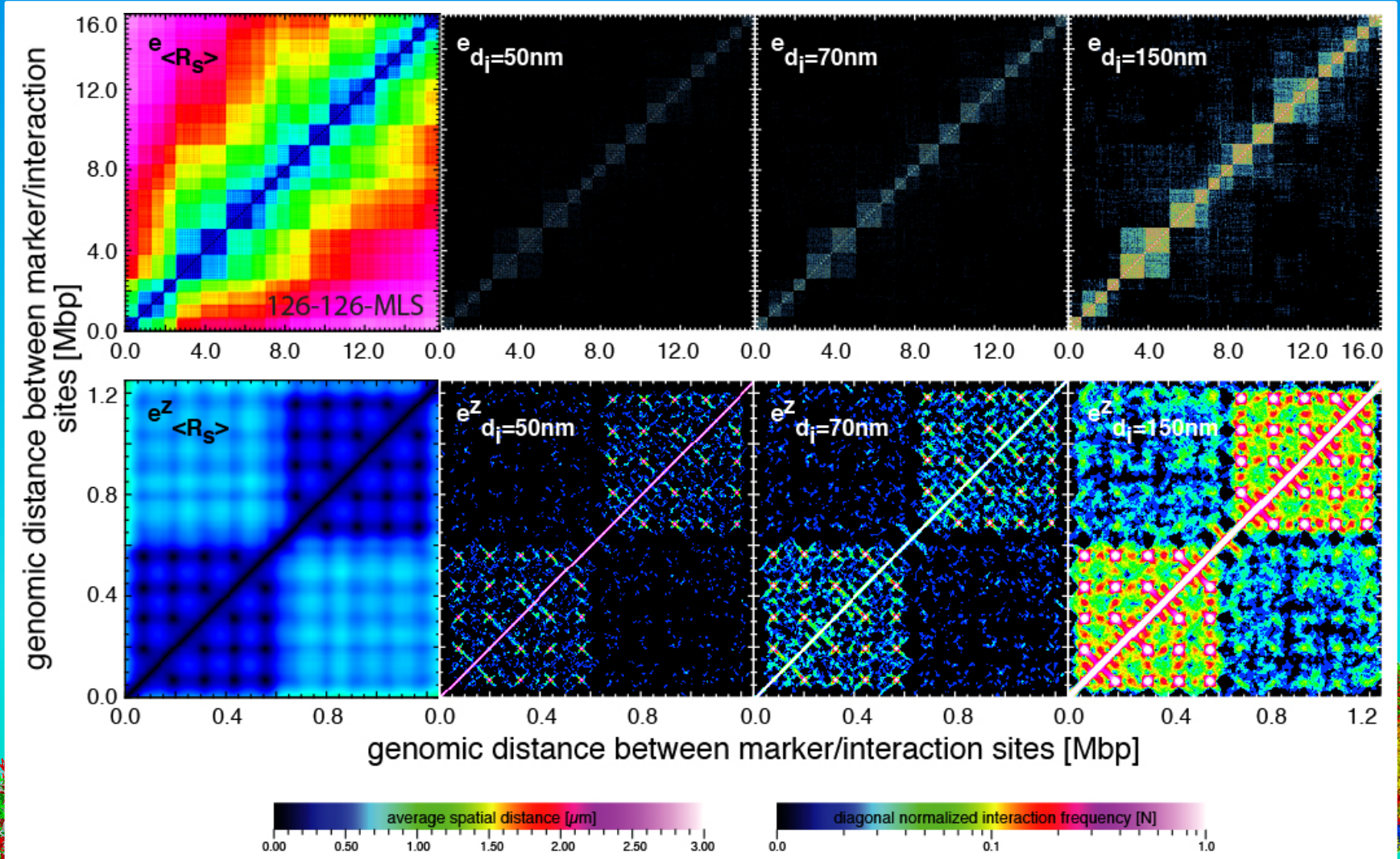


~ 380 kbp



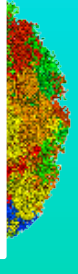
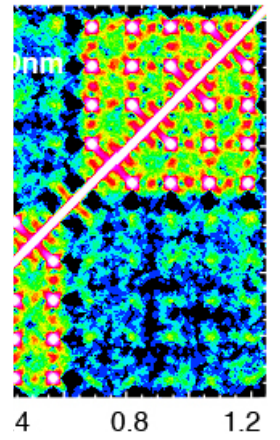
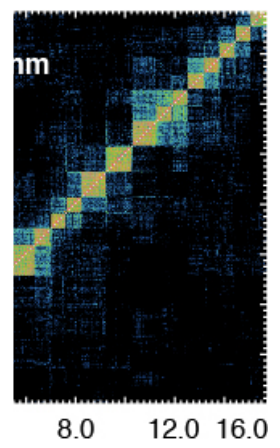
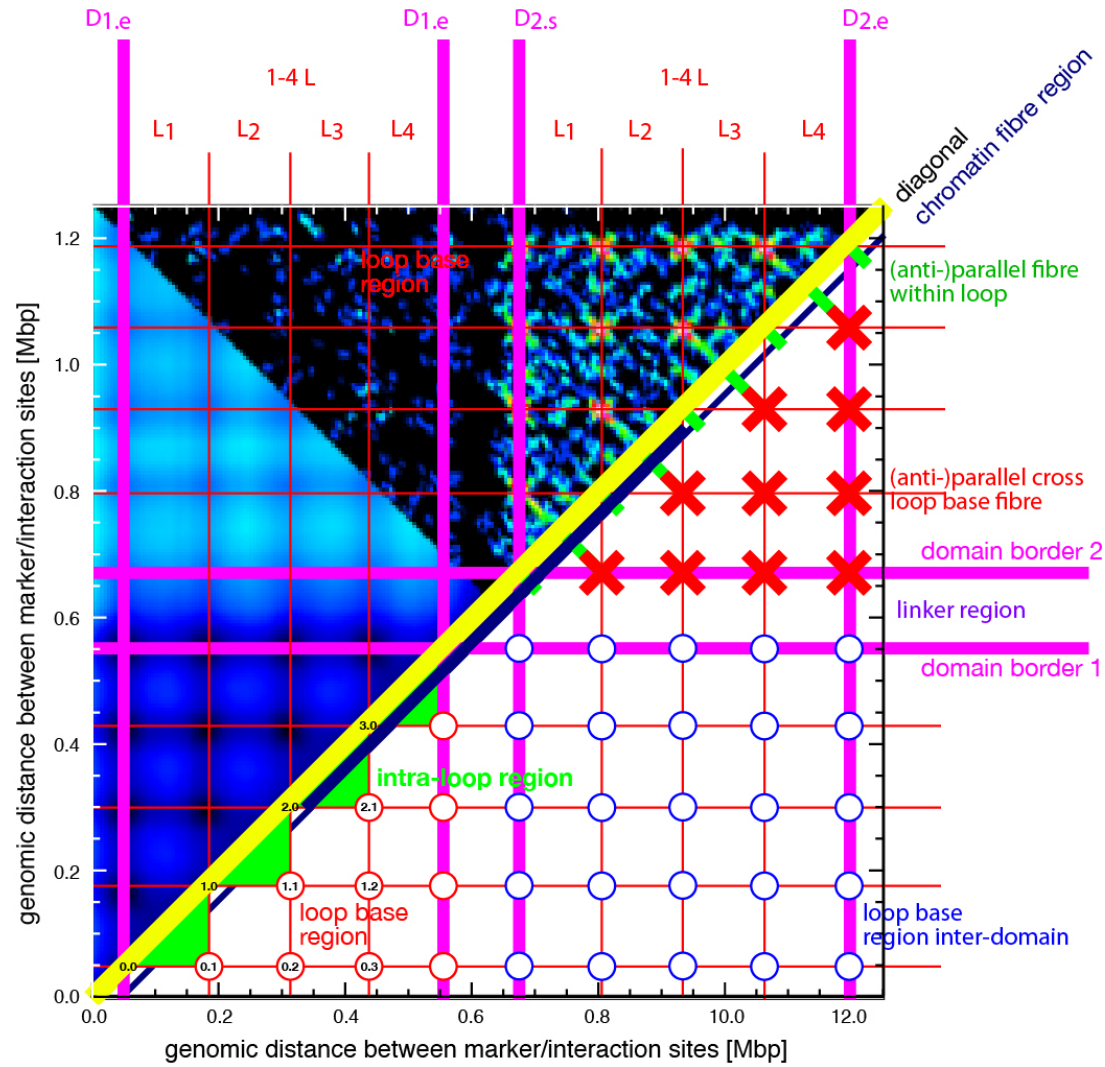
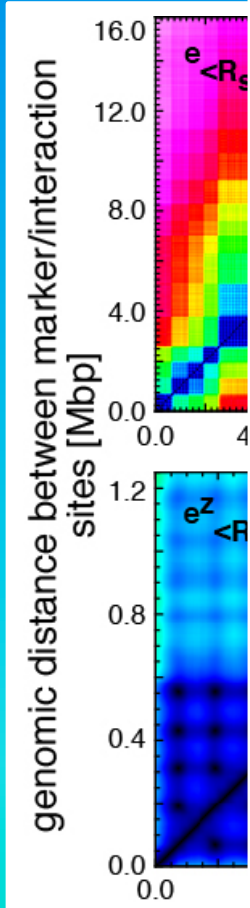
Simulated Interaction Maps

Simulated spatial distance maps as well as simulated interaction maps result in the representation of every parameter variation, and also exhibit the fine-structure describing the loop base as well as rosette core. Thus from the quasi-fibre to the entire chromosome the architecture can be understood in detail.



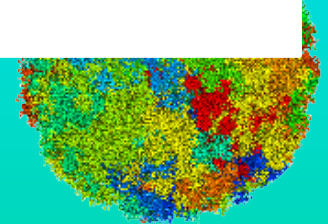
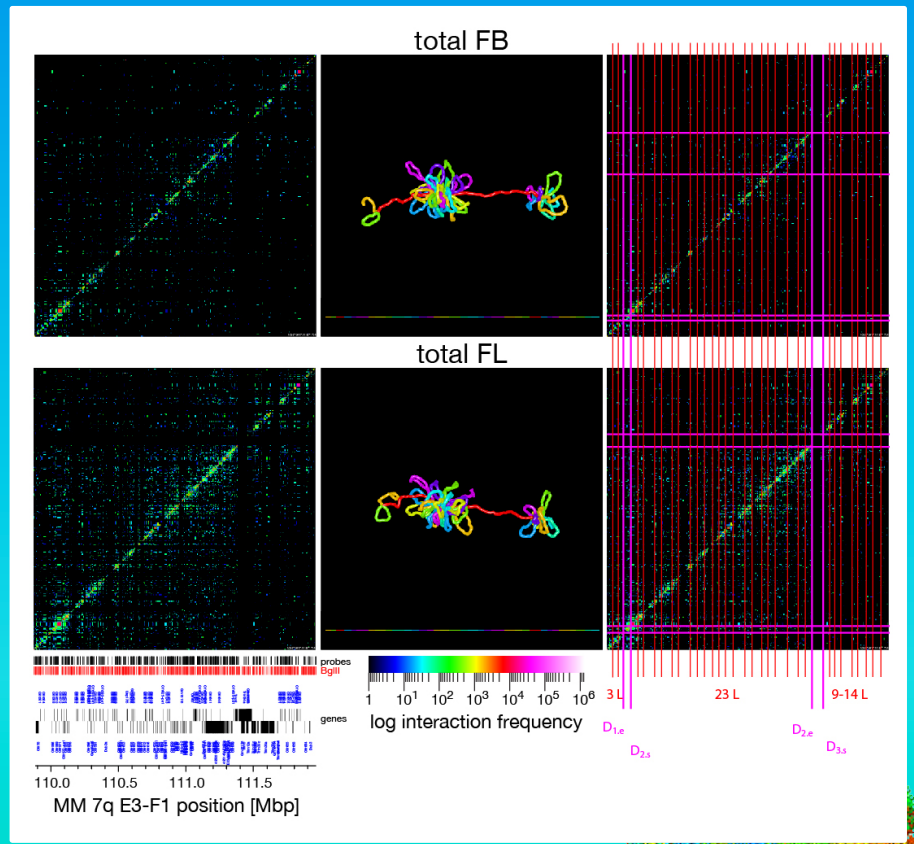
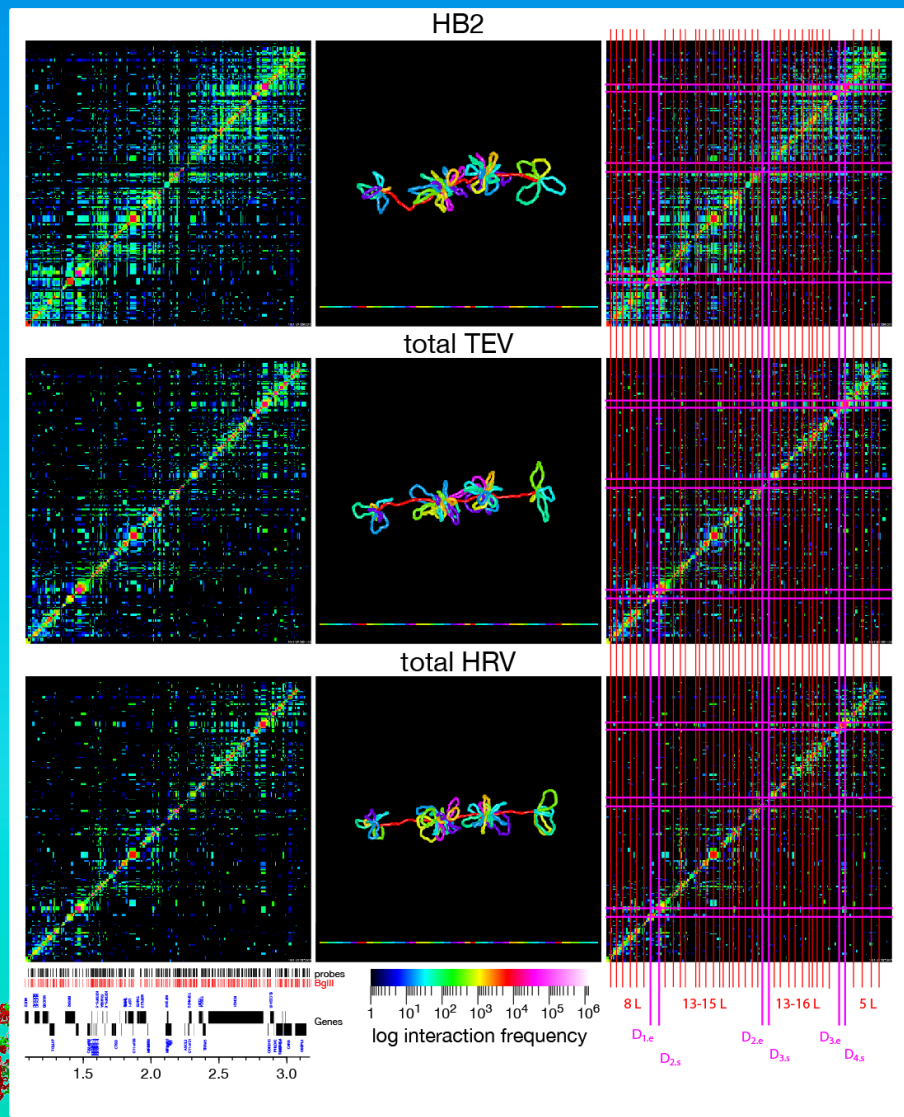
Simulated Interaction Maps

Simulated spatial distance maps as well as simulated interaction maps result in the representation of every parameter variation, and also exhibit the fine-structure describing the loop base as well as rosette core. Thus from the quasi-fibre to the entire chromosome the architecture can be understood in detail.



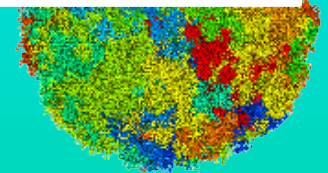
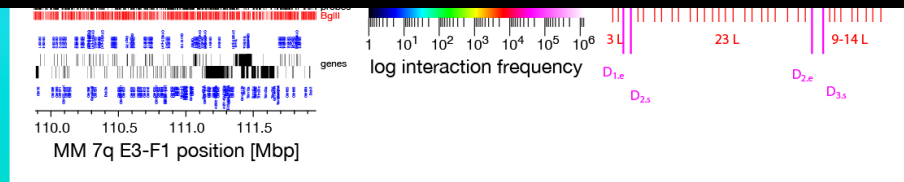
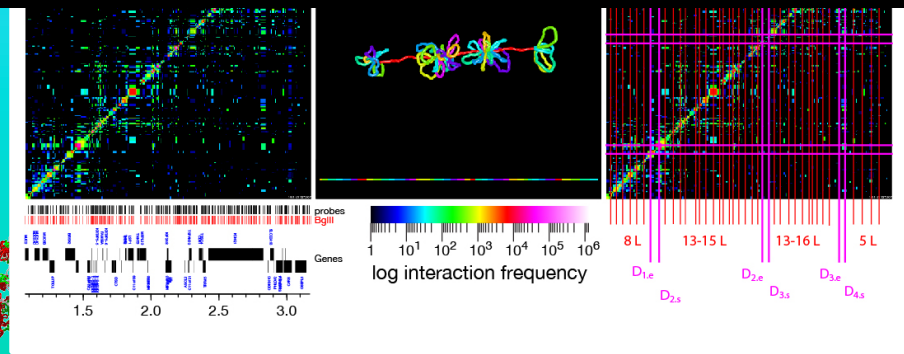
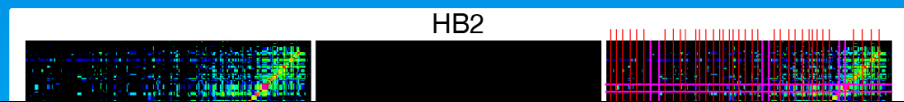
Variation of a Consensus Architecture Scheme

The difference between different cell types, functional states or even species is minor despite depending on the region. From this, the chromatin fibre conformation, loop position, and their association into loop aggregates/rosettes can be derived, simulated by polymer models and finally visualized.



Variation of a Consensus Architecture Scheme

The difference between different cell types, functional states or even species is minor despite depending on the region. From this, the chromatin fibre conformation, loop position, and their association into loop aggregates/rosettes can be derived, simulated by polymer models and finally visualized.



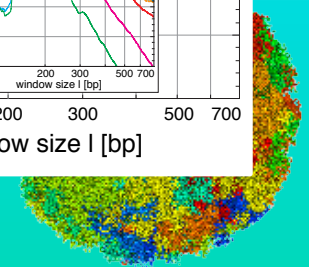
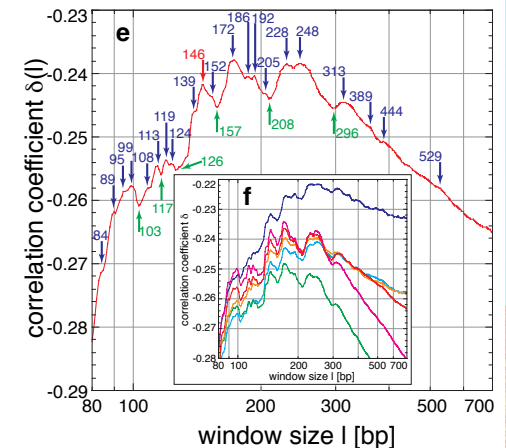
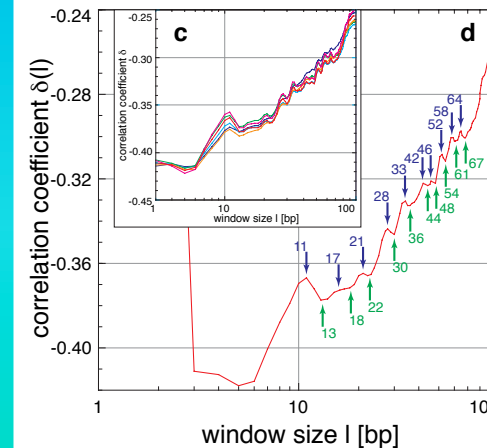
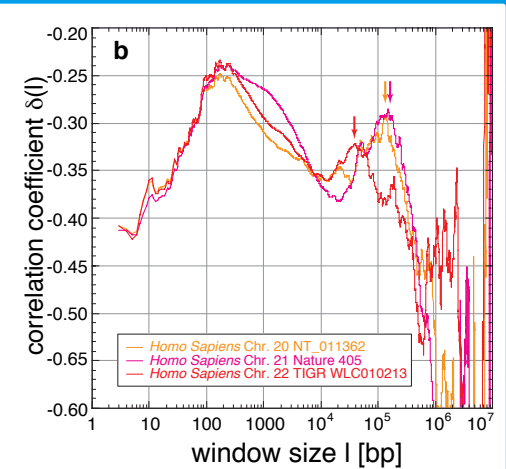
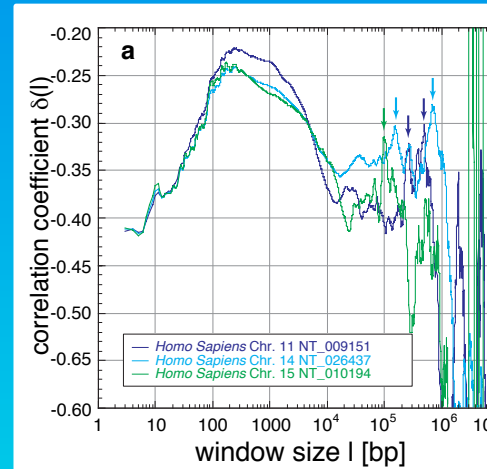
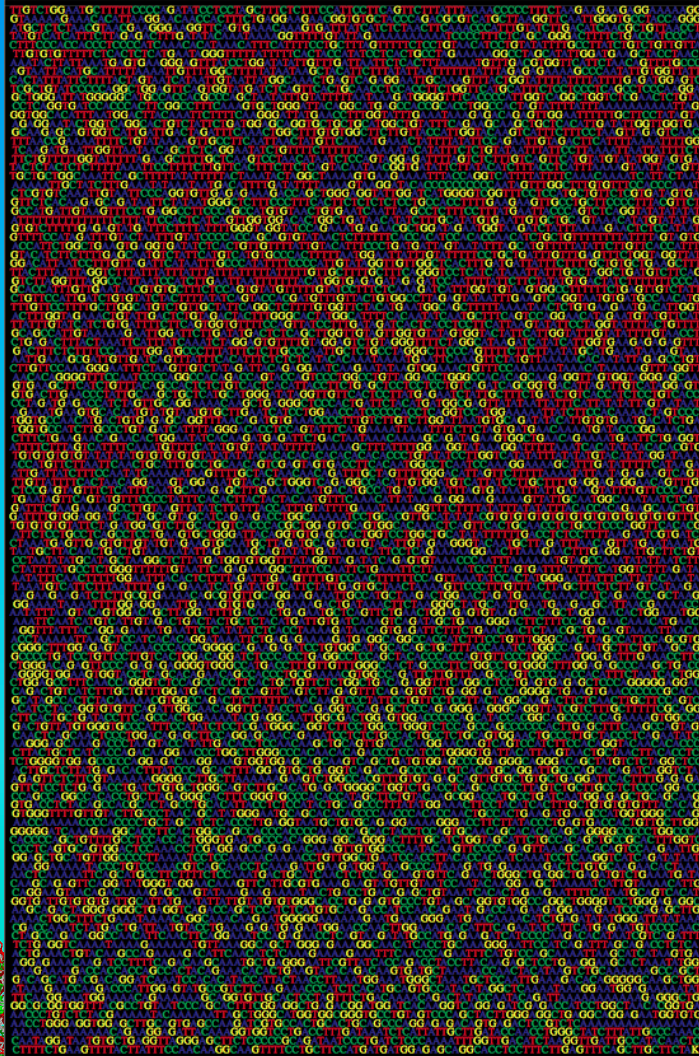
Variation of a Consensus Architecture Scheme

The difference between different cell types, functional states or even species is minor despite depending on the region. From this, the chromatin fibre conformation, loop position, and their association into loop aggregates/rosettes can be derived, simulated by polymer models and finally visualized.



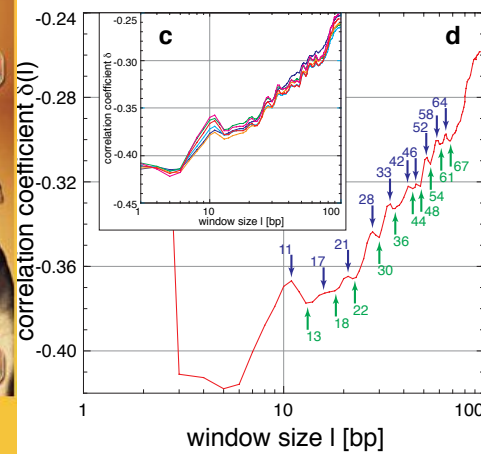
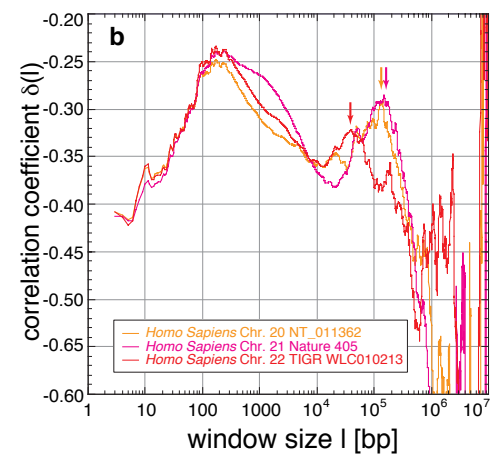
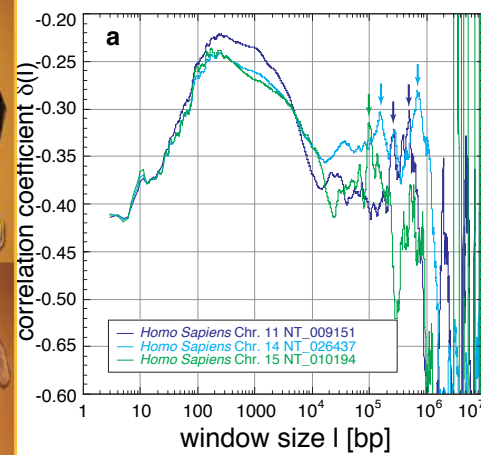
DNA Sequence Organization

Determination of the concentration fluctuation function $C(l)$ and its local slope the correlation coefficient $\delta(l)$ are an indication for the i) degree of long-rang scaling behaviour, ii) general multi-scaling, and iii) fine-structure features, which all are connected to all levels of genome organization and especially also the three-dimensional genome architecture.



DNA Sequence Organization

Determination of the concentration fluctuation function $C(l)$ and its local slope the correlation coefficient $\delta(l)$ are an indication for the i) degree of long-rang scaling behaviour, ii) general multi-scaling, and iii) fine-structure features, which all are connected to all levels of genome organization and especially also the three-dimensional genome architecture.

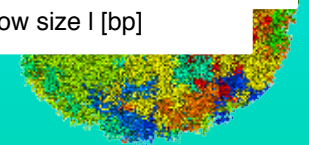
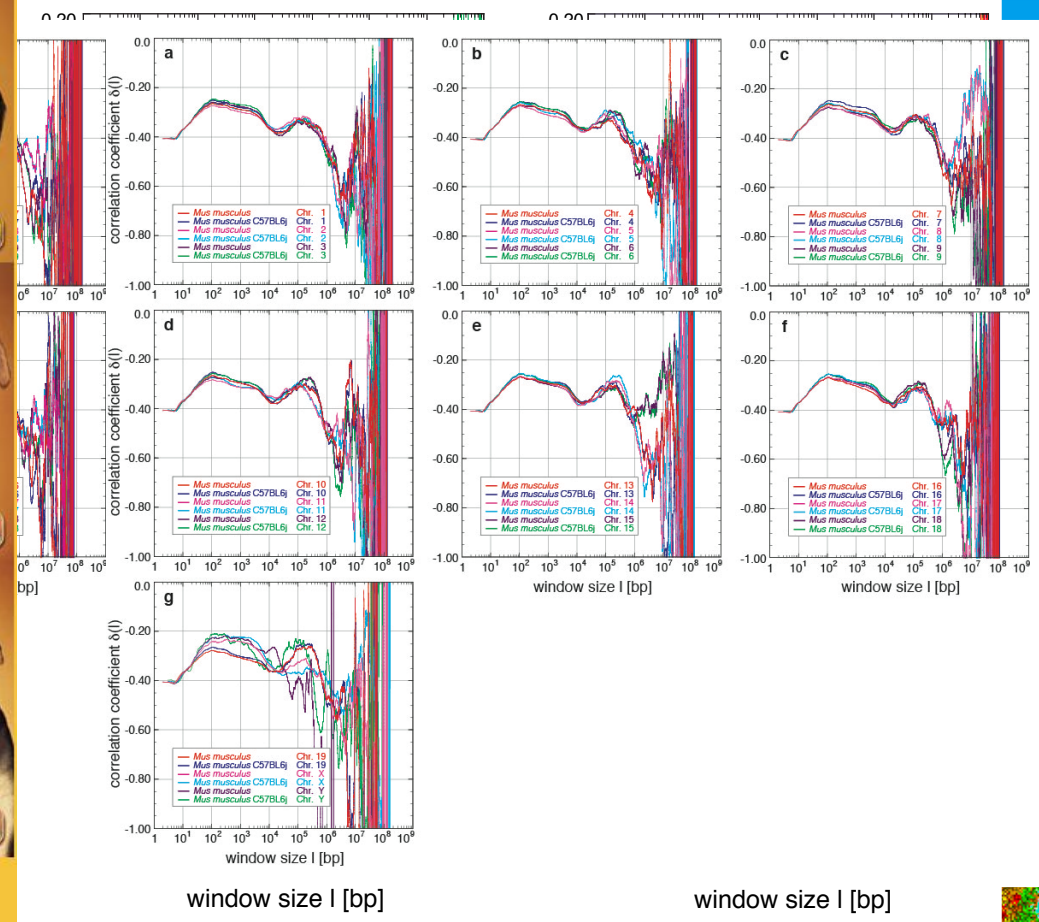


DNA Sequence Organization

Determination of the concentration fluctuation function $C(l)$ and its local slope the correlation coefficient $\delta(l)$ are an indication for the i) degree of long-rang scaling behaviour, ii) general multi-scaling, and iii) fine-structure features, which all are connected to all levels of genome organization and especially also the three-dimensional genome architecture.

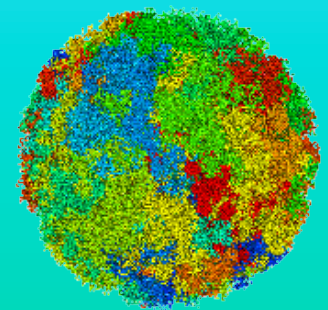
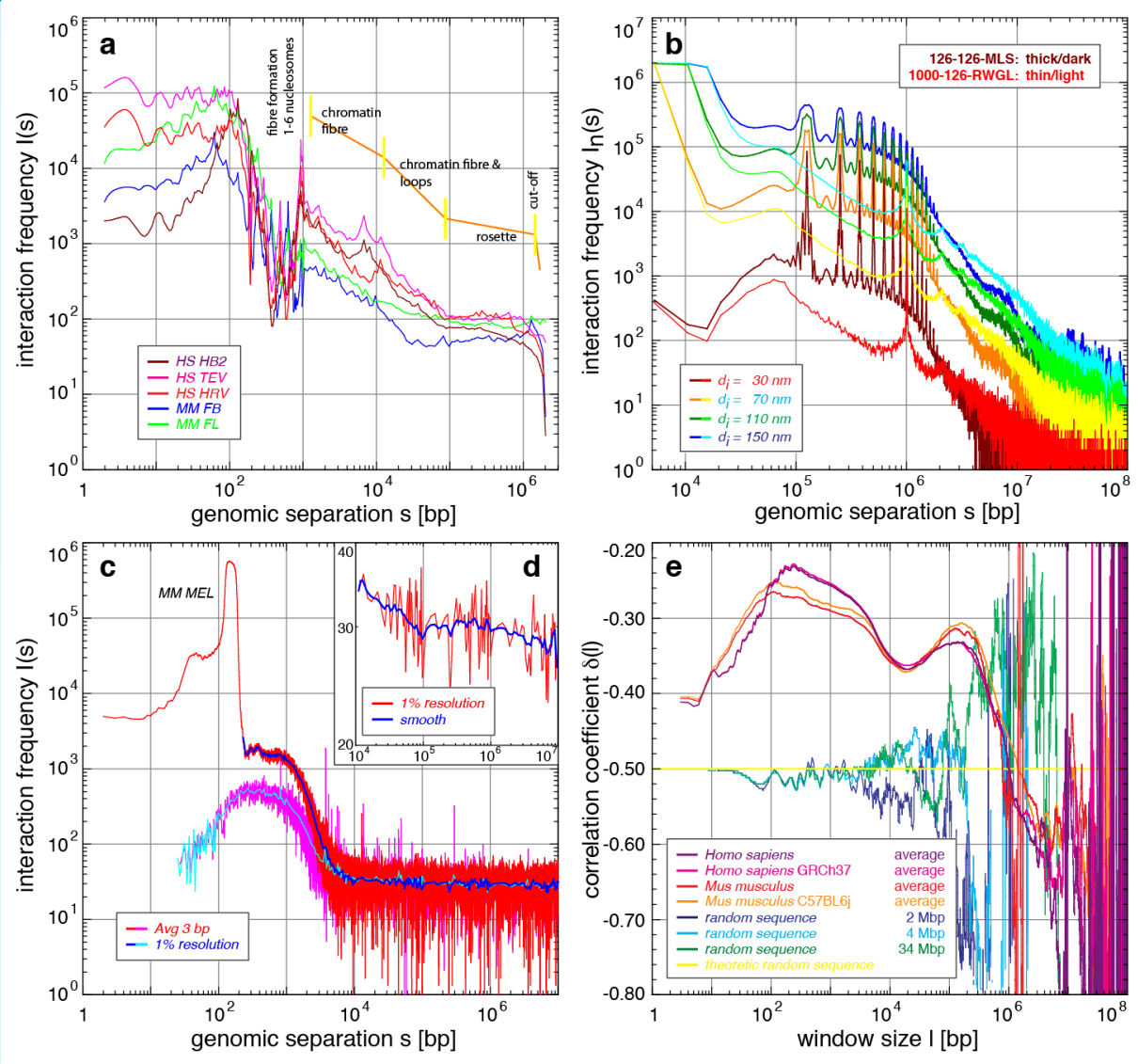


 FunFire.de



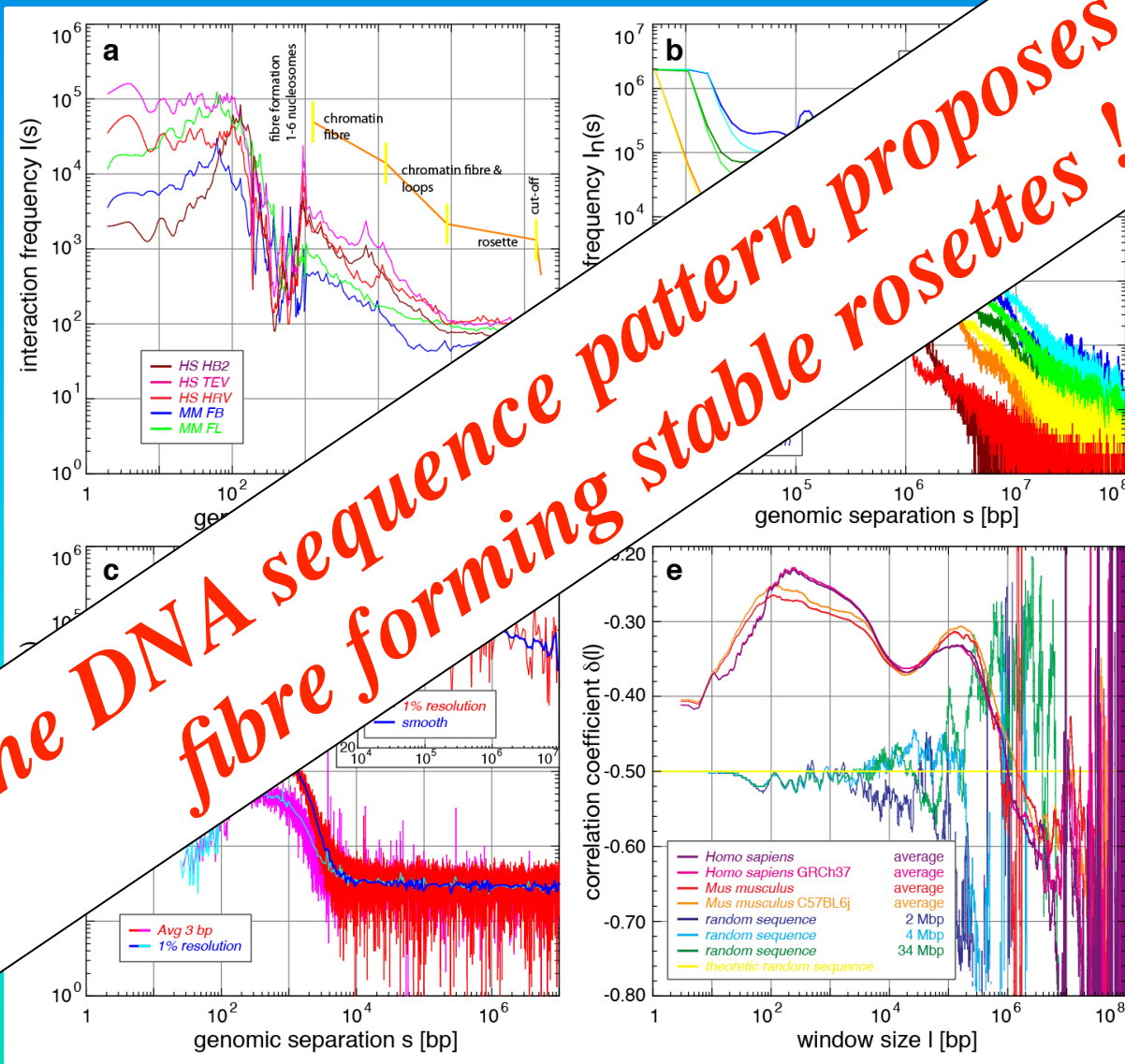
Scaling Analysis

Scaling analysis show again the entire bandwidth of architectural effects in an aggregated manner. Beyond, they show the scale bridging of the structures and the evolutionary holistic entanglement between the 3D architecture and the DNA sequence organization itself.

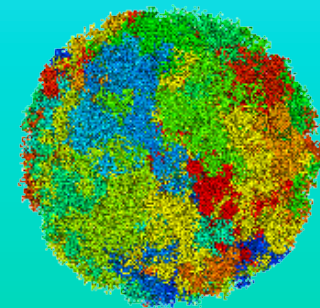


Scaling Analysis

Scaling analysis show again the entire bandwidth of architectural effects in an aggregated manner. Beyond, they show the scale bridging of the structures and the evolutionary holistic entanglement between the 3D architecture and the DNA sequence organization itself.

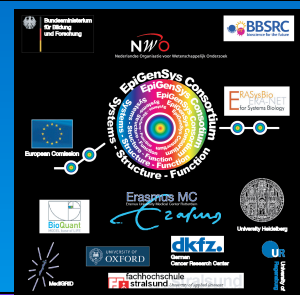


Also the DNA sequence pattern proposes a quasi-fibre forming stable rosettes !

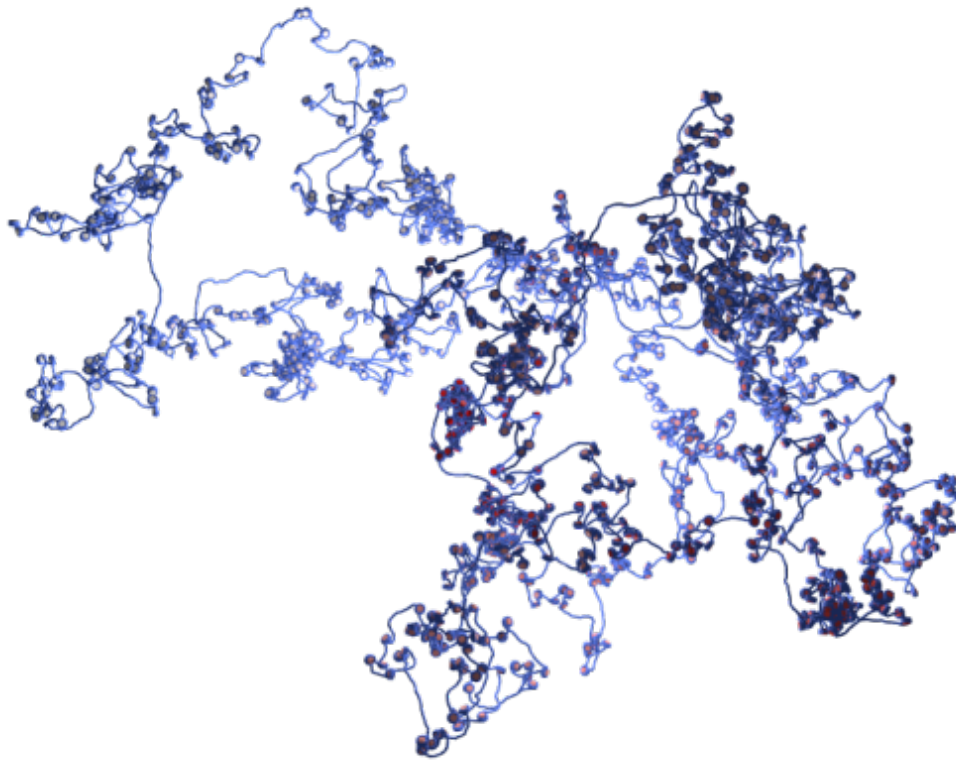


Simulation of Chromatin Quasi-Fibres

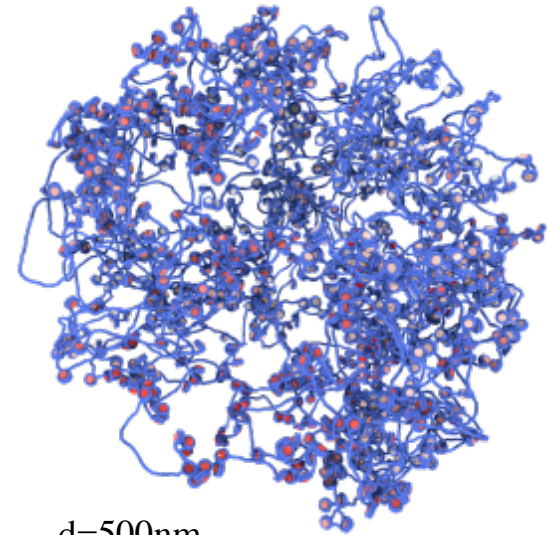
The position of nucleosomes influence greatly the structure of chromatin fibers done on super-computers. Here a dedicated workflow is applied, with which overlapping nucleosome populations can be analyzed and the best positioning of nucleosomes by Monte Carlo simulated annealing can be achieved. For an actual locus in a spherical confinement then a 3D independent nucleosome fiber conformation can be simulated.



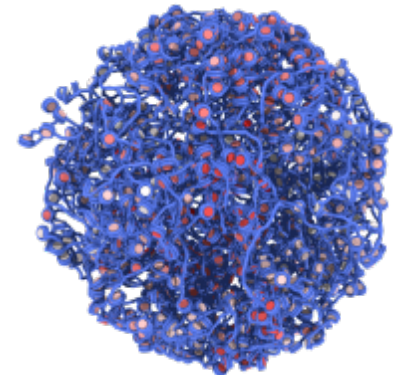
Monte Carlo Simulation of SAMD4A Mouse ES Cells



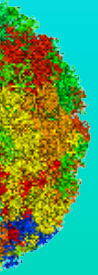
d=1000nm



d=500nm



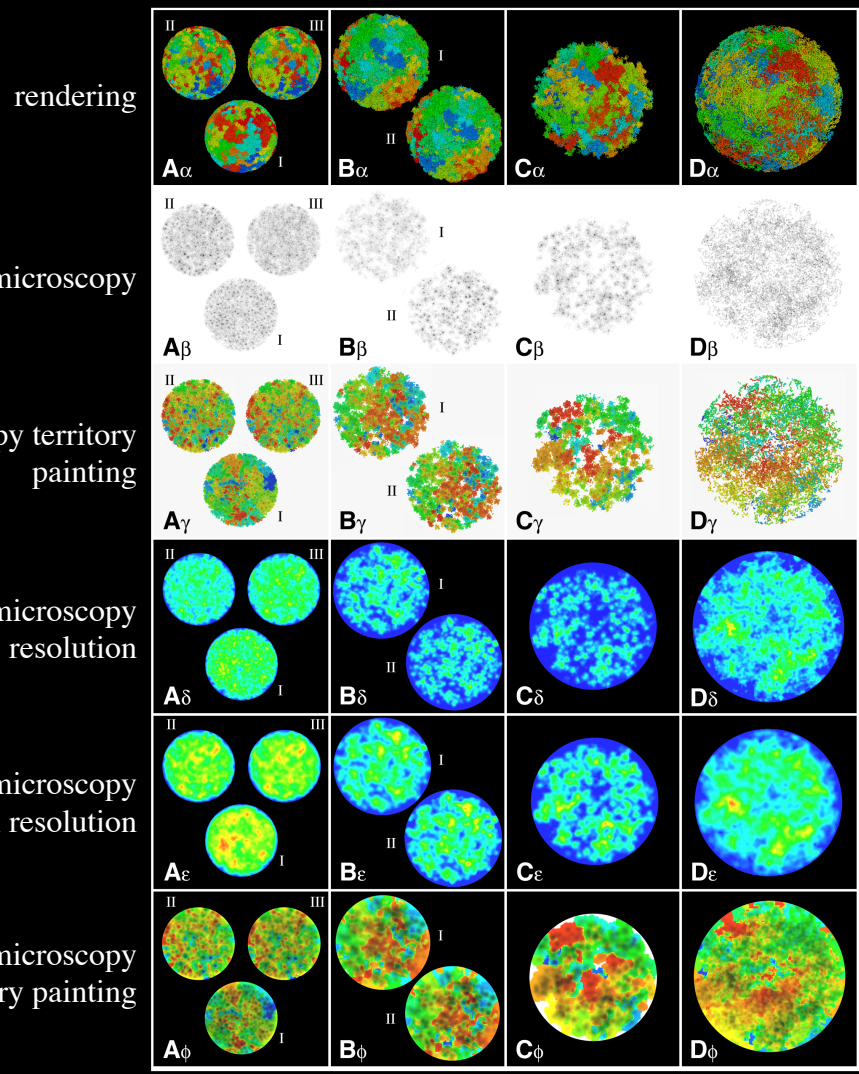
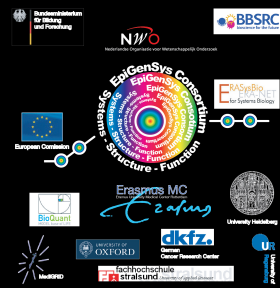
d=200nm



From Fiber Topology to Nuclear Morphology

Chromosome territories form in the RW/GL and the MLS model. However, only the MLS model leads distinct subcompartments and low chromosome and subcompartment overlap. Best agreement is reached for an MLS model with 80 to 120 kbp loops and linkers in nuclei with 8 to 10 μm diameter.

The simulated nuclear morphology reflects the chromosome fiber topology of different models in detail.

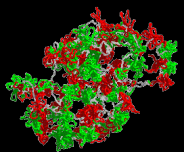
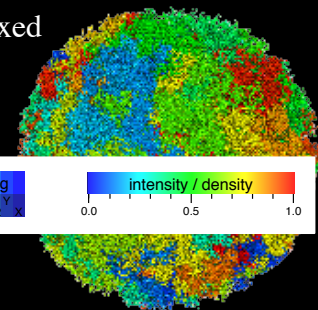


A: MLS in 6 μm nucleus
 I: 63 kbp loops, 63 kbp linkers
 II: 63 kbp loops, 252 kbp linkers
 III: 126 kbp loops, 252 kbp linkers

B: MLS in 8 μm nucleus
 I: 126 kbp loops, 126 kbp linkers
 II: 84 kbp loops, 126 kbp linkers

C: MLS in 10 μm nucleus
 126 kbp loops, 126 kbp linker,
 not totally relaxed

D: RW/GL in 12 μm nucleus
 5 Mbp loops
 not totally relaxed



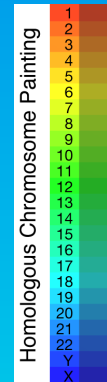
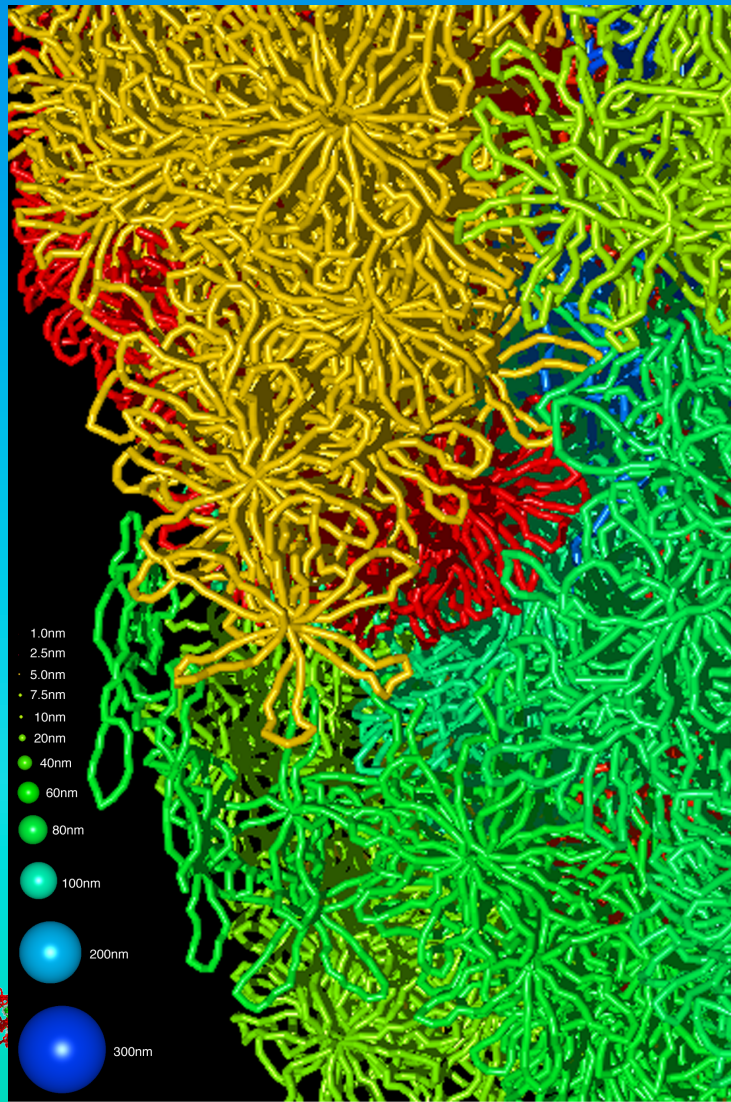
100x objective, theoretic resolution

63x objective, real resolution

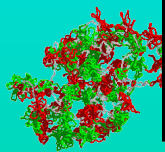
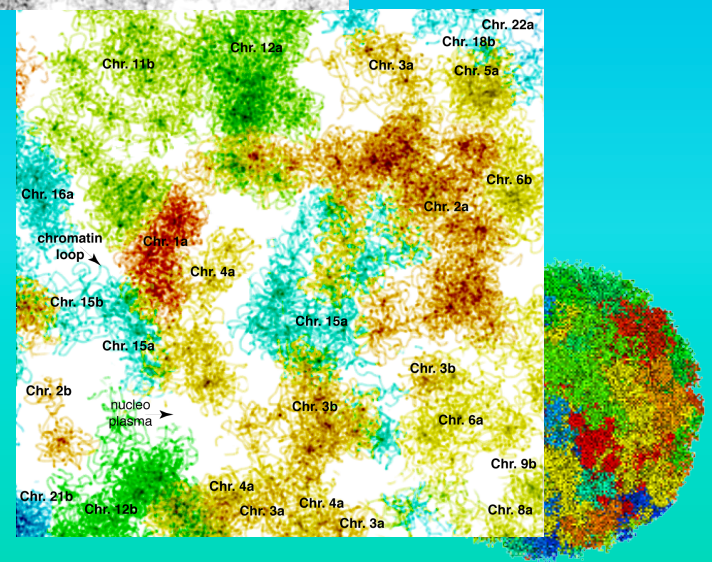
territory painting

Fine Morphology of Nuclei

High resolution rendering and simulated electron microscopy including territory painting reveal not only again the model details but also that any location in the nucleus is accessible to biological molecules <15 nm in diameter and that even the Extended Interchromosomal Domain hypothesis is oversimplified.

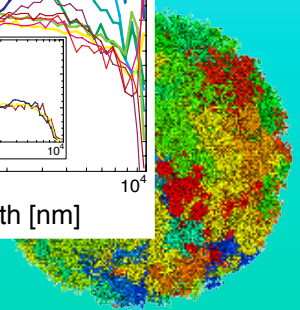
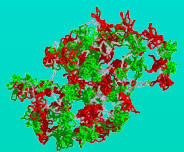
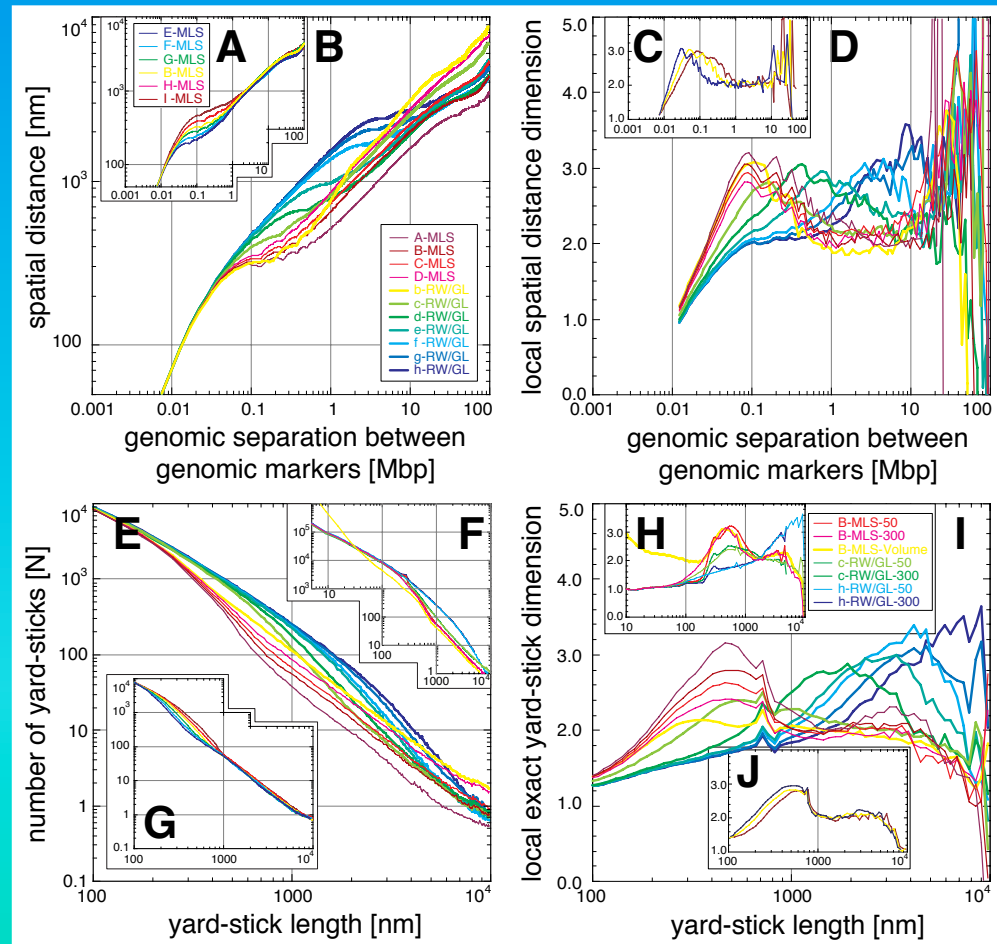
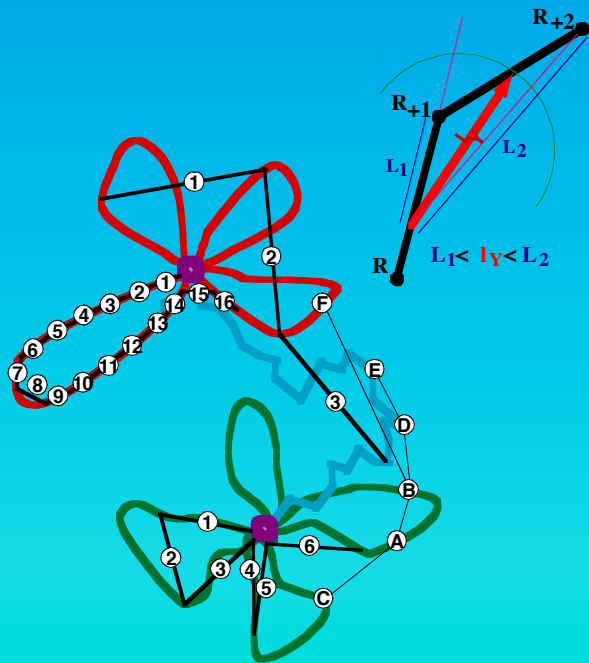


MLS models with 126 kbp loops and linkers in a 10 μm nucleus.



Scaling of the Chromatin Fiber Topology

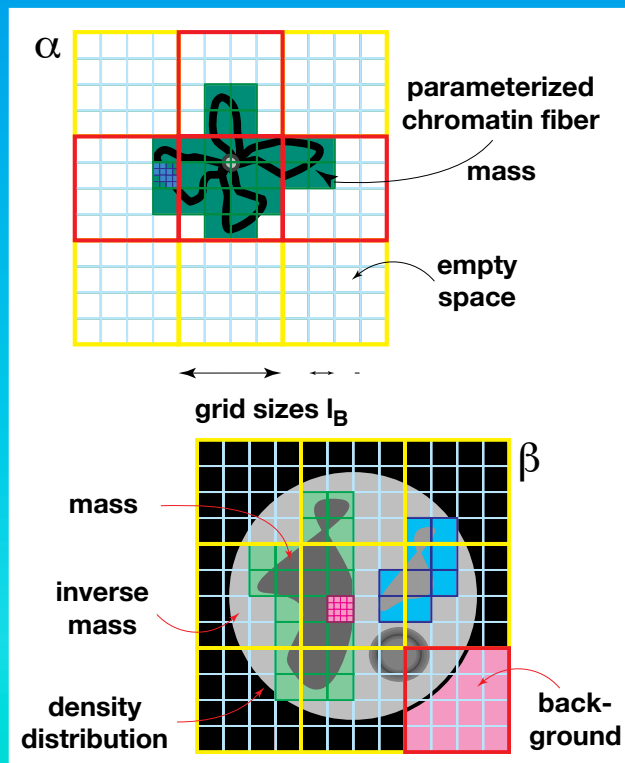
The spatial-distance and exact yard-stick dimension distinguish between the simulated models in detail. The MLS model shows a globular and fine-structured multi scaling behaviour due to the loops forming rosettes. This agrees with DNA fragmentation by Carbon ion irradiation and the appearance of fine-structured multi-scaling long-range correlations found in the sequential organization of genomes.



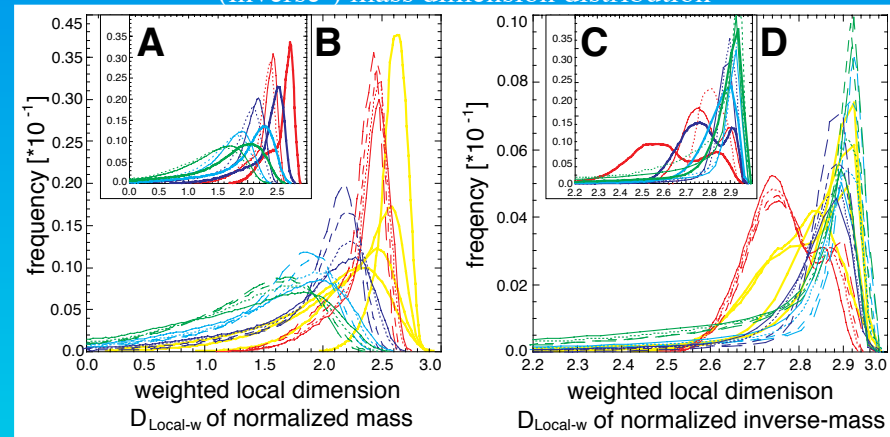
Scaling of the Chromatin Morphology & Distribution

The local (inverse-) mass dimension distinguishes between the models in detail and show also a multi-scaling behaviour with globular feature for the MLS model like the scaling of the fiber topology. With the mass dimension as function of intensity separates very well between different nuclei *in vivo*.

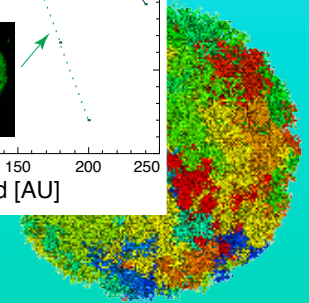
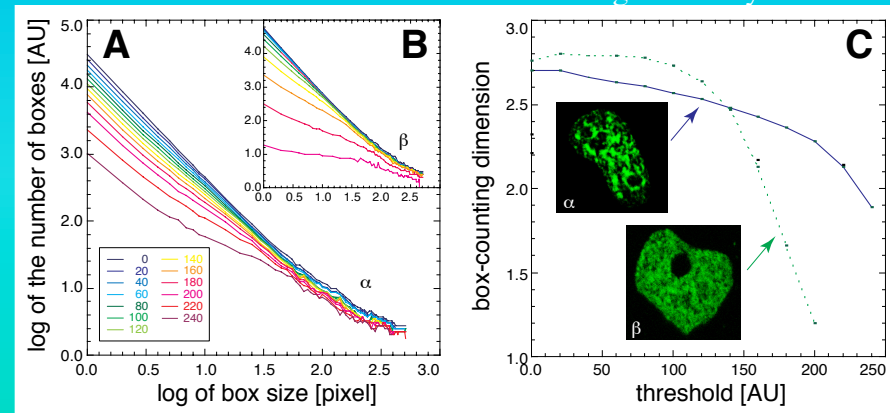
Consequently, the chromatin morphology is causally and quantitatively connected to the fiber topology.



(inverse-) mass dimension distribution

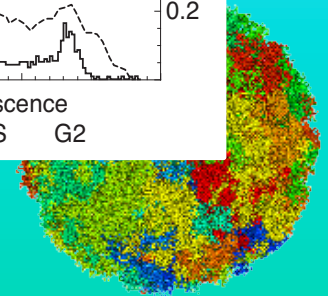
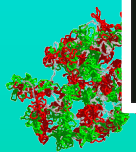
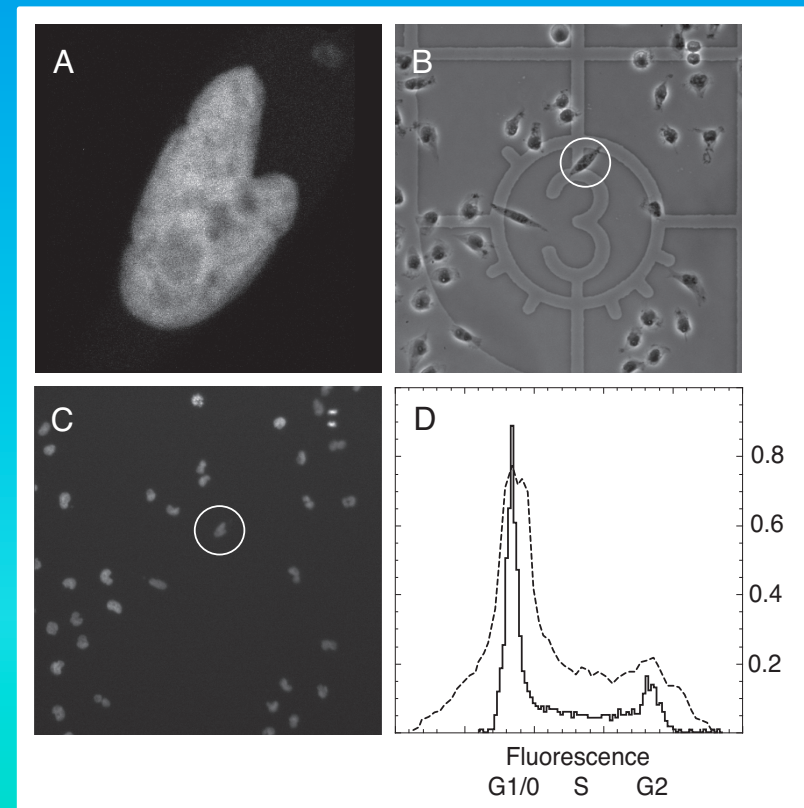
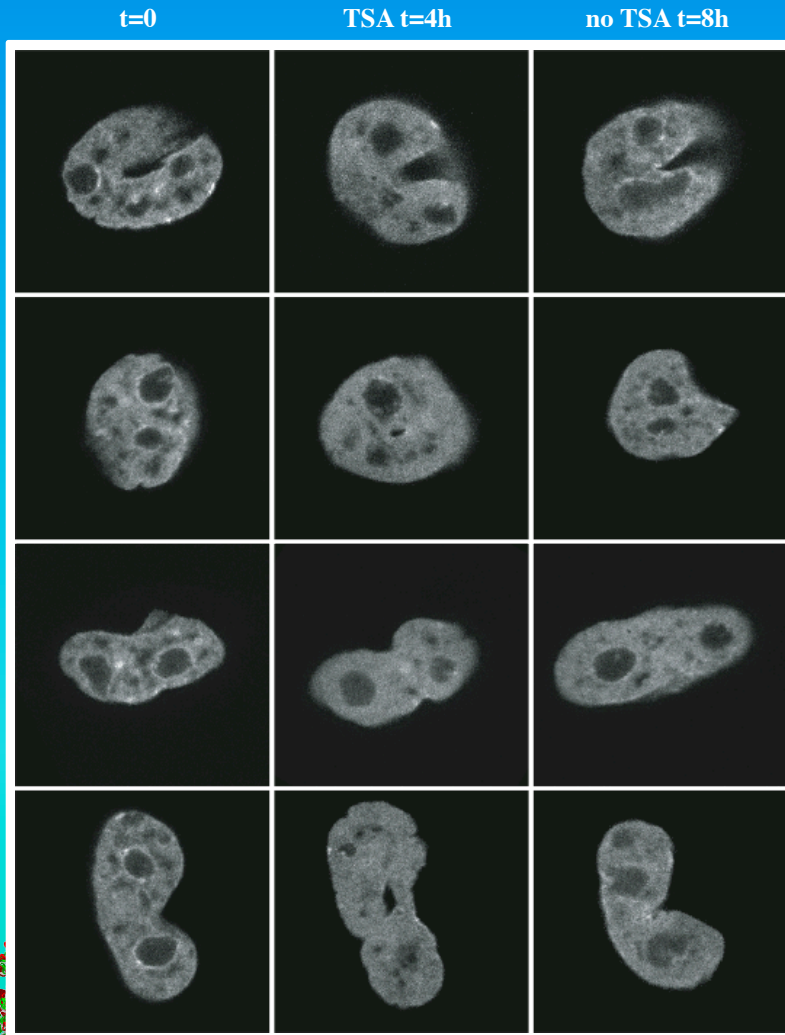


mass dimension as function of image intensity



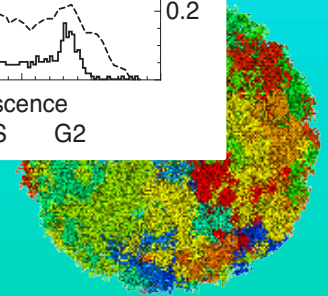
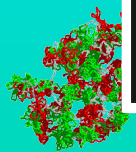
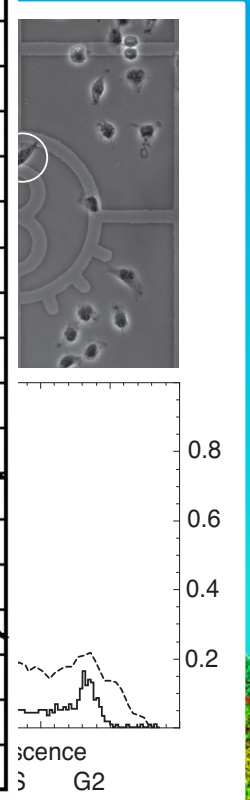
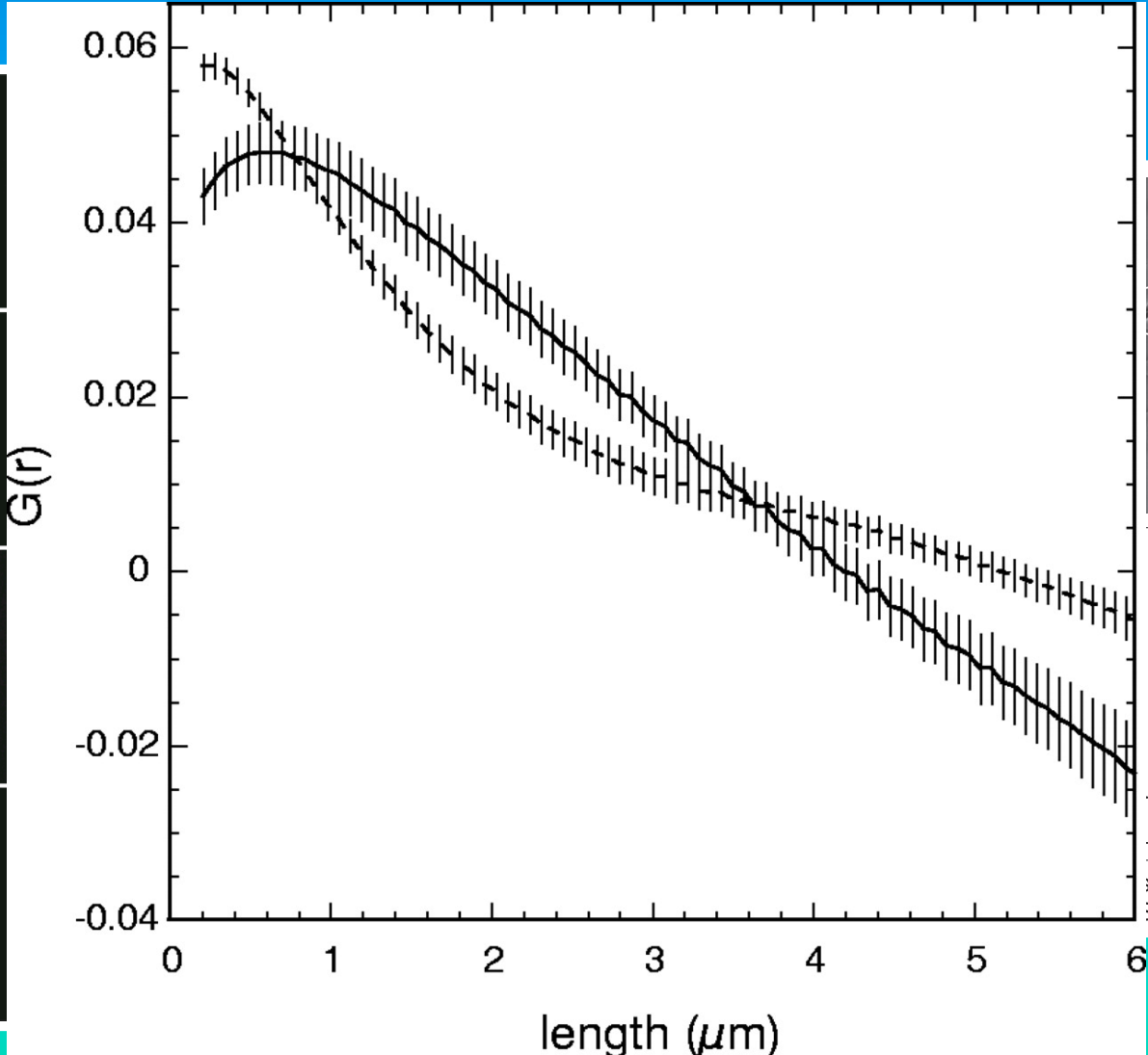
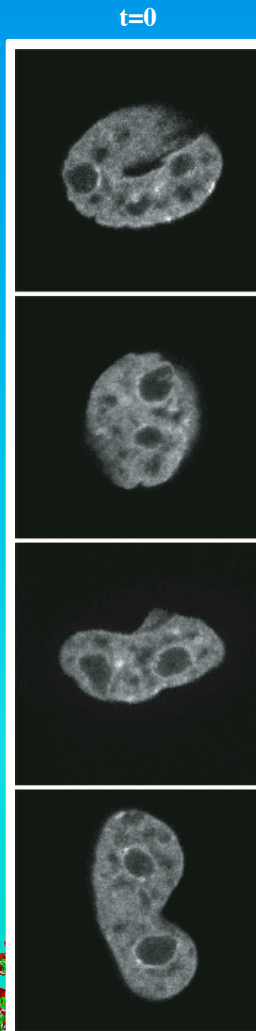
Quantified TSA induced Morphology Changes

Trichostatin A induced histone acetylation can be quantified by *in vivo* H2A-GFP confocal images and image correlation spectroscopy (iFCS), which is a scaling analysis, and reveals the opening of chromatin, and thus reorganization changes on scales from 0.2 to $\sim 1\mu\text{m}$, consistent with MLS models.



Quantified TSA induced Morphology Changes

Trichostatin A induced histone acetylation can be quantified by *in vivo* H2A-GFP confocal images and image correlation spectroscopy (iFCS), which is a scaling analysis, and reveals the opening of chromatin, and thus reorganization changes on scales from 0.2 to $\sim 1\mu\text{m}$, consistent with MLS models.



Diffusion of Particles in the Nucleus

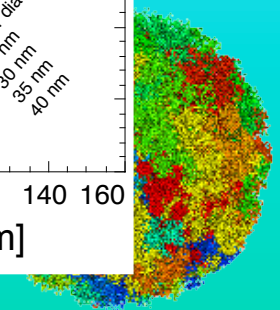
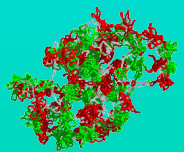
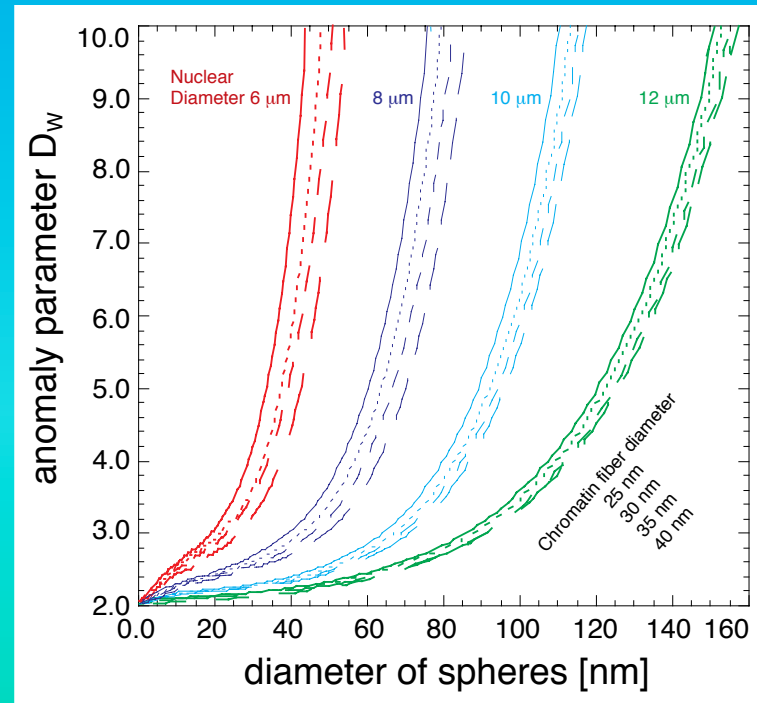
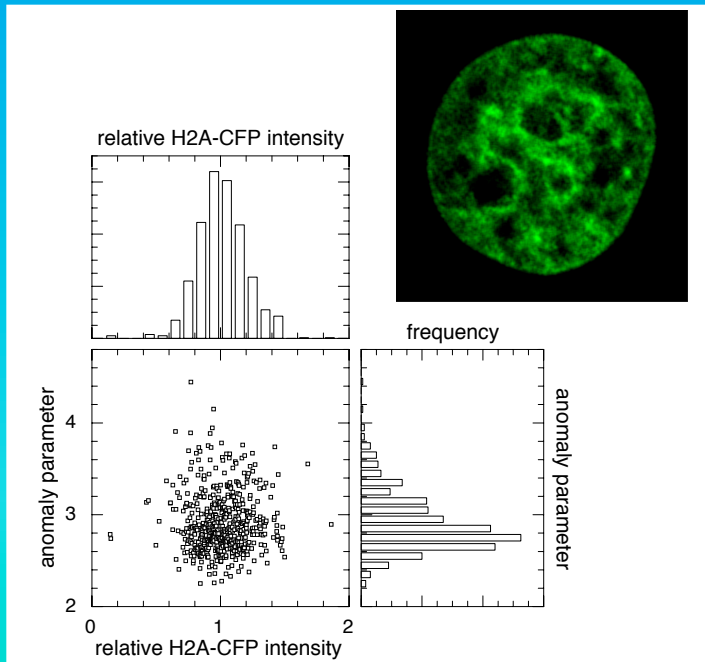
Due to the volume and spatial relationships in the nucleus typical particles reach almost any location in the nucleus by moderately obstructed diffusion: a 10 nm particle moves 1 to 2 μm within 10 ms.

The structural influence on the obstruction degree is random for Alexa 568 as function of the chromatin distribution visualized by H2A CFP in vivo and measured by fluorescence correlation spectroscopy (FCS)



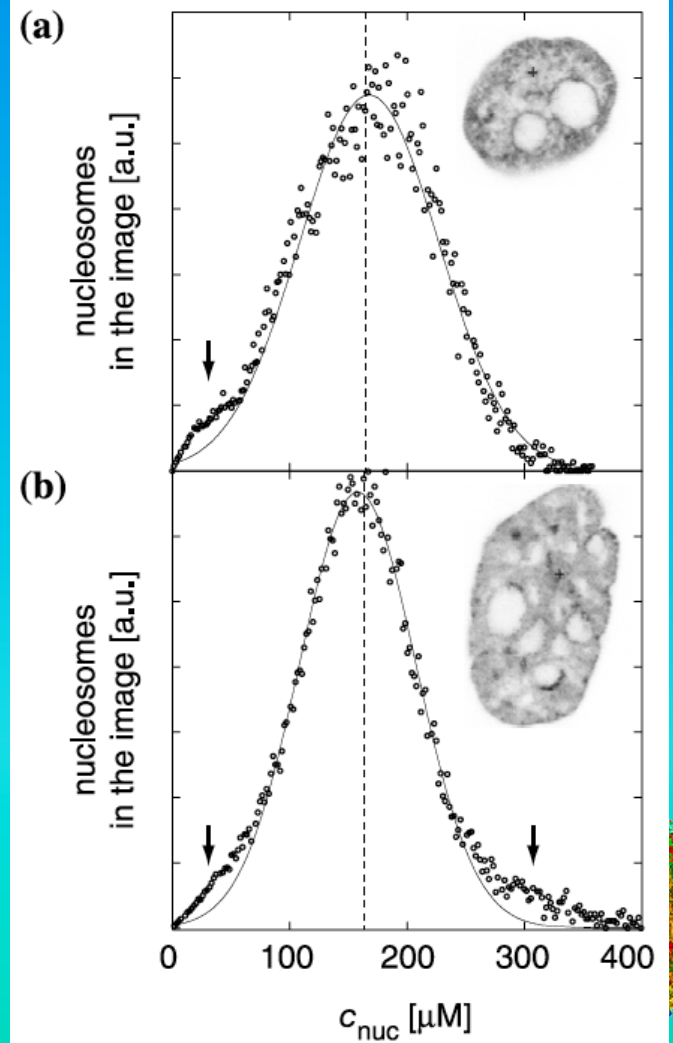
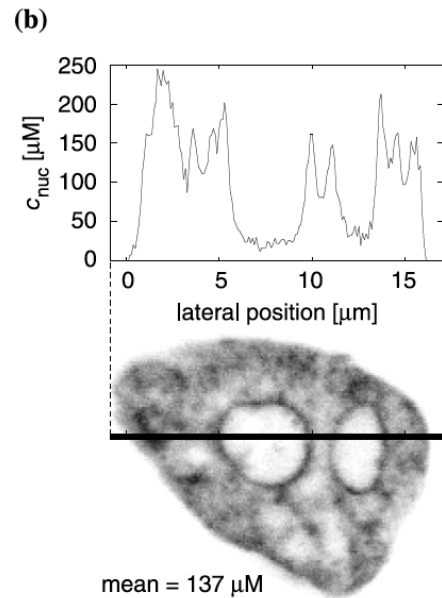
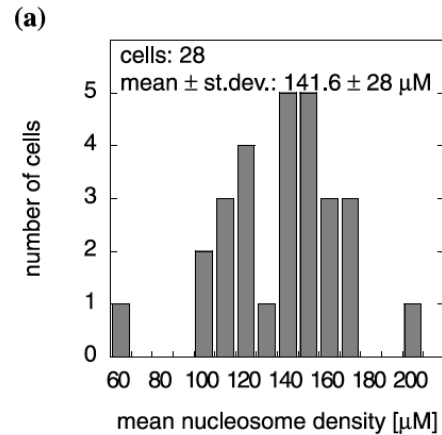
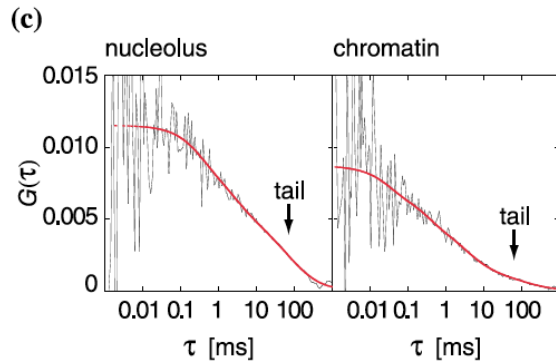
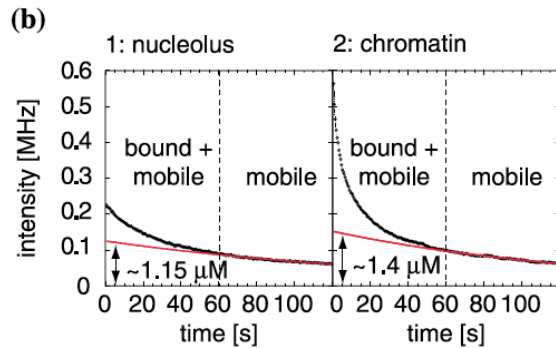
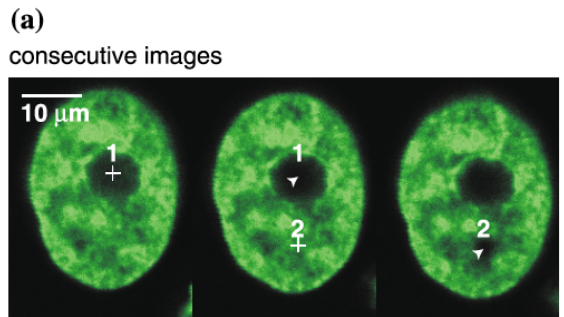
$$\langle r^2 \rangle \propto t^{2/D_w}$$

Nuclear diameter [μm]	Nuclear Volume [μm^3]	Mean Nucleosome Concentration [μM]	Chromatin Volume Fraction [%]	Mean Isotropic Mesh Spacing [nm]
6	115	251	20.1	41
8	268	107	8.6	64
10	523	55	4.4	90
12	904	32	2.6	117



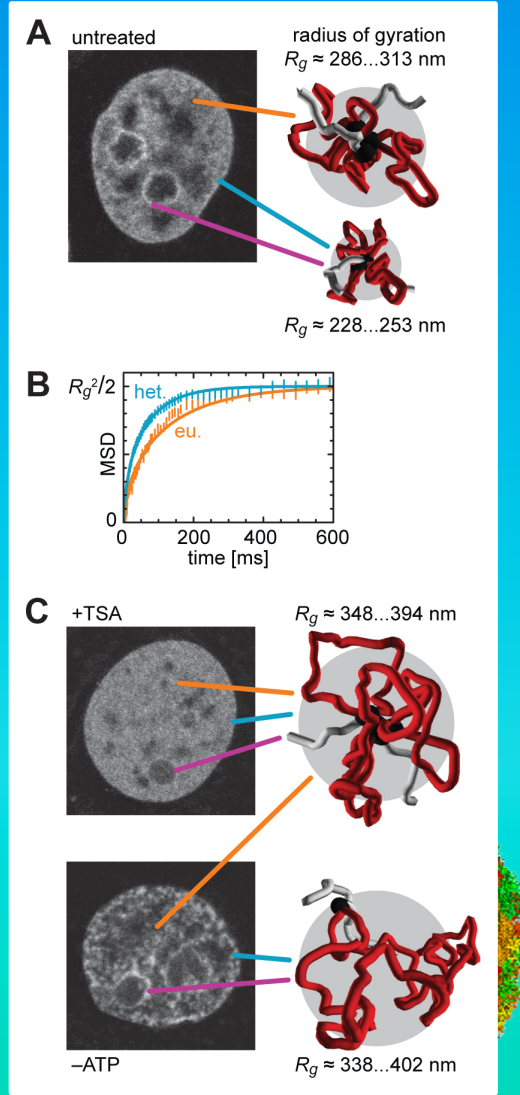
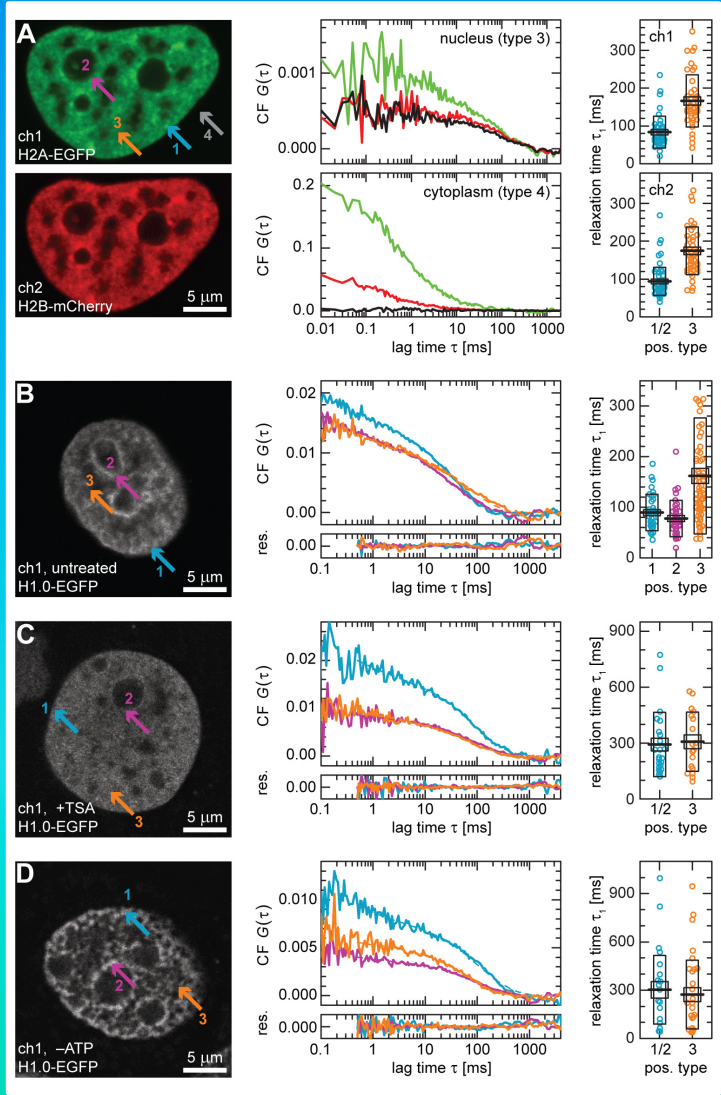
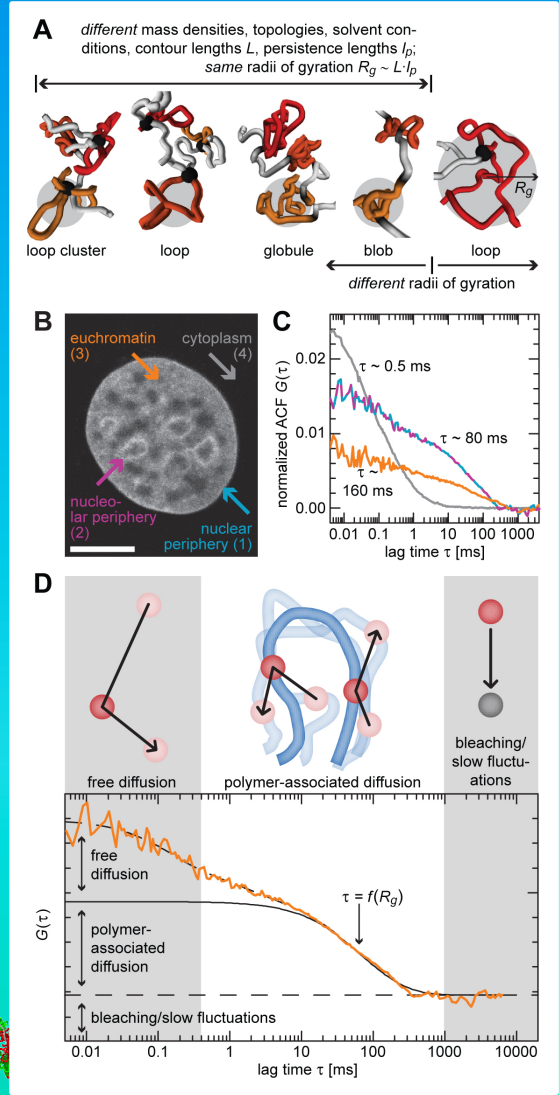
In Vivo Nucleosome Concentrations and 3D architecture

Counting nucleosomes in living cells with a combination of fluorescence correlation spectroscopy (FCS) and confocal laser scanning microscopy (CLSM) reveals the association of nucleosomes and their kinetics as well as again the typical expected distribution of a multi-loop aggregate/rosette.



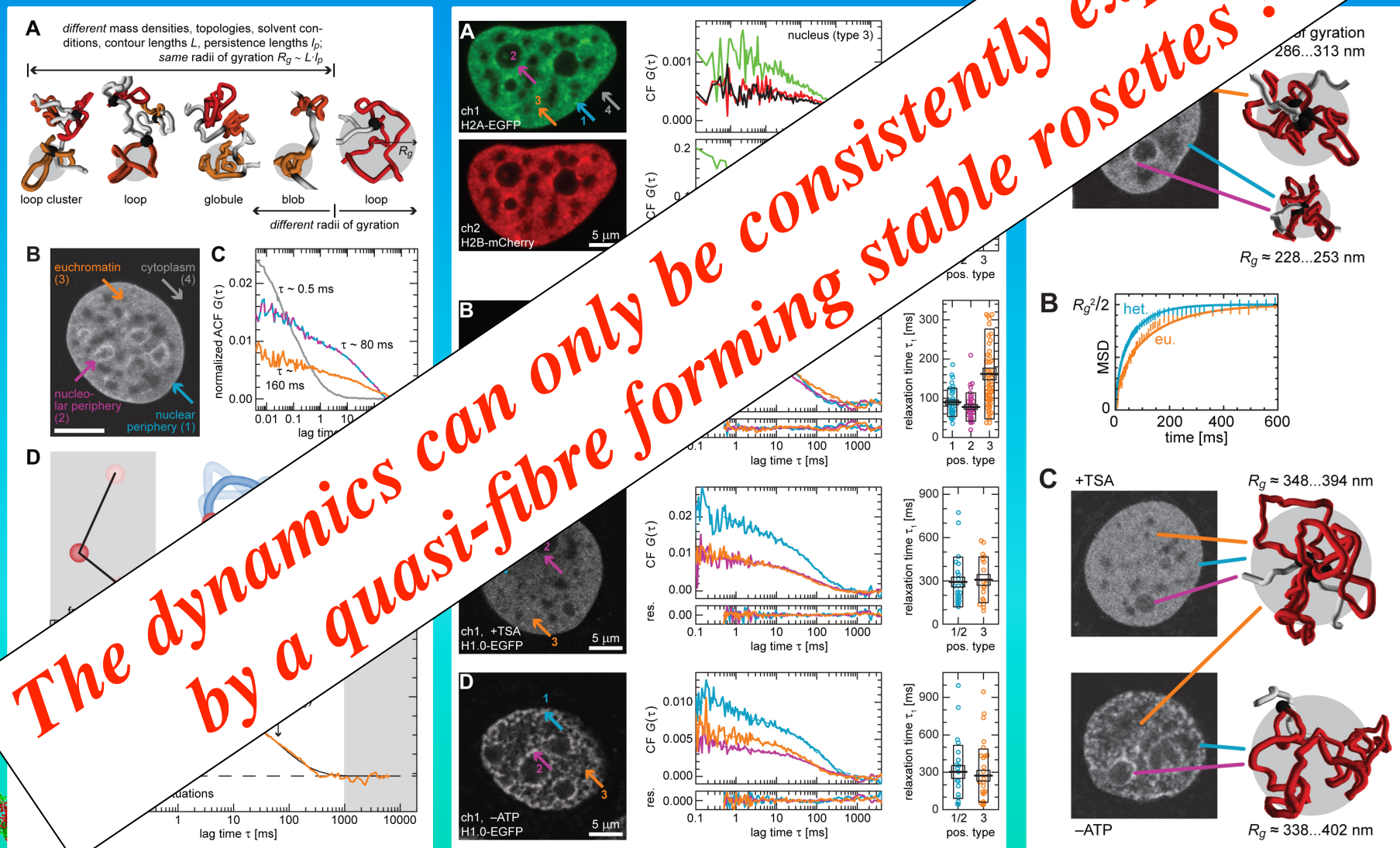
In Vivo Dynamics and 3D architecture

Fluorescence correlation spectroscopy (FCS) also reveals the dynamics of nucleosomes bound to DNA, i.e. FCS measures the movement of the chromatin quasi-fibre and its constraining architecture. This shows again a differentially compacted quasi-fibre folded into multi-loop aggregates/rosettes with functional differences as to e.g. hetero- and euchromatin or induced disturbances chromatin fiber (de-)condensation (+TSA, -ATP)



In Vivo Dynamics and 3D architecture

Fluorescence correlation spectroscopy (FCS) also reveals the dynamics of nucleosomes bound to DNA, i.e. FCS measures the movement of the chromatin quasi-fibre and its constraining architecture. This shows again differentially compacted quasi-fibre folded into multi-loop aggregates/rosettes with functional differences, e.g. hetero- and euchromatin or induced disturbances chromatin fiber (de-)condensation (+TSA)



The dynamics can only be consistently explained by a quasi-fibre forming stable rosettes!

Conclusion

The compacted chromatin quasi-fibre, folds into stable loop-aggregates connected by a linker !

Every structural level of nuclear organization including its dynamics is connected and represented in all the other levels in a holistic systems genomics manner.



Parameter/Observable			Simulation Single Chromosomes						Simulation Whole Nuclei						General Comparison		
Architectural Level	Observable Class	Spec. Feature	Applic. & Quality	Topological Parameter Dependence				Modell	Applic. & Quality	Topological Parameter Dependence					Modell	Experiment vs. Simulation	
				L _s /R _s	LI _s	C _{VOL}	EV			L _s /R _s	LI _s	NUC _{VOL}	EV	Chrom _s		Comp. Degree	Modell
Morphology: Chromatin Fibre to Nucleus	Morphology	Rendering	+++	+++	+++	+++	+++	MLS	+++	+++	+++	+++	+++	-	MLS	+	MLS
		EM	ND; but similar to the simulation of whole nuclei.	+	+	+	+++	+	-	~MLS	+	~MLS +					
		FISH-EM		++	++	++	+++	++	+++	~MLS	+	~MLS +					
		CLSM		+	+	++	+++	+	-	MLS	++	MLS ++					
		FISH-CLSM		++	++	+++	+++	++	+++	MLS	+++	MLS +++					
Mass	+++	+		+	+++	++	+++	≈MLS	+	≈MLS							
Nucleus	Radial Distribution Nuclei	Density	+++	+	+	+++	++	+++	≈MLS	+	≈MLS						
		CLSM-Image Distribution	Intensity	+++	+	+	+++	++	-	MLS	+++	MLS +++					
		Mass	+++	+	+	+++	++	-	MLS	+++	MLS +++						
	Chromosome Position	Distance Mass Centre	+++	+	++	+++	++	+++	~MLS	+	~MLS +						
		Mass	+++	++	+++	++	+	+++	MLS	+	MLS +						
Chromosome	Radial Distribution Chromosomes	Density	+++	++	+++	+++	++	MLS	+++	++	+++	++	+	+++	MLS	+	MLS +
		Territory Shape	Roundness	++	+	+++	++	+	+++	MLS	++	MLS ++					
		Territory Distance	Nearest	+++	+	++	+++	+	+++	MLS	++	MLS ++					
		Arbitrary	+++	+	++	+++	+	+++	MLS	++	MLS ++						
		Territory CLSM/Interaction	Volume CLSM	+++	+	++	+++	++	+++	MLS	+++	MLS +++					
		Overlap CLSM	+++	+	++	+++	++	+++	MLS	+++	MLS +++						
		Subchromosomal Domain	SD Radial Distribution	Mass	+++	+++	+	+	+	MLS	+++	+++	+	+	~+	-	MLS
	SD Distance	Density	+++	+++	+	+	+	MLS	+++	+++	+	+	~+	-	MLS	+++	MLS +++
		Genetically Adjacent	+++	++	+++	+	+	MLS	+++	++	+++	+	~+	-	MLS	+++	MLS +++
		Spatial Arbitrary	+++	+	+	++	++	MLS	+++	+	+	+++	~+	-	MLS	+++	MLS +++
		Spatial Nearest	+++	++/+	+++/+	++	++	MLS	+++	++/+	+++/+	+/+	~+	-	MLS	+++	MLS +++
		SD CLSM/Interaction	Volume CLSM	+++	+++	+	+	~+	-	MLS	+++	+++	+	+	~+	-	MLS
Chromatin Loop/Fibre	Spatial Distance	Position Independent	+++	+++	+++	-/+	++	MLS	+++	+++	+++	-/+	+	-/+	MLS	+++	MLS +++
		Position Dependent	++++	+++	+++	-/+	++	MLS	++++	+++	+++	-/+	+	-/+	MLS	+++	MLS +++
		Marker Ensemble	++++	+++	+++	-/+	++	MLS	++++	+++	+++	-/+	+	-/+	MLS	+++	MLS +++

Evolutionary Architecture Perspective

Only a compacted chromatin quasi-fibre, folded into stable loop-aggregates connected by a linker allows to guaranty the functional informational requirements of genomes:

i) storage stability/flexibility, ii) readout, and iii) replication !



➤ Storage stability/flexibility:

The packaging ratio/scale into a quasi-fibre and stable loops forming rosettes is optimal for the physical stability of genomes, while it is flexible enough to allow functional differences as well as react to entropic and other damages.

➤ Readout:

The dynamics this architecture allows expression/regulation by self-organization into (in-)active units already in proximity, and guaranties at the same time accessibility to and from the information for factors as well transcripts.

➤ Replication:

The 2D knot-free topology as well as the packaging ratio/scale into a quasi-fibre and stable loops forming rosettes, allows concatenation free replication with low error/damage rate due to the easy block-wise proximity organization as well as the easy physical (de-)condensation during cell division.

Form follows function and function follows form!

Evolutionary Architecture Perspective

Only a compacted chromatin quasi-fibre, folded into stable loop-aggregates connected by a linker allows to guaranty the functional informational requirements of genomes:

i) storage stability/flexibility, ii) readout, and iii) replication !

➤ **Storage stability/flexibility:**

The packaging ratio/scale into a quasi-fibre and stable loops is optimal for the physical stability of genomes, while it is flexible to accommodate differences as well as react to entropic and other damages.

➤ **Readout:**

The dynamics this architecture is achieved by self-organization into (in-)active units already in proximity, and accessibility to and from the information for factors as well transcription.

➤ **Replication:**

The 2D structure of the genome allows the packaging ratio/scale into a quasi-fibre and stable loops form a replication free replication with low error/damage rate due to the easy replication as well as the easy physical (de-)condensation during cell division.

Genomes are an Evolutionary Holistic Form-Function Entanglement !

Form follows function and function follows form!

Acknowledgements

Thanks go to all the lab local lab members, those people who supported this work in the last decades, the institutions providing their infrastructure, and the national and international computing infrastructures.

Special thanks go to the reviewers, the EraSysBio+ initiative and the national and EU funding bodies.



Erasmus MC

Nick Kepper
Michael Lesnussa
Anis Abuseiris
A.M. Ali Imam

Petros Kolovos
Harmen J. G. van de Werken
Jessica Zuin
Christel E. M. Kockx
Rutger W. W. Brouwer
Wilfred F. J. van Ijken
Kerstin S. Wendt
Frank G. Grosveld

Erasmus Medical Center and BioQuant & German Cancer Research Center

High-Performance Computing Center Stuttgart, University of Stuttgart; Supercomputing Center Karlsruhe, University of Karlsruhe; Computing Center, Deutsches Krebsforschungszentrum Heidelberg (DKFZ)

Erasmus Medical Center, Hogeschool Rotterdam, The Fraunhofer Society, The German MediGRID and Services@MediGRID
The German D-Grid Initiatives, The German Ministry for Science and Technology, The Dutch Science Organization (NOW)
The European EGEE Initiative, The European EDGES Consortium, The German Society for Human Ecology, The
International Society for Human Ecology, The European Commission

Cell Biology & Biophysics

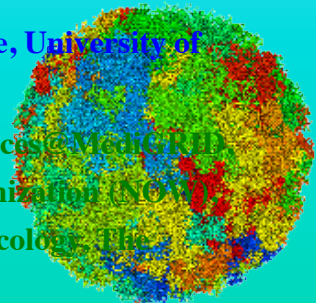
EMBL

Malte Wachsmuth

EpiGenSys

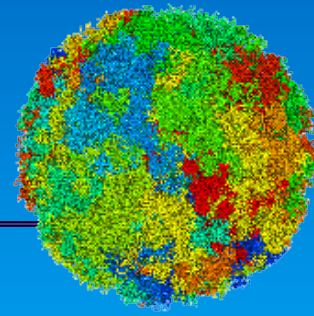
EraSysBio+ Consortium Labs

Peter R. Cook
Gernot Längst
Tobias A. Knoch
Karsten Rippe
Gero Wedemann



Acknowledgements

Thanks go also to all those people who supported this work in the last decades,
the institutions providing their infrastructure, and the national and international computing infrastructures.

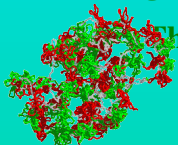


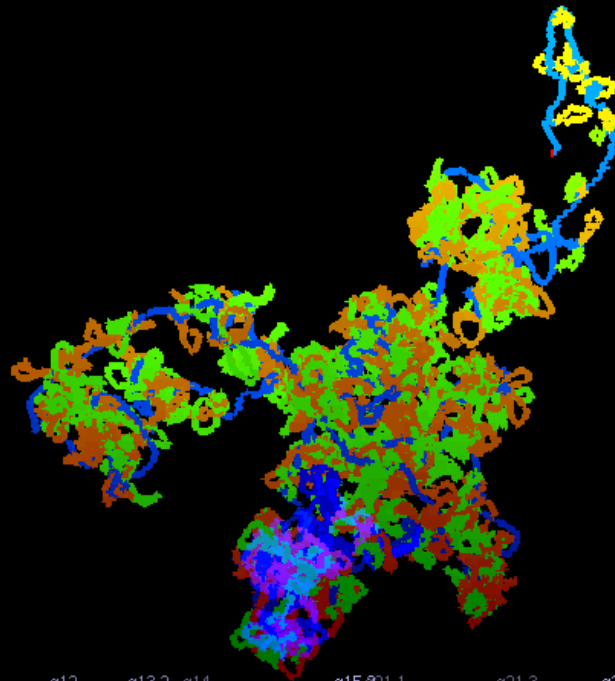
	Biophysical Genomics, Cell Biology, Erasmus MC	Biological Sciences, UCSD	The Cremer Labs	
Cell Biology & Biophysics	Petros Kolovos	Suchit Jhunjhunwala	Joachim Rauch	
EMBL	Anis Abuseiris	Menno van Zelm	Irina Solovei	Biophysics of Macromolecules DKFZ
Malte Wachsmuth	Michael Lesnussa	Cornelis Murre	Michael Hausmann	Gabriele Müller
Biophysics, LMU	Rob de Graaf	Clinical Genetics Erasmus MC	Christoph Cremer	Waldemar Waldeck
Thomas Weidemann	Nick Kepper	Bert Eussen	Thomas Cremer	Jörg Langowski
CALTECH	Frank Grossveld	Annelies de Klein		
Katalin Fejes-Toth	LMU Munich		Molecular Genetics DKFZ	Supercomputing Center Karlsruhe
Genome Org & Function BioQuant/DKFZ	Peter Quicken	University Braunschweig	Karsten Richter	
Karsten Rippe	Anna Friedl	Markus Göker	Peter Lichter	Rudolph Lohner

Erasmus Medical Center and BioQuant & German Cancer Research Center

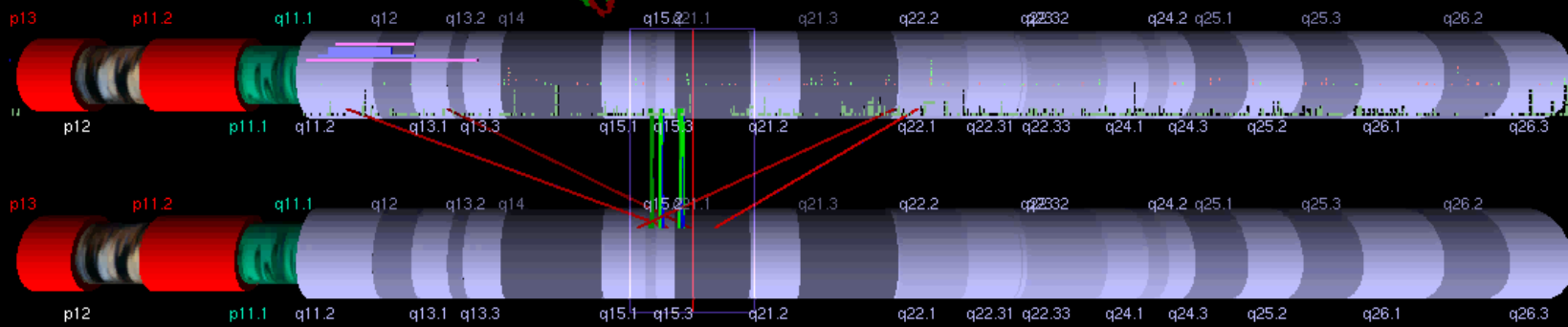
**High-Performance Computing Center Stuttgart, University of Stuttgart; Supercomputing Center Karlsruhe, University of
Karlsruhe; Computing Center, Deutsches Krebsforschungszentrum Heidelberg (DKFZ)**

**Erasmus Medical Center, Hogeschool Rotterdam, The Fraunhofer Society, The German MediGRID and Services@MediGRID,
The German D-Grid Initiatives, The German Ministry for Science and Technology, The Dutch Science Organization (NOW),
The European EGEE Initiative, The European EDGES Consortium, The German Society for Human Ecology, The
International Society for Human Ecology,
The European Commission**





15
 Decipher
 Affy100KXba
 Refseqb36



43750000

15

1:500000

A Systems Genomic Approach
Combining Simulations and Experiments Reveals
the
Detailed 3D Multi-Loop Aggregate/Rosette Chromatin Architecture
and
Functional Dynamic Organization of Genomes

Knoch, T. A.

*Netherlands Society on Biomolecular Modelling Fall Meeting, Boothzaal, University Library
De Uithof, Utrecht University, Utrecht, The Netherlands, 16th November, 2016.*

Abstract

The dynamic three-dimensional chromatin architecture of genomes and the obvious co-evolutionary connection to its function – the storage and expression of genetic information – is still debated after ~170 years of research. With a systems genomics approach combining quantitative polymer super-computer simulations, analytical models, and scaling analysis of both architecture and DNA sequence, with experimentally novel selective high-throughput chromosomal interaction capture (T2C) and novel *in vivo* 2D fluorescence correlation spectroscopy (2D-FCS) techniques, we determined and cross-proved finally the architecture of genomes with unprecedented molecular resolution and dynamic range from single base pairs to entire chromosomes: for several genetic loci of different species, cell type, cell cycle, and functional states a chromatin quasi-fibre exists with 5 ± 1 nucleosome per 11 nm, which folds into stable(!) 40-100 kbp loops forming stable(!) aggregates/rosettes which are connected by a ~50 kbp chromatin linker.

A priori, Monte Carlo and Brownian Dynamics methods were used to simulate the Multi-Loop-Subcompartment (MLS) model, in which ~100 kbp loops form rosettes, connected by a linker, and the Random-Walk/Giant-Loop (RW/GL) topology, in which 1-5 Mbp loops are attached to a flexible backbone. Both the MLS and the RW/GL model form chromosome territories but only the MLS rosettes result in distinct subcompartments visible with light microscopy and low overlap of chromosomes, -arms and subcompartments. The MLS morphology, the size of subcompartments and chromatin density distribution of simulated confocal (CLSM) images agree with the expression of fusionproteins from the histones with the autofluorescent proteins which also revealed different interphase morphologies for different cell lines. Even small changes of the model parameters induced significant rearrangements of the chromatin morphology. Thus, pathological diagnoses are closely related to structural changes on the chromatin level. Review and comparison of experimental to simulated spatial distance measurements between genomic markers as function of their genomic separation, as well as DNA fragment distributions after ion-irradiation also favour the above mentioned architecture and dynamics. Most importantly experiments with newly developed T2C and *in vivo* 2D-FCS techniques proof all this independently and allow the exact quantitative determination of parameters with unprecedented resolution. Finally, we find a fine-structured multi-scaling behaviour of both the simulated and experimentally determined architecture and the DNA sequence, showing for the first time directly the tight entanglement between architecture and DNA sequence.

The found organization has fundamental consequences for the entire system of the storage and expression of genetic information as well as for its investigation: E.g. this architecture, its dynamics, and accessibility balance stability and flexibility ensuring genome integrity and variation enabling gene expression/regulation by self-

organization of (in-)active units already in proximity. Thus, our systems genomics approach opens the door to “architectural and dynamic sequencing” and “virtual systems simulation” of genomes at a resolution where a genome mechanics with corresponding uncertainty principles applies. Consequently, this will lead now to a detailed understanding of genomes with fundamental new insights and huge novel perspectives for diagnosis, treatment and genome engineering efforts in the future.

Corresponding author email contact: TA.Knoch@taknoch.org

Keywords:

Genome, genomics, genome organization, genome architecture, structural sequencing, architectural sequencing, systems genomics, coevolution, holistic genetics, genome mechanics, genome statistical mechanics, genomic uncertainty principle, multilism genotype-phenotype, genome function, genetics, gene regulation, replication, transcription, repair, homologous recombination, simultaneous co-transfection, cell division, mitosis, metaphase, interphase, cell nucleus, nuclear structure, nuclear organization, chromatin density distribution, nuclear morphology, chromosome territories, subchromosomal domains, chromatin loop aggregates, chromatin rosettes, chromatin loops, chromatin quasi fibre, chromatin density, persistence length, spatial distance measurement, histones, H1.0, H2A, H2B, H3, H4, mH2A1.2, DNA sequence, complete sequenced genomes, molecular transport, obstructed diffusion, anomalous diffusion, percolation, long-range correlations, fractal analysis, scaling analysis, exact yard-stick dimension, box-counting dimension, lacunarity dimension, local nuclear dimension, nuclear diffuseness, parallel super computing, grid computing, volunteer computing, polymer model, analytic mathematical model, Brownian Dynamics, Monte Carlo, fluorescence *in situ* hybridization (FISH), targeted chromatin capture (T2C) confocal laser scanning microscopy, fluorescence correlation spectroscopy, spatial precision distance microscopy, super-resolution microscopy, two dimensional fluorescence correlations spectroscopy (2D-FCS) auto-fluorescent proteins, CFP, GFP, YFP, DsRed, fusion protein, *in vivo* labelling, information browser, visual data base access, holistic viewing system, integrative data management, extreme visualization, three-dimensional virtual environment, virtual paper tool, human ecology, e-human grid ecology, society, social systems, e-social challenge, inverse tragedy of the commons, grid phenomenon, micro-sociality, macro-sociality, autopoietic tragedy of social sub-systems, micro subsystems, macro subsystems, micro operationality, macro operationality, grid psychology micro riskmanagement, macro riskmanagement.

Literature References

- Knoch, T. A.** Dreidimensionale Organisation von Chromosomen-Domänen in Simulation und Experiment. (Three-dimensional organization of chromosome domains in simulation and experiment.) *Diploma Thesis*, Faculty for Physics and Astronomy, Ruperto-Carola University, Heidelberg, Germany, 1998, and TAK Press, Tobias A. Knoch, Mannheim, Germany, ISBN 3-00-010685-5 and ISBN 978-3-00-010685-9 (soft cover, 2rd ed.), ISBN 3-00-035857-9 and ISBN 978-3-00-0358857-0 (hard cover, 2rd ed.), ISBN 3-00-035858-7, and ISBN 978-3-00-035858-6 (DVD, 2rd ed.), 1998.
- Knoch, T. A., Münkkel, C. & Langowski, J.** Three-dimensional organization of chromosome territories and the human cell nucleus - about the structure of a self replicating nano fabrication site. *Foresight Institute - Article Archive*, Foresight Institute, Palo Alto, CA, USA, <http://www.foresight.org>, 1- 6, 1998.
- Knoch, T. A., Münkkel, C. & Langowski, J.** Three-Dimensional Organization of Chromosome Territories and the Human Interphase Nucleus. *High Performance Scientific Supercomputing*, editor Wilfried Juling, Scientific Supercomputing Center (SSC) Karlsruhe, University of Karlsruhe (TH), 27- 29, 1999.
- Knoch, T. A., Münkkel, C. & Langowski, J.** Three-dimensional organization of chromosome territories in the human interphase nucleus. *High Performance Computing in Science and Engineering 1999*, editors Krause,

- E. & Jäger, W., High-Performance Computing Center (HLRS) Stuttgart, University of Stuttgart, Springer Berlin-Heidelberg-New York, ISBN 3-540-66504-8, 229-238, 2000.
- Bestvater, F., **Knoch, T. A.**, Langowski, J. & Spiess, E. GFP-Walking: Artificial construct conversions caused by simultaneous cotransfection. *BioTechniques* 32(4), 844-854, 2002.
- Gil-Parado, S., Fernández-Montalván, A., Assfalg-Machleidt, I., Popp, O., Bestvater, F., Holloschi, A., **Knoch, T. A.**, Auerswald, E. A., Welsh, K., Reed, J. C., Fritz, H., Fuentes-Prior, P., Spiess, E., Salvesen, G. & Machleidt, W. Ionomycin-activated calpain triggers apoptosis: A probable role for Bcl-2 family members. *J. Biol. Chem.* 277(30), 27217-27226, 2002.
- Knoch, T. A. (editor)**, Backes, M., Baumgärtner, V., Eysel, G., Fehrenbach, H., Göker, M., Hampl, J., Hampl, U., Hartmann, D., Hitzelberger, H., Nambena, J., Rehberg, U., Schmidt, S., Weber, A., & Weidemann, T. Humanökologische Perspektiven Wechsel - Festschrift zu Ehren des 70. Geburtstags von Prof. Dr. Kurt Egger. Human Ecology Working Group, Ruperto-Carola University of Heidelberg, Heidelberg, Germany, 2002.
- Knoch, T. A.** Approaching the three-dimensional organization of the human genome: structural-, scaling- and dynamic properties in the simulation of interphase chromosomes and cell nuclei, long- range correlations in complete genomes, *in vivo* quantification of the chromatin distribution, construct conversions in simultaneous co-transfections. *Dissertation*, Ruperto-Carola University, Heidelberg, Germany, and TAK†Press, Tobias A. Knoch, Mannheim, Germany, ISBN 3-00-009959-X and ISBN 978-3-00-009959-5 (soft cover, 3rd ed.), ISBN 3-00-009960-3 and ISBN 978-3-00-009960-1 (hard cover, 3rd ed.), ISBN 3-00-035856-9 and ISBN 978-3-00-010685-9 (DVD, 3rd ed.) 2002.
- Westphal, G., van den Berg-Stein, S., Braun, K., **Knoch, T. A.**, Dümmerling, M., Langowski, J., Debus, J. & Friedrich, E. Detection of the NGF receptors TrkA and p75NTR and effect of NGF on the growth characteristics of human tumor cell lines. *J. Exp. Clin. Canc. Res.* 21(2), 255-267, 2002.
- Westphal, G., Niederberger, E., Blum, C., Wollman, Y., **Knoch, T. A.**, Dümmerling, M., Rebel, W., Debus, J. & Friedrich, E. Erythropoietin Receptor in Human Tumor Cells: Expression and Aspects Regarding Functionality. *Tumori* 88(2), 150-159, 2002.
- Gil-Parado, S., Popp, O., **Knoch, T. A.**, Zahler, S., Bestvater, F., Felgenträger, M., Holoshi, A., Fernández-Montalván, A., Auerswald, E. A., Fritz, H., Fuentes-Prior, P., Machleidt, W. & Spiess, E. Subcellular localization and subunit interactions of over-expressed human μ -calpain. *J. Biol. Chem.* 278(18), 16336-15346, 2003.
- Knoch, T. A.** Towards a holistic understanding of the human genome by determination and integration of its sequential and three-dimensional organization. *High Performance Computing in Science and Engineering 2003*, editors Krause, E., Jäger, W. & Resch, M., High-Performance Computing Center (HLRS) Stuttgart, University of Stuttgart, Springer Berlin-Heidelberg-New York, ISBN 3- 540-40850-9, 421-440, 2003.
- Wachsmuth, M., Weidemann, T., Müller, G., Urs W. Hoffmann-Rohrer, **Knoch, T. A.**, Waldeck, W. & Langowski, J. Analyzing intracellular binding and diffusion with continuous fluorescence photobleaching. *Biophys. J.* 84(5), 3353-3363, 2003.
- Weidemann, T., Wachsmuth, M., **Knoch, T. A.**, Müller, G., Waldeck, W. & Langowski, J. Counting nucleosomes in living cells with a combination of fluorescence correlation spectroscopy and confocal imaging. *J. Mol. Biol.* 334(2), 229-240, 2003.
- Fejes Tóth, K., **Knoch, T. A.**, Wachsmuth, M., Frank-Stöhr, M., Stöhr, M., Bacher, C. P., Müller, G. & Rippe, K. Trichostatin A induced histone acetylation causes decondensation of interphase chromatin. *J. Cell Science* 117, 4277-4287, 2004.
- Ermiler, S., Kronic, D., **Knoch, T. A.**, Moshir, S., Mai, S., Greulich-Bode, K. M. & Boukamp, P. Cell cycle-dependent 3D distribution of telomeres and telomere repeat-binding factor 2 (TRF2) in HaCaT and HaCaT-myc cells. *Europ. J. Cell Biol.* 83(11-12), 681-690, 2004.
- Kost, C., Gama de Oliveira, E., **Knoch, T. A.** & Wirth, R. Spatio-temporal permanence and plasticity of foraging trails in young and mature leaf-cutting ant colonies (*Atta spp.*). *J. Trop. Ecol.* 21(6), 677- 688, 2005.
- Winnefeld, M., Grewenig, A., Schnölzer, M., Spring, H., **Knoch, T. A.**, Gan, E. C., Rommelaere, J. & Cziepluch, C. Human SGT interacts with BAG-6/Bat-3/Scythe and cells with reduced levels of either protein display persistence of few misaligned chromosomes and mitotic arrest. *Exp. Cell Res.* 312, 2500-2514, 2006.

- Sax, U., Weisbecker, A., Falkner, J., Viezens, F., Yassene, M., Hartung, M., Bart, J., Krefting, D., **Knoch, T. A.** & Semler, S. Grid-basierte Services für die elektronische Patientenakte der Zukunft. *E-HEALTH-COM - Magazin für Gesundheitstelematik und Telemedizin*, 4(2), 61-63, 2007.
- de Zeeuw, L. V., **Knoch, T. A.**, van den Berg, J. & Grosveld, F. G. Erasmus Computing Grid - Het bouwen van een 20 TeraFLOP virtuele supercomputer. *NIOC proceedings 2007 - het perspective of lange termijn*. editor Frederik, H. NIOC, Amsterdam, The Netherlands, 52-59, 2007.
- Rauch, J., **Knoch, T. A.**, Solovei, I., Teller, K. Stein, S., Buiting, K., Horsthemke, B., Langowski, J., Cremer, T., Hausmann, M. & Cremer, C. Lightoptical precision measurements of the Prader- Willi/Angelman Syndrome imprinting locus in human cell nuclei indicate maximum condensation changes in the few hundred nanometer range. *Differentiation* 76(1), 66-82, 2008.
- Sax, U., Weisbecker, A., Falkner, J., Viezens, F., Mohammed, Y., Hartung, M., Bart, J., Krefting, D., **Knoch, T. A.** & Semler, S. C. Auf dem Weg zur individualisierten Medizin - Grid-basierte Services für die EPA der Zukunft. *Telemedizinführer Deutschland 2008*, editor Jäckel, A. Deutsches Medizinforum, Minerva KG, Darmstadt, ISBN 3-937948-06-6, ISBN-13 9783937948065, 47-51, 2008.
- Drägestein, K. A., van Capellen, W. A., van Haren, J. Tsibidis, G. D., Akhmanova, A., **Knoch, T. A.**, Grosveld, F. G. & Galjart, N. Dynamic behavior of GFP-CLIP-170 reveals fast protein turnover on microtubule plus ends. *J. Cell Biol.* 180(4), 729-737, 2008.
- Jhunjhunwala, S., van Zelm, M. C., Peak, M. M., Cutchin, S., Riblet, R., van Dongen, J. J. M., Grosveld, F. G., **Knoch, T. A.**⁺ & Murre, C.⁺ The 3D-structure of the Immunoglobulin Heavy Chain Locus: implications for long-range genomic interactions. *Cell* 133(2), 265-279, 2008.
- Krefting, D., Bart, J., Beronov, K., Dzhimova, O., Falkner, J., Hartung, M., Hoheisel, A., **Knoch, T. A.**, Lingner, T., Mohammed, Y., Peter, K., Rahm, E., Sax, U., Sommerfeld, D., Steinke, T., Tolxdorff, T., Vossberg, M., Viezens, F. & Weisbecker, A. MediGRID - Towards a user friendly secured grid infrastructure. *Future Generation Computer Systems* 25(3), 326-336, 2008.
- Knoch, T. A.**, Lesnussa, M., Kepper, F. N., Eussen, H. B., & Grosveld, F. G. The GLOBE 3D Genome Platform - Towards a novel system-biological paper tool to integrate the huge complexity of genome organization and function. *Stud. Health. Technol. Inform.* 147, 105-116, 2009.
- Knoch, T. A.**, Baumgärtner, V., de Zeeuw, L. V., Grosveld, F. G., & Egger, K. e-Human Grid Ecology: Understanding and approaching the Inverse Tragedy of the Commons in the e-Grid Society. *Stud. Health. Technol. Inform.* 147, 269-276, 2009.
- Dickmann, F., Kaspar, M., Löhnhardt, B., **Knoch, T. A.**, & Sax, U. Perspectives of MediGRID. *Stud. Health. Technol. Inform.* 147, 173-182, 2009.
- Knoch, T. A.**, Göcker, M., Lohner, R., Abuseiris, A. & Grosveld, F. G. Fine-structured multi-scaling long-range correlations in completely sequenced genomes - features, origin and classification. *Eur. Biophys. J.* 38(6), 757-779, 2009.
- Dickmann, F., Kaspar, M., Löhnhardt, B., Kepper, N., Viezens, F., Hertel, F., Lesnussa, M., Mohammed, Y., Thiel, A., Steinke, T., Bernarding, J., Krefting, D., **Knoch, T. A.** & Sax, U. Visualization in health-grid environments: a novel service and business approach. *LNCS 5745*, 150-159, 2009.
- Dickmann, F., Kaspar, M., Löhnhardt, B., Kepper, N., Viezens, F., Hertel, F., Lesnussa, M., Mohammed, Y., Thiel, A., Steinke, T., Bernarding, J., Krefting, D., **Knoch, T. A.** & Sax, U. Visualization in health-grid environments: a novel service and business approach. *Grid economics and business models - GECON 2009 Proceedings, 6th international workshop, Delft, The Netherlands*. editors Altmann, J., Buyya, R. & Rana, O. F., GECON 2009, LNCS 5745, Springer-Verlag Berlin Heidelberg, ISBN 978-3-642-03863-1, 150-159, 2009.
- Estrada, K.* , Abuseiris, A.* , Grosveld, F. G., Uitterlinden, A. G., **Knoch, T. A.**⁺ & Rivadeneira, F.⁺ GRIMP: A web- and grid-based tool for high-speed analysis of large-scale genome-wide association using imputed data. *Bioinformatics* 25(20), 2750-2752, 2009.
- de Wit, T., Dekker, S., Maas, A., Breedveld, G., **Knoch, T. A.**, Langeveld, A., Szumska, D., Craig, R., Bhattacharya, S., Grosveld, F. G.⁺ & Drabek, D. Tagged mutagenesis of efficient minos based germ line transposition. *Mol. Cell Biol* 30(1), 66-77, 2010.
- Kepper, N., Schmitt, E., Lesnussa, M., Weiland, Y., Eussen, H. B., Grosveld, F. G., Hausmann, M. & **Knoch T. A.**, Visualization, Analysis, and Design of COMBO-FISH Probes in the Grid-Based GLOBE 3D Genome Platform. *Stud. Health Technol. Inform.* 159, 171-180, 2010.

- Kepper, N., Ettig, R., Dickmann, F., Stehr, R., Grosveld, F. G., Wedemann, G. & **Knoch, T. A.** Parallel high-performance grid computing: capabilities and opportunities of a novel demanding service and business class allowing highest resource efficiency. *Stud. Health Technol. Inform.* 159, 264-271, 2010.
- Skrowny, D., Dickmann, F., Löhnhardt, B., **Knoch, T. A.** & Sax, U. Development of an information platform for new grid users in the biomedical field. *Stud. Health Technol. Inform.* 159, 277-282, 2010.
- Knoch, T. A.**, Baumgärtner, V., Grosveld, F. G. & Egger, K. Approaching the internalization challenge of grid technologies into e-Society by e-Human “Grid” Ecology. *Economics of Grids, Clouds, Systems, and Services – GECON 2010 Proceedings*, 7th International Workshop, Ischia, Italy, editors Altman, J., & Rana, O. F., Lecture Notes in Computer Science (LNCS) 6296, Springer Berlin Heidelberg New York, ISSN 0302-9743, ISBN-10 3-642-15680-0, ISBN-13 978-3-642-15680-9, 116-128, 2010.
- Dickmann, F., Brodhun, M., Falkner, J., **Knoch, T. A.** & Sax, U. Technology transfer of dynamic IT outsourcing requires security measures in SLAs. *Economics of Grids, Clouds, Systems, and Services – GECON 2010 Proceedings*, 7th International Workshop, Ischia, Italy, editors Altman, J., & Rana, O. F., Lecture Notes in Computer Science (LNCS) 6296, Springer Berlin Heidelberg New York, ISSN 0302-9743, ISBN-10 3-642-15680-0, ISBN-13 978-3-642-15680-9, 1-115, 2010.
- Knoch, T. A.** Sustained Renewability: approached by systems theory and human ecology. *Renewable Energy 2*, editors M. Nayeripour & M. Keshti, Intech, ISBN 978-953-307-573-0, 21-48, 2011.
- Kolovos, P., **Knoch, T. A.**, F. G. Grosveld, P. R. Cook, & Papantonis, A. Enhancers and silencers: an integrated and simple model for their function. *Epigenetics and Chromatin 5(1)*, 1-8, 2012.
- Dickmann, F., Falkner, J., Gunia, W., Hampe, J., Hausmann, M., Herrmann, A., Kepper, N., **Knoch, T. A.**, Lauterbach, S., Lippert, J., Peter, K., Schmitt, E., Schwardmann, U., Solodenko, J., Sommerfeld, D., Steinke, T., Weisbecker, A. & Sax, U. Solutions for Biomedical Grid Computing - Case Studies from the D-Grid Project Services@MediGRID. *JOCS 3(5)*, 280-297, 2012.
- Estrada, K., Abuseiris, A., Grosveld, F. G., Uitterlinden, A. G., **Knoch, T. A.** & Rivadeneira, F. GRIMP: A web- and grid-based tool for high-speed analysis of large-scale genome-wide association using imputed data. *Dissection of the complex genetic architecture of human stature and osteoporosis*. cumulative dissertation, editor Estrada K., Erasmus Medical Center, Erasmus University Rotterdam, Rotterdam, The Netherlands, ISBN 978-94-6169-246-7, 25-30, 1st June 2012.
- van de Corput, M. P. C., de Boer, E., **Knoch, T. A.**, van Cappellen, W. A., Quintanilla, A., Ferrand, L., & Grosveld, F. G. Super-resolution imaging reveals 3D folding dynamics of the β -globin locus upon gene activation. *J. Cell Sci.* 125 (Pt 19), 4630-4639, 2012.
- da Silva, P. S. D., Delgado Bieber, A. G., Leal, I. R., **Knoch, T. A.**, Tabarelli, M., Leal, I. R., & Wirth, R. Foraging in highly dynamic environments: leaf-cutting ants adjust foraging trail networks to pioneer plant availability. *Entomologia Experimentalis et Applicata 147*, 110-119. 2013.
- Zuin, J., Dixon, J. R., van der Reijden, M. I. J. A., Ye, Z., Kolovos, P., Brouwer, R. W. W., van de Corput, M. P. C., van de Werken, H. J. G., **Knoch, T. A.**, van IJcken, W. F. J., Grosveld, F. G., Ren, B. & Wendt, K. S. Cohesin and CTCF differentially affect chromatin architecture and gene expression in human cells. *PNAS 111(3)*, 9906-1001, 2014.
- Kolovos, P., Kepper, N., van den Werken, H. J. G., Lesnussa, M., Zuin, J., Brouwer, R. W. W., Kockx, C. E. M., van IJcken, W. F. J., Grosveld, F. G. & **Knoch, T. A.** Targeted Chromatin Capture (T2C): A novel high resolution high throughput method to detect genomic interactions and regulatory elements. *Epigenetics & Chromatin 7:10*, 1-17, 2014.
- Diermeier, S., Kolovos, P., Heizinger, L., Schwartz, U., Georgomanolis, T., Zirkel, A., Wedemann, G., Grosveld, F. G., **Knoch, T. A.**, Merkl, R., Cook, P. R., Längst, G. & Papantonis, A. TNF α signalling primes chromatin for NF-kB binding and induces rapid and widespread nucleosome repositioning. *Genome Biology 15(12)*, 536-548, 2014.
- Knoch, T. A.**, Wachsmuth, M., Kepper, N., Lesnussa, M., Abuseiris, A., A. M. Ali Imam, Kolovos, P., Zuin, J., Kockx, C. E. M., Brouwer, R. W. W., van de Werken, H. J. G., van IJcken, W. F. J., Wendt, K. S. & Grosveld, F. G. The detailed 3D multi-loop aggregate/rosette chromatin architecture and functional dynamic organization of the human and mouse genomes. *bioRxiv preprint*, 16.07.2016.
- Kolovos, P., Georgomanolis, T., Koeflerle, A., Larkin, J. D., Brant, J., Nikolić, M., Gusmao, E. G., Zirkel, A., **Knoch, T. A.**, van IJcken, W. F. J., Cook, P. R., Costa, I. G., Grosveld, F. G. & Papantonis, A. Binding of nuclear kappa-B to non-canonical consensus sites reveals its multimodal role during the early inflammatory response. *Genome Research 26(11)*, 1478-1489, 2016.

- Wachsmuth, M., **Knoch, T. A.** & Rippe, K. Dynamic properties of independent chromatin domains measured by correlation spectroscopy in living cells. *Epigenetics & Chromatin* 9:57, 1-20, 2016.
- Knoch, T. A.**, Wachsmuth, M., Kepper, N., Lesnussa, M., Abuseiris, A., A. M. Ali Imam, Kolovos, P., Zuin, J., Kockx, C. E. M., Brouwer, R. W. W., van de Werken, H. J. G., van IJcken, W. F. J., Wendt, K. S. & Grosveld, F. G. The detailed 3D multi-loop aggregate/rosette chromatin architecture and functional dynamic organization of the human and mouse genomes. *Epigenetics & Chromatin* 9:58, 1-22, 2016.